UNIVERSITY OF CALIFORNIA
SANTA CRUZ

ANTIBODIES, DIET, AND THE MICROBIOTA: BACTERIAL-DEPENDENT INDUCTION OF ANTI-FIBER ANTIBODIES AND HOW THEY INFLUENCE MICROBIAL BIOLOGY

A dissertation submitted in partial satisfaction
of the requirements for the degree of

DOCTOR OF PHILOSOPHY

in

MICROBIOLOGY AND ENVIRONMENTAL TOXICOLOGY

by

Giovanni Vega
August 2026

The Dissertation of Giovanni Vega
is approved:

_____
Professor Michael L. Patnode, Chair

_____
Professor Victoria Auerbuch Stone

_____
Professor Rebecca DuBois

_____
Donald Smith
Interim Vice Provost and
Dean of Graduate Studies

Table of Contents

Abstract viii

Acknowledgements x

Chapter 1: Antibody Production in Response to Ingested Antigens 1

Introduction: 2

Antibody diversification and effector function: 2

T cell-dependent antibody generation: 3

T cell-independent antibody generation: 4

Natural antibodies against carbohydrates: 6

Host consequences of glycan-specific antibody production: 8

Conclusion: 8

Chapter 2: Gut Bacteria Prime Host Antibody Responses Against Ingested Dietary Fiber Glycans 10

Abstract: 11

Introduction: 11

Results: 13

Humans produce circulating IgM and secreted IgA specific for dietary fiber glycans 13

Ingestion of fiber induces glycan-specific anti-fiber IgM and IgA 16

Induction of anti-fiber antibodies requires exposure to gut microbes 25

Culturable commensal gut bacteria enable the induction of fiber-specific antibodies 43

Monoclonal antibodies specific for diverse plant glycans bind the surfaces of gut microbes 49
Methods: 56
Mice 56
Human Samples 56
Mouse feeding experiments 57
Bacterial samples for mouse colonization 57
Mouse sample collections 58
Fiber glycan bead library 59
Anti-fiber antibody detection assay 60
ELISA 60
Microbial flow cytometry 61
V4 16S rDNA sequencing 62
Statistics and Reproducibility 62
Chapter 3: Antibody-mediated interactions with gut microbes 64
Introduction: 65
Results: 68
Gut bacteria degrade antibodies through protease-dependent mechanisms 68
Human IgG does not broadly support bacterial growth under nitrogen-limited conditions 71
Anti-fiber antibodies modulate bacterial interactions with dietary glycans 79
Discussion: 85

Methods: **88**

Mouse sample collections (cecal contents) **88**

Antibody degradation assays **88**

Mouse cecal contents **88**

Bacterial culture supernatants **89**

Bacterial growth assays **90**

Blocking microbial adhesion **90**

Blocking glycan hydrolysis **91**

Bibliography: **92**

List of Figures and Tables

Chapter 2: Gut Bacteria Prime Host Antibody Responses Against Ingested Dietary Fiber Glycans 10

Fig. 1. Adults and children produce circulating anti-fiber IgM against dietary glycans 15

Fig. 2. Fiber supplementation induces circulating and secreted fiber-specific antibodies 20

Extended Data Fig. 1. Mice produce circulating anti-fiber IgG and IgA. 22

Extended Data Fig. 2. Induction of anti-psyllium antibodies does not require T cells. 24

Fig. 3. Microbes are required for the induction of anti-fiber antibodies 30

Extended Data Fig. 3. Absence of anti-fiber response in Germ-free mice. 32

Extended Data Fig. 4. Circulating response against psyllium in conventionally-raised Swiss Webster mice. 33

Extended Data Fig. 5. Germ-free husbandry conditions do not inhibit the induction of anti-psyllium antibodies. 35

Extended Data Fig. 6. Antibiotic treatment does not inhibit the induction of circulating anti-psyllium IgM. 37

Extended Data Fig. 7. Psyllium feeding alters gut microbiota composition. 38

Extended Data Fig. 8. Galactomannan feeding induces circulating anti-galactomannan IgM. 40

Extended Data Fig. 9. Diverse bacterial isolates are not sufficient for the induction of circulating anti-psyllium IgM. 42

Fig. 4. Mouse-derived communities of culturable isolates sensitize mice to psyllium 46

Extended Data Fig. 10. Culturable mouse microbiota enables germ-free mice to generate anti-psyllium antibodies. 48

Fig. 5. Plant glycans are detected on bacterial surfaces 52

Chapter 3: Antibody-mediated interactions with gut microbes 64

Figure 1. Gut bacterial communities degrade antibodies through protease-dependent mechanisms. 70

Figure 2. Human IgG does not support bacterial growth. 72

Table 1. Human IgG does not support bacterial growth 73

Table 2. Bacterial isolates using polygalacturonate (PPC) as a sole carbon source 81

Figure 3. Fiber-specific monoclonal antibodies inhibit bacterial adhesion but do not prevent glycan hydrolysis or bacterial growth 84

Abstract

ANTIBODIES, DIET, AND THE MICROBIOTA: BACTERIAL-DEPENDENT INDUCTION OF ANTI-FIBER ANTIBODIES AND HOW THEY INFLUENCE MICROBIAL BIOLOGY

Giovanni Vega

Gut microbes synthesize protein and glycan antigens that stimulate circulating and secreted antibody responses. Hosts are also continuously exposed to structurally diverse plant glycans through dietary fiber, yet whether these foreign glycans similarly stimulate antibody production remains unclear. This dissertation introduces dietary glycans as immunostimulatory structures by demonstrating the presence of antibodies that recognize dietary fiber. It further examines the prerequisites for the induction of anti-fiber antibodies and their potential effects on microbial interactions with dietary glycans.

The first chapter of this dissertation reviews T cell-dependent, T cell-independent, and natural-antibody responses to ingested antigens and the host consequences of glycan-specific antibodies.

The second chapter demonstrates the presence of circulating and secreted anti-fiber antibodies in humans and mice. Dietary supplementation experiments in mice showed that ingestion of individual fibers induced antibodies that preferentially recognized the supplemented fiber. These responses depended on microbial exposure, as germ-free mice and mice colonized with several minimal microbial communities failed to respond to dietary supplementation. By contrast, microbial communities containing bacteria that bound dietary glycans *in vivo* enabled antibody induction, suggesting a mechanism through which gut microbes sensitize the host to dietary fiber.

The third chapter explores functional interactions among antibodies, gut bacteria, and microbial metabolism. Gut microbial communities degraded mouse IgA and IgG through protease-dependent mechanisms yet purified human IgG did not broadly support the growth of bacterial isolates under nitrogen-limited conditions. In addition, glycan-specific antibodies

reduced bacterial adhesion to glycan-coated beads but did not inhibit glycan hydrolysis or bacterial growth under the conditions tested.

This work identifies an uncharacterized interaction among diet, the gut microbiota, and host immunity that may influence bacterial access to dietary nutrients in the intestinal environment.

Acknowledgements

The work accomplished in this dissertation would not have been possible without the love and support of many people throughout my Ph.D. journey.

First, I would like to thank Michael L. Patnode for his mentorship and guidance, and for providing me with an opportunity to grow as an independent scientist. I sincerely appreciate you giving me the opportunity to be one of the first students in your lab. I would like to thank the members of my Ph.D. committee, Victoria Auerbuch Stone and Rebecca DuBois, who have helped guide me through my project. I would also like to thank Brandt Warecki. Brandt, thank you for sparking my interest in science and allowing me to further explore this curiosity in the Sullivan lab. You taught me the foundational skills I have as a scientist that I have since passed on to my mentees, in the hope that I could do for them what you did for me.

Through this journey, I have not only grown as a scientist but as a person, and for that, I thank everyone mentioned here and all the people I do not have the chance to mention. Abdul Rahman Ibn Asadullah and Angel Pelayo, you are my friends who have stood the test of time. Abdul, the words I have for you cannot be expressed through writing. You have been there every step of the way with me, and it is safe to say that I would not be obtaining this doctoral degree without you, and for that, thank you. Angel, you have shown me countless times that you will always have a home for me. You are a caring person who is willing to help anyone with whatever is needed. Without you, I would not have Bubba in my life, who means the world to me, and for that, thank you.

Kyle Medina and Sophia Almendras, you have been my friends since our undergraduate years, and it makes me so happy that we are still in each other's lives. Kyle, your compassion, energy, and ability to empathize with other people make you a one-of-a-kind person. You have taught me how to grow emotionally and spiritually as a person, and for that, thank you. Choo, you have a passion for art that I have never seen in anyone else.

Although we don't see each other as much, you always find a way to paint the day a little brighter whenever you are around. You have taught me how to view the world with brighter colors, and for that, thank you.

Bo Huey Chiang, Adam Lentz, Christina Yang, Cristobal Morfin, Raymond Lopez, Khurshid Iranpur, and Ibette Valle, you have all made my Ph.D. journey one of the best experiences ever. Bo, you are my lab brother. You always made sure I never felt alone through this journey, and for that, thank you. Adam, you are the kindest soul ever who never fails to bring around a warm energy, and for that, thank you. Christina, you are my amazing partner, and you have gone above and beyond not only for me, but for all our friends. I have countless memories with you that always cheer me up whenever I feel down, and for that, thank you. Cris, your overall knowledge about the world will never stop amazing me. The facts you know are something I will never forget, and for that, thank you. Ray, you are one of the most independent people I have ever met and have given me an example of the person I want to become, and for that, thank you. Khurshid, you went from my mentee to my close friend. Exploring Hawaii with you was an experience that I will never forget, and for that, thank you. Ibette, you were one of the best housemates I ever had. I will always remember our late-night Fridays listening to new music and playing games all night long, and for that, thank you.

Zane Blake Groves, you are no longer with us, but your presence will remain with me forever. You would make every achievement, no matter the size, feel like the biggest accomplishment anyone has ever achieved. For teaching me that all wins should be celebrated and for countless other things, thank you.

Finally, I would like to thank my family. They have always been there for me and given me a reason to continue with this journey. Jackie Vega and Lizette Vega, thank you for always making time to hang out with me whenever I visited home. I would always look forward to seeing you and telling you all about my progress and listening to everything you have also accomplished. My mom, Lucia Vega Uriostegui, is one of the most humble yet

inspiring people ever. She has sacrificed so much for my sisters and me to have the lives we live. We would, undoubtedly, not be where we are today without her. Everything I have accomplished is for you, and I hope it makes you proud.

Ama, todo esto es para ti, te quiero mucho y gracias por todo lo que hiciste por mis hermanas y por mí.

Chapter 2 is a preprint titled “Gut Bacteria Prime Host Antibody Responses Against Ingested Dietary Fiber Glycans,” which was posted on bioRxiv in August 2026. I planned and designed the experiments with Michael L. Patnode, conducted experiments with assistance from the coauthors, analyzed the data, and prepared all the figures. I also wrote and edited the manuscript with Michael L. Patnode and assistance from the other coauthors. Michael L. Patnode directed and supervised the research that forms this chapter.

A portion of the introduction to Chapter 3 was adapted from the review “Bacterial interactions on nutrient-rich surfaces in the gut lumen,” by Bo Huey Chiang, Giovanni Vega, Sarah C. Dunwoody, and Michael L. Patnode, published in *Infection and Immunity* in 2024 (doi: 10.1128/iai.00480-23). The adapted text was written by me.

.

Chapter 1: Antibody Production in Response to Ingested Antigens

Giovanni Vega[1,2] and Michael L. Patnode[1,*]

[1] Department of Microbiology and Environmental Toxicology, University of California, Santa Cruz, Santa Cruz, CA, 95064 USA.

[2] Graduate Program in Biological Sciences and Engineering, University of California, Santa Cruz, Santa Cruz, CA, 95064 USA.

* Correspondence: mpatnode@ucsc.edu

Introduction:

The gastrointestinal tract is continuously exposed to protein and carbohydrate antigens derived from the host diet and the microbiota. Protein antigens commonly induce T cell-dependent (TD) responses, while repetitive carbohydrate structures can cross-link B cell receptors and stimulate T cell-independent (TI) responses (Noelle and Snow, 1990; Allman et al. 2019; Kappler and Hennet, 2020). However, carbohydrates conjugated to carrier proteins or associated with other immunogenic structures can recruit T cell help and induce TD responses (Kappler and Hennet, 2020).

Some antibodies that recognize carbohydrates are present prior to exposure with the recognized antigen and are referred to as natural antibodies (NAbs) (Holodick et al. 2017; Palma et al. 2018). Although many NAbs participate in TI immune responses, NAbs and TI antibodies are not synonymous. In this review, we explore antibodies produced against orally encountered antigens, with a focus on TI and natural antibodies that recognize carbohydrates and their effects on the host.

Antibody diversification and effector function:

Following activation, B cells can alter the affinity and effector functions of the antibodies they produce through somatic hypermutation (SHM) and class-switch recombination (CSR). During affinity maturation, SHM introduces mutations into the variable regions of antibody genes. B cells that produce antibodies with increased affinity for an antigen can then be preferentially selected and expanded (Mishra and Mariuzza, 2018). Selected B cells can differentiate into antibody-secreting plasma cells or memory B cells, allowing the host to maintain antigen-specific antibodies and respond more rapidly during subsequent antigen exposures (Kurosaki et al. 2010).

Early antibody responses commonly produce IgM, which remains the predominant isotype in many TI and natural-antibody responses (Allman et al. 2019; Holodick et al. 2017).

B cells can also undergo CSR, which changes the antibody isotype without changing the antigen recognized by the antibody. Unlike SHM, which alters the variable region, CSR changes the antibody constant region and its resulting effector functions (Stavnezer et al. 2008). Signals delivered through CD40/CD40L, T cell-derived cytokines, and innate immune pathways can promote CSR and influence the antibody isotype that is produced (Cerutti, 2008; He et al. 2007; McAdam et al. 2001; Stavnezer et al. 2008). For example, IgG can mediate systemic immune functions, while IgA can be transported across mucosal surfaces and released into the intestinal lumen (Cerutti, 2008).

T cell-dependent antibody generation:

After binding a protein antigen, B cells can internalize and process it before displaying peptide fragments on major histocompatibility complex class II molecules. Recognition of the peptide-MHC class II complex allows helper T cells to provide CD40L and cytokine signals that support B cell activation, proliferation, and entry into germinal centers (McAdam et al. 2001; Noelle and Snow, 1990; Stavnezer et al. 2008). Early mouse studies helped establish the importance of T cells in TD responses, as mice lacking a functional thymus exhibited impaired antibody production because they could not generate the mature T cells needed to activate B cells (Noelle and Snow, 1990; Vinuesa and Chang, 2013).

Oral exposure to protein antigens can result in antigen-specific systemic and mucosal antibodies. In one study, infants with food intolerance had elevated antigen-specific IgA and IgG against ovalbumin, soy, or cow's milk proteins compared with control infants, while IgM did not differ between the groups (McDonald et al. 1984). In a separate human study, ingestion of capsules containing killed *Streptococcus mutans* induced circulating anti-*S. mutans* IgA-producing cells that were proposed to migrate to mucosal tissues and contribute to secretory IgA production (Czerkinsky et al. 1987). TD responses against orally administered antigens have also been examined using hapten 4-hydroxy-3-nitrophenylacetyl

conjugated to the protein carrier cholera toxin (NP-CT). Repeated oral exposure with NP-CT induced antigen-specific IgA in the serum and small intestine of mice. Analysis of NP-specific IgA-producing B cells showed that the response was affinity matured, with related B cell clones detected across multiple Peyer's patches (Bergqvist et al. 2013). Together, these studies demonstrate that oral ingestion can induce systemic and mucosal antibody responses.

T cell-independent antibody generation:

Unlike TD responses, TI responses do not require B cells to present peptides to cognate helper T cells. TI responses can be divided into type 1 (TI-1) and type 2 (TI-2) responses based on the antigen. TI-1 antigens activate B cells through innate immune receptors in addition to the B cell receptor, with bacterial LPS acting through TLR4 as a common example. In contrast, TI-2 antigens contain repetitive epitopes that extensively cross-link B cell receptors. Bacterial capsular polysaccharides commonly act as TI-2 antigens because their carbohydrate epitopes are repeatedly displayed across the bacterial surface (Allman et al. 2019; Kappler and Hennet, 2020).

B1 and marginal-zone B cells are major contributors to TI responses, although the participating B cell population depends on the antigen and anatomical site. B1 cells are established early in development and differ from conventional follicular B2 cells (Hayakawa and Hardy, 2000; Martin and Kearney, 2001). B1 cells are further divided into B1a and B1b populations based partly on CD5 expression. B1a cells are generally CD5-positive and are major contributors to steady-state NAb production, whereas CD5-negative B1b cells can expand following exposure to microbial polysaccharides and contribute to induced TI responses (Martin and Kearney, 2001; Holodick et al. 2017; Marshall et al. 2012). Immunization of mice with the Vi capsular polysaccharide from *Salmonella* Typhi induced B1b cell proliferation and Vi-specific antibody-secreting cells. These responses were retained

in mice lacking T cells, supporting the classification of Vi as a TI antigen (Marshall et al. 2012). Marginal-zone B cells are classified as B2 cells, can also respond rapidly to repetitive antigens, and are important for responses against blood-borne bacterial polysaccharides (Martin et al. 2001; He et al. 2007; Macpherson et al. 2000).

B cell populations and antibody repertoires continue to develop after birth, and infants generally respond less effectively to unconjugated polysaccharides than older children and adults (Basha et al. 2014; Wilson and Kollmann, 2008). For example, responses against capsular polysaccharides from *Haemophilus influenzae* type b and *Streptococcus pneumoniae* are limited in young children (Wilson and Kollmann, 2008). Linking a polysaccharide to a protein carrier, however, can overcome this limitation. A carbohydrate-specific B cell recognizes the polysaccharide portion of the conjugate, internalizes the complete structure, and presents peptides from the carrier protein to a helper T cell. This interaction allows the B cell to receive T cell help and generate a response with increased class switching and memory (Kappler and Hennet, 2020).

Although TI responses are commonly dominated by IgM, they are not restricted to this isotype. B cell receptor engagement can act together with innate signals and cytokines to promote B cell proliferation, plasma cell differentiation, and CSR. CD40- and CD40L-deficient mice retained antibody responses against TI antigens, demonstrating that antibody production and isotype switching can occur without conventional CD40-mediated T cell help (Kawabe et al. 1994; Renshaw et al. 1994). At mucosal surfaces, microbial products can stimulate intestinal epithelial and innate immune cells to produce APRIL and BAFF. These cytokines act through receptors that include transmembrane activator and CAML interactor (TACI) to promote B cell survival, differentiation, and class switching to IgA or IgG (Castigli et al. 2005; He et al. 2010). In addition, intestinal bacteria can induce epithelial production of APRIL and support TI switching to IgA in human B cells (He et al. 2007).

TI responses have traditionally been associated with less affinity maturation and memory than conventional TD responses. However, some anti-carbohydrate responses

generate persistent B cell populations and enhanced responses following antigen re-exposure. Following exposure with *Enterobacter cloacae* expressing α-1,3-dextran, marginal-zone B cells contributed to the initial production of dextran-specific antibodies, while dextran-specific B1b cells expanded and produced an increased response following bacterial re-exposure (Foote and Kearney, 2009). TI-2 immunization has also generated antigen-experienced B cells that persisted after the primary response and responded to subsequent antigen exposure (Obukhanych and Nussenzweig, 2006). These findings do not establish that TI responses generate memory equivalent to conventional TD memory. Instead, they show that some carbohydrate antigens generate persistent or memory-like B cell populations whose characteristics depend on the antigen, responding B cell subset, and signals present during activation (Allman et al. 2019; Zubler, 2001).

Natural antibodies against carbohydrates:

TI and natural antibodies are related but describe different features of an antibody response. TI refers to how a B cell is activated, whereas natural refers to the presence of an antibody before exposure with the recognized antigen. NAbs frequently contain germline-encoded or minimally mutated variable regions and can exhibit relatively low affinity and polyreactive binding (Holodick et al. 2017; Palma et al. 2018). This polyreactivity allows a single antibody to recognize multiple related or unrelated structures. B1a cells are major producers of steady-state NAbs, although marginal-zone and other B cell populations can also contribute (Holodick et al. 2017; Palma et al. 2018).

The B1 cell repertoire develops early in life and reflects both developmental programming and environmental exposure. B1 cells mainly originate during fetal development and are maintained throughout adulthood (Hayakawa and Hardy, 2000; Wong et al. 2019). These developmental processes establish B cell clones capable of recognizing particular structures, while subsequent antigen exposure can select or expand those clones. For

example, neonatal exposure to commensal bacterial antigens promoted the selection and expansion of B1 cells recognizing N-acetylglucosamine (New et al. 2020). Therefore, one way to influence an antibody's abundance is through microbial exposure.

Another study identified NAbs from BALB/c mice that recognized 3-fucosyllactosamine, levan, and dextran (Kimura et al. 1989). To examine the effects of exogenous antigen exposure, another study compared conventionally raised mice with germ-free mice maintained on a chemically defined, ultrafiltered diet. Germ-free mice had lower levels of antibodies against levan and dextran than conventionally raised mice, suggesting that microbial or environmental exposure expanded these antibody populations. In contrast, anti-3-fucosyllactosamine levels were comparable between the groups, indicating that this reactivity developed under conditions of limited exogenous antigen exposure (Bos et al. 1989). However, the persistence of anti-3-fucosyllactosamine antibodies does not establish that exposure to all structurally related antigens was absent.

Humans also produce antibodies against diverse carbohydrate structures. One prominent example is the natural anti-Gal antibody, which recognizes the α-Gal epitope (Galα1-3Galβ1-4GlcNAc-R). Anti-Gal antibodies can interact with related carbohydrate structures expressed by members of the human microbiota, providing a potential mechanism through which microbial exposure influences their abundance (Galili et al. 1988). Glycan-array studies have also identified circulating IgM, IgG, and IgA antibodies that recognize a broad range of carbohydrate structures in human serum (Bovin et al. 2012; Huflejt et al. 2009). Human sera also contain IgM and IgG antibodies against N-acetylglucosaminyl-N-acetylmuramyl dipeptide, a component of the bacterial cell wall (Pinegin et al. 1995). However, detecting an anti-carbohydrate antibody in healthy serum does not establish whether it was present before exposure or induced by microbes.

Host consequences of glycan-specific antibody production:

Whether generated through TD, TI, or natural-antibody pathways, glycan-specific antibodies can influence how the host responds to microbes displaying these glycans on their surface. The pentameric structure of IgM allows it to bind multiple copies of a repetitive carbohydrate epitope simultaneously. Antigen-bound IgM can activate the classical complement pathway and promote complement deposition on the recognized surface. Antibodies can also agglutinate microbes, promote their uptake by phagocytic cells, and block microbial attachment to host tissues. These functions allow pre-existing NAbs and rapidly induced TI antibodies to provide protection before a conventional TD response has fully developed.

Antibodies against bacterial capsular polysaccharides provide a direct example of protection mediated by anti-carbohydrate antibodies. Vi-specific antibodies derived from B1b cells were sufficient to protect mice against bacteria expressing the Vi antigen (Marshall et al. 2012). Antibodies against capsular polysaccharides from Haemophilus influenzae type b and Streptococcus pneumoniae can also protect against invasive infection, forming the basis for vaccines targeting these carbohydrates (Wilson and Kollmann, 2008).

Antibodies at mucosal surfaces can regulate microbes without directly killing them. Secretory IgA can bind microbial surface antigens and limit contact between bound microbes and the intestinal epithelium through a process known as immune exclusion. Depending on the microbe and antibody specificity, IgA binding can also affect microbial localization, colonization, and gene expression within the intestine (Mantis et al. 2011, Harris et al. 2006, Corthésy 2013, and Joglekar et al. 2019). These functions allow antibodies to regulate microbes while limiting immune activation at the intestinal surface.

Conclusion:

Antibodies against orally encountered antigens can be generated through several pathways. Protein antigens commonly induce TD responses, while repetitive carbohydrates can activate

B cells through TI mechanisms. Natural antibodies provide an additional source of carbohydrate recognition that is present before deliberate immunization, although the abundance and composition of these antibodies can still be influenced by microbial exposure. Together, these pathways generate antibodies against dietary proteins and carbohydrate structures expressed by commensal microbes and pathogens.

Anti-carbohydrate antibodies can protect against infection and regulate interactions between intestinal bacteria and the host. However, most studies have focused on antibodies against microbial glycans, and considerably less is known about responses to dietary carbohydrates. Understanding how dietary glycans induce antibodies and how these antibodies affect the intestinal environment will help define another way in which diet, the microbiota, and the immune system interact.

Chapter 2: Gut Bacteria Prime Host Antibody Responses Against Ingested Dietary Fiber Glycans

Giovanni Vega[1,2], Carolina Agudelo[3], Meghan E. Graham[1], Elyza A. Do[4], Jasmin Akter[5], Rashidul Haque[5], Nicolette Hernandez-Kaempf[1], Khurshid R. Iranpur[1,2], Abigail Renfro[1], Ansel Hsiao[4], Ashley R. Wolf[3], and Michael L. Patnode[1,*]

[1] Department of Microbiology and Environmental Toxicology, University of California, Santa Cruz, Santa Cruz, CA, 95064 USA.

[2] Graduate Program in Biological Sciences and Engineering, University of California, Santa Cruz, Santa Cruz, CA, 95064 USA.

[3] Division of Infectious Diseases and Vaccinology, School of Public Health, University of California, Berkeley, Berkeley, CA, 94720, USA; Center for Computational Biology, University of California, Berkeley, Berkeley, CA, 94720, USA.

[4]Department of Microbiology and Plant Pathology, University of California, Riverside, Riverside, CA, 92521, USA.

[5]International Centre for Diarrhoeal Disease Research, Bangladesh (icddr,b); Dhaka, Bangladesh

* Correspondence: mpatnode@ucsc.edu

Abstract:

Protein and glycan antigens synthesized by gut microbes stimulate circulating and secreted antibody production. Despite continuous exposure of hosts to the plant glycans that constitute dietary fiber, it remains unclear whether these foreign structures induce mucosal immune responses. We report that humans and mice generate antibodies specific for common glycans in plant foods. Oral exposure to individual fiber types induced T cell-independent, glycan-specific IgM and IgA. The induction of anti-fiber antibodies required colonization by particular microbes, since germ-free mice and mice harboring representatives of several bacterial phyla failed to respond. The OMM12 model community was sufficient to rescue antibody induction, and dietary fiber glycans were detected on the surfaces of OMM12 microbes, suggesting a route by which bacteria trigger anti-fiber immune responses. Our results reveal a direct impact of dietary fiber on the adaptive immune system with implications for host control of fiber breakdown by bacteria in the gut lumen.

Introduction:

Dietary fiber is an abundant component of nearly all mammalian diets and is composed of ingested carbohydrates that are not susceptible to degradation by host enzymes. In typical human diets, fiber is composed primarily of high molecular weight plant cell wall polysaccharides, which serve as the major energy and carbon source for the most abundant gut bacterial taxa (Flint et al. 2012). Mechanisms by which the host can modulate microbial metabolism may provide evolutionary advantages (Miller and Bäumler 2021; Rivera-Chávez et al. 2016), yet it is unclear whether, or how, microbial access to carbohydrates in the gut lumen is subject to host control. Although plant cell wall polysaccharides have not previously been considered immunogenic in their ingested forms, antibodies targeting these glycans could have an outsized impact on microbial food webs in the gut. Immune responses against microbial polysaccharides are crucial for host protection and form the basis of several

existing vaccines (Astronomo and Burton 2010; Finn 2004). Antibodies against capsular polysaccharides and lipopolysaccharides are typically produced through a T cell-independent pathway that results in strong IgM responses (Allman et al. 2019; Wortis et al. 1995). Additionally, association of these glycans with intact bacteria or a carrier protein can lead to an enhanced response, including long-term immunity and antibody class-switching (Snapper 2016; Pollard et al. 2009).

Gut bacteria bind with high affinity and specificity to dietary fiber glycans (Patnode et al. 2021), raising the possibility that microbial cell surfaces might be coated with fiber glycans *in vivo* and that these bacteria initiate bystander immune responses against plant polysaccharides. We reasoned that fiber glycans have the potential to trigger antibody responses in mammals because they are (i) physically associated with bacteria that can induce co-stimulation of B cells via innate immune receptors, (ii) abundant in the intestinal lumen offering the chance for repeated exposure throughout life, and (iii) distinct from host glycans suggesting that circulating naive B cell clones might recognize these non-self structures. Here, we employed screening approaches using glycan coated beads (Patnode et al. 2019) and detected antibodies specific for dietary fiber produced during steady state in humans and mice. We found that dietary fiber supplementation regimens modulate anti-fiber antibodies on short timescales. Gnotobiotic mice colonized with individual strains, model consortia, and microbial communities of native complexity revealed that exposure to specific microbes is required to sensitize mice to dietary fiber. Together, these results uncover a new class of immune responses directed against diet and raise the prospect of an inducible mode of host control over fiber-degrading bacteria in the gut.

Results:

Humans produce circulating IgM and secreted IgA specific for dietary fiber glycans

To determine whether humans produce antibodies that recognize dietary fiber glycans, we measured IgM reactivity in serum samples from adults (n=17, 20-41 years old) and their children (n=19, 3-4 years old) at two timepoints one week apart **(Fig. 1a)**. We used multi-color flow cytometry to analyze a pooled library of microscopic magnetic beads coated with distinct glycan preparations representing the major classes of plant cell wall polysaccharides and tagged with unique fluorescent barcodes (Patnode et al. 2021). Each glycan preparation has been characterized by mass spectrometry with respect to monosaccharide composition and glycosidic linkages present (Patnode et al. 2021). This screen revealed significant IgM binding to 30 bead types, including those coated with plant polysaccharides commonly found in human diets such as cell wall hemicelluloses (xylans and galactomannans) and multiple components of pectins **(Fig. 1b and Table S1a)**. Serum collected from the same donors one week apart showed that many anti-fiber IgM profiles were consistent **(Table S1a)**, including 15 fiber types displaying strong correlations between the two timepoints across donors (Spearman's rho > 0.7, **Fig. 1b and Table S1a**). IgM reactivity was higher in children compared to adults for 6 out of the 56 bead types in the library, despite the generally observed increase in IgM levels with increasing age (Bayram et al. 2019; Jazayeri et al. 2013). We did not observe significant correlations between the antibody profiles of mothers and their own children, with samples instead clustering by age group. Based on the known correspondence between IgA specificity in breast milk and at other mucosal sites including the intestine (Usami et al. 2021; Bourges et al. 2008), we tested pooled human colostrum and observed IgA binding to arabinogalactan A, galactan, oat-beta glucan, psyllium, and rhamnogalacturonan K **(Fig. 1c and Table S1b)**. These data demonstrate that humans produce circulating fiber-specific IgM under steady state conditions and also secrete anti-fiber IgA (sIgA) with similar glycan specificities.

Fig. 1. Adults and children produce circulating anti-fiber IgM against dietary glycans

(a) Schematic illustrating serum collected from mother-child pairs at two timepoints (one week apart). Serum was screened by flow cytometry for circulating anti-fiber IgM using a library of magnetic beads coated with 56 distinct glycan preparations. (b) Heatmap showing human serum IgM binding to glycan-coated beads (blue to red color scale). The plotted values show the average signal of week 0 and week 1 collections (black *, Paired t test, $q < 0.1$, FC >= 1.5 at both timepoints versus empty beads; green *, Student's t test, $q < 0.05$, FC >= 1.25 at both timepoints between adults and children). The rows represent individual donors and samples are clustered (Ward's minimum variance) by binding profile (rightmost column indicates sample age group; adults, white; children, green). The bottom row (white to pink color scale) shows Spearman's correlations between the two timepoints. (c) Human colostrum was tested for the presence of anti-fiber IgA using the glycan-coated bead library. The row represents the average of 3 technical replicates. Heatmap values are corrected by subtracting the average of 3 secondary-only controls and the average of 2 empty bead populations.

Fig. 1

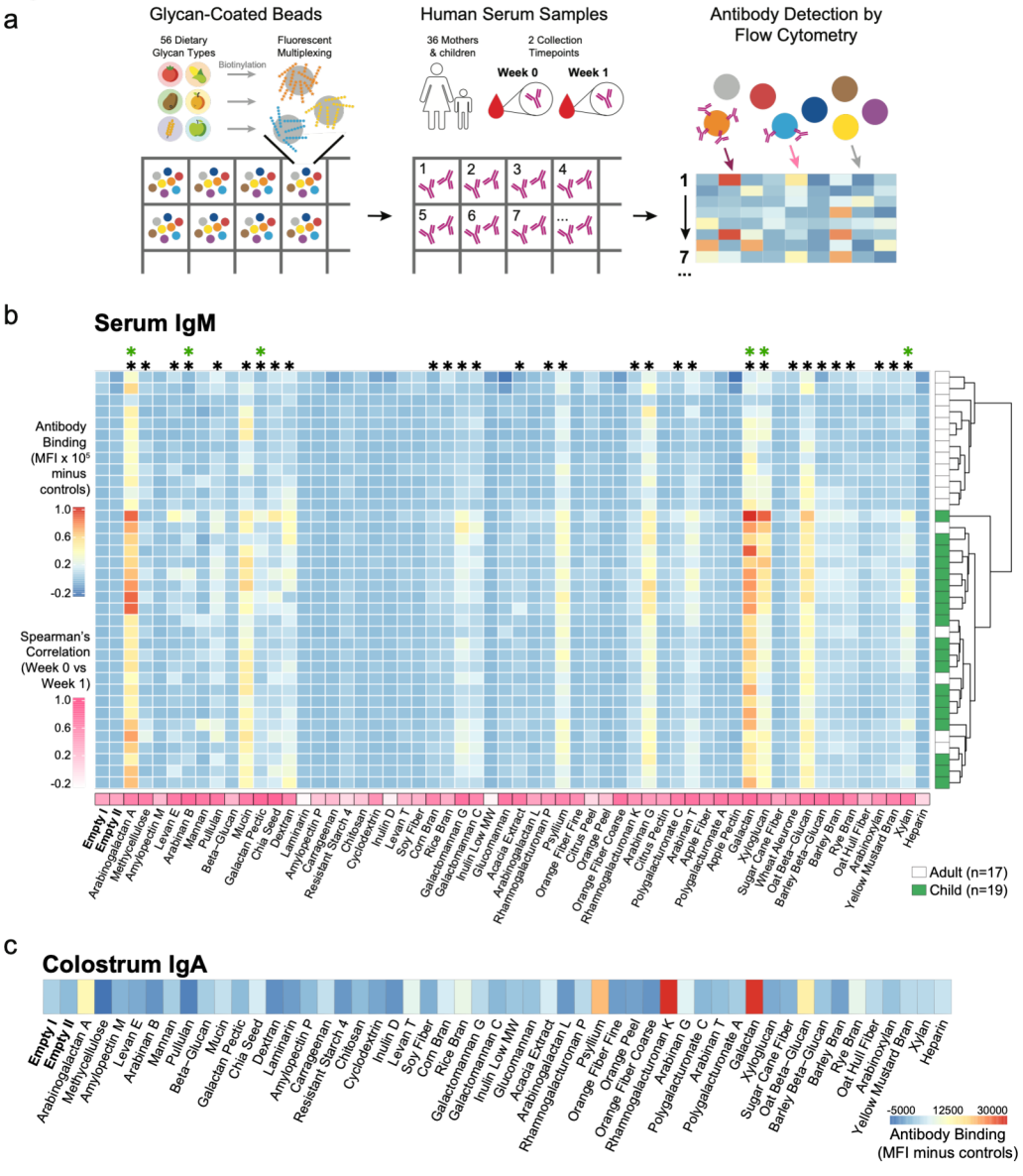
a
Glycan-Coated Beads
56 Dietary Glycan Types
Biotinylation
Fluorescent Multiplexing
Human Serum Samples
36 Mothers & children
2 Collection Timepoints
Week 0
Week 1
Antibody Detection by Flow Cytometry
b
Serum IgM
Antibody Binding (MFI x 10^5 minus controls)
Spearman's Correlation (Week 0 vs Week 1)
Adult (n=17)
Child (n=19)
c
Colostrum IgA
Antibody Binding (MFI minus controls)

Ingestion of fiber induces glycan-specific anti-fiber IgM and IgA

To determine whether oral exposure to dietary fiber influences the levels of fiber-specific antibodies, we compared circulating anti-fiber antibodies in C57BL/6 mice bred for four generations on either a standard mouse chow control diet or a diet with low levels of microbially accessible fibers ("low fiber diet"). The low fiber diet led to significantly lower circulating IgM reactivity against plant glycans including arabinans and xylans **(Fig. 2a and Table S2a)**, which are ubiquitous cell wall polysaccharides that are present in the corn and wheat ingredients in standard mouse chow. Mouse IgM reactivity was similar to that observed in humans **(Fig. 1b)**, consistent with the abundance of these structures in both mouse and human diets. Serum IgG and IgA bound a small and distinct set of bead types, and only the binding to levan and porcine mucin were significantly reduced in the low fiber diet group **(Extended Data Fig. 1a-b and Table S3a-b)**. Together, these data indicate that consumption of a diet containing abundant fiber induces antibody responses against a broad range of plant polysaccharides.

The observed dependence of anti-fiber antibodies on diet suggested that exposure to a variety of diverse plant polysaccharides was responsible for distinct antibody responses. However, this could alternatively indicate the presence of polyreactive antibodies that broadly recognize many unrelated glycan structures. To determine whether antibody responses to fiber are glycan-specific, we fed C57BL/6 mice food-grade psyllium husk, which contains a beta-1,4-xylose backbone densely substituted with xylose and arabinose side chains variably capped with terminal galacturonic acid. Psyllium was selected because (i) it is one of the fiber supplements most commonly consumed by humans (Martellet et al. 2022; Mysonhimer and Holscher 2022; Llewellyn et al. 2018), (ii) anti-psyllium IgM exhibited a large fold-change in mice fed a control versus low fiber diet **(Fig. 2a)**, and (iii) humans produce anti-psyllium IgM and IgA **(Fig. 1b-c)**. Mice were maintained for 12 days on either a control mouse chow diet or that same diet supplemented with 9.2% w/w psyllium, followed by administration of a low fiber

diet for 5 days to limit sequestration of secreted anti-psyllium IgA by structurally similar xylans in normal chow **(Fig. 2b)**. No difference in mouse weight was observed between the two groups during feeding **(Fig. 2c)**. Circulating anti-psyllium IgM in mice fed a psyllium diet was 3-fold higher than in the control group **(Fig. 2d-e and Table S2b)**. Higher levels of antibodies targeting rhamnogalacturonan from karaya (2.4-fold) were detected in these mice, potentially reflecting the glycan epitopes that this fiber shares with psyllium (Patnode et al. 2021). The antibodies induced by psyllium supplementation were notably glycan-specific, as there was no detectable increase for fiber types with only subtle differences from psyllium in glycan structure (more sparsely substituted wheat arabinoxylan and beechwood xylan) and the highest signal for other unrelated fiber types was 7.1-fold lower than for psyllium. Measurement of anti-psyllium IgM by ELISA produced similar results, with mice eating a psyllium diet exhibiting 3.5-fold higher levels than control animals **(Fig. 2f)**. Total serum IgM in the two diet groups was comparable **(Fig. 2g)**, indicating that the anti-psyllium IgM induction reflects a change in antibody repertoire rather than a broad increase in IgM abundance.

Antibodies that recognize glycans and other non-protein antigens are commonly produced via T cell-independent pathways (Allman et al. 2019; Wortis et al. 1995). To determine whether the induction of fiber-specific antibodies is dependent on T cells, we fed C57BL/6 wild-type and *Tcrb*$^{-/-}$*Tcrd*$^{-/-}$ mice psyllium for 12 days followed by a low fiber diet for 5 days, as above. Two days prior to fiber feeding, all groups of mice exhibited comparable circulating anti-fiber IgM profiles, with the exception of reactivity against coarse orange fiber, arabinan G, and arabinan T, which were elevated in T cell-deficient mice **(Extended Data Fig. 2a-b and Table S4a)**. Upon psyllium feeding, both wild-type and T cell-deficient mice exhibited a >2-fold increase in circulating anti-psyllium IgM **(Fig. 2h, Extended Data Fig. 2c-d, and Table S4b)**, indicating that T cell help is not required for the induction of circulating anti-psyllium IgM.

The oral route of host exposure to dietary fiber led us to ask whether a secreted IgA response accompanies the circulating IgM response against ingested plant glycans. Mice fed psyllium produced 2.6-fold higher levels of anti-psyllium IgA in cecal contents compared to mice eating the control diet, as measured by flow cytometry **(Fig. 2i-j and Table S2c)**. These mice also exhibited higher levels of anti-galactan IgA, but the limited galactose detected in psyllium glycans (Patnode et al. 2021) suggests that this represents a response to a microbial or alternate dietary antigen. ELISA confirmed the induction of anti-psyllium IgA in mice fed psyllium (9.3-fold induction; **Fig. 2k**). Psyllium did not increase total secreted IgA levels **(Fig. 2l)** and induction of anti-psyllium IgA was T cell-independent (4.2-fold increase in wild-type mice and 5-fold increase in *Tcrb*$^{-/-}$ *Tcrd*$^{-/-}$ mice) **(Fig. 2m)**. Taken together, these results demonstrate that ingestion of dietary fiber stimulates the production of circulating anti-fiber IgM and secreted anti-fiber IgA independent of T cell help.

Fig. 2. Fiber supplementation induces circulating and secreted fiber-specific antibodies

(a) Anti-fiber IgM was measured in serum from C57BL/6 mice eating normal chow (2920X, Envigo) or a low fiber diet (TD.130343, Envigo) by flow cytometry using a glycan-coated bead library. Each row shows the average of 7-8 mice. Results are representative of 2 independent experiments. (b) Schematic illustrating C57BL/6 mice fed a control or 9.2% w/w psyllium-supplemented diet for 12 days followed by a low fiber diet for 5 days. Brackets depict dietary fiber in the cecal contents sequestering anti-fiber antibodies and blocking their detection. Cecal contents and serum were collected on day 17. (c) Mouse weights throughout a representative feeding experiment. (d) Anti-fiber IgM in serum on day 17. Each row represents the average of 5 mice. (e) Individual values for anti-psyllium IgM in serum on day 17. (f) ELISA for anti-psyllium IgM in serum on day 17 (Student's t test, ***$p < 0.001$). (g) Quantification of total serum IgM on day 17. Results for (c - g) are representative of >3 independent experiments. (h) Anti-psyllium IgM in serum from wild-type or *Tcrb*$^{-/-}$*Tcrd*$^{-/-}$ C57BL/6 mice on day 17 of the experimental feeding protocol shown in b (Student's t test, ***$p < 0.001$ and ****$p < 0.0001$). Results are representative of 3 independent experiments. (i) Anti-fiber IgA in cecal contents on day 17. Each row represets the average of 5 mice. (j) Individual values for anti-psyllium IgA in cecal contents on day 17. (k) ELISA for anti-psyllium IgA in cecal contents on day 17 (Student's t test, ****$p < 0.0001$). (l) Quantification of total cecal IgA on day 17. Results for (i-l) are representative of 3 independent experiments. (m) Anti-psyllium IgA in cecal contents from wild-type or *Tcrb*$^{-/-}$*Tcrd*$^{-/-}$ C57BL/6 mice on day 17 of the experimental feeding protocol shown in B (Student's t test, *$p < 0.05$ and **$p < 0.01$). Results are representative of 3 independent experiments. For heatmaps, the plotted values are normalized by subtracting the average of 3 secondary-only controls. When linear values are shown (a and d), the average of 2 empty bead populations are subtracted (*, Student's t test, $q < 0.05$, FC >= 1.5). (i) The plotted values are normalized by subtracting the average of 3 secondary-only controls and log2 transformed (*, Student's t test and $q < 0.05$). (e and j) * $q < 0.05$ and ** $q < 0.01$. Dotted lines, background signal (average of 3 secondary-only controls); bars, mean + SD.

Fig. 2

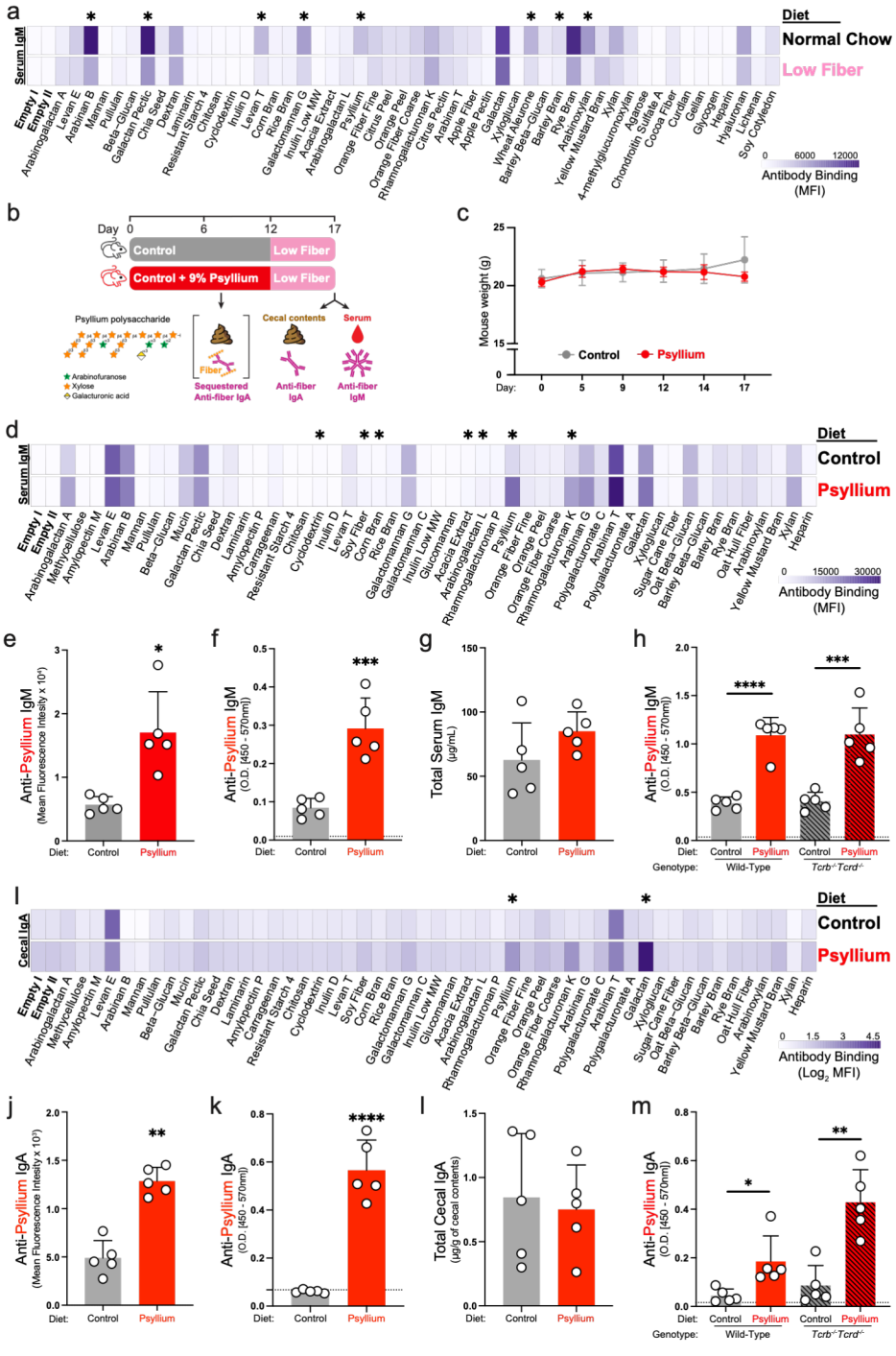
a
Diet
Normal Chow
Low Fiber
Serum IgM
Antibody Binding (MFI)
b
Day 0 6 12 17
Control
Control + 9% Psyllium
Low Fiber
Psyllium polysaccharide
Arabinofuranose
Xylose
Galacturonic acid
Fiber
Cecal contents
Serum
Sequestered Anti-fiber IgA
Anti-fiber IgA
Anti-fiber IgM
c
Mouse weight (g)
Control
Psyllium
Day:
d
Diet
Control
Psyllium
Serum IgM
Antibody Binding (MFI)
e
Anti-Psyllium IgM
(Mean Fluorescence Intesity x 10³)
f
Anti-Psyllium IgM
(O.D. [450 - 570nm])
g
Total Serum IgM
(µg/mL)
h
Anti-Psyllium IgM
(O.D. [450 - 570nm])
Genotype:
Wild-Type
Tcrb⁻/⁻Tcrd⁻/⁻
i
Diet
Control
Psyllium
Cecal IgA
Antibody Binding (Log₂ MFI)
j
Anti-Psyllium IgA
(Mean Fluorescence Intesity x 10³)
k
Anti-Psyllium IgA
(O.D. [450 - 570nm])
l
Total Cecal IgA
(µg/g of cecal contents)
m
Anti-Psyllium IgA
(O.D. [450 - 570nm])

Extended Data Fig. 1. Mice produce circulating anti-fiber IgG and IgA.

(a and b) Anti-fiber IgG (a) and IgA (b) was measured in serum from C57BL/6 mice eating normal chow or a low fiber diet by flow cytometry using a glycan-coated bead library. Each row shows the average of 7-8 mice. Results are representative of 2 independent experiments. Heatmap values are corrected by subtracting the average of 3 secondary-only controls and the average of 2 empty bead populations (*, Student's t test, $q < 0.05$, FC >= 1.5).


a
Diet
Normal Chow
Low Fiber
0
1500
3000
Antibody Binding (MFI)
Serum IgG
*
Empty I
Empty II
Arabinogalactan A
Methylcellulose
Amylopectin M
Levan E
Arabinan B
Mannan
Pullulan
Beta-Glucan
Mucin
Galactan Pectic
Chia Seed
Dextran
Laminarin
Amylopectin P
Carrageenan
Resistant Starch 4
Chitosan
Cyclodextrin
Inulin D
Levan T
Soy Fiber
Corn Bran
Rice Bran
Galactomannan G
Galactomannan C
Inulin Low MW
Glucomannan
Acacia Extract
Arabinogalactan L
Rhamnogalactouronan P
Psyllium
Orange Fiber Fine
Citrus Peel
Orange Fiber Coarse
Rhamnogalactouronan K
Arabinan G
Citrus Pectin
Polygalacturonate C
Arabinan T
Apple Fiber
Polygalacturonate A
Apple Pectin
Galactan
Xyloglucan
Sugar Cane Fiber
Wheat Aleurone
Oat Beta-Glucan
Barley Beta-Glucan
Barley Bran
Rye Bran
Oat Hull Fiber
Arabinoxylan
Yellow Mustard Bran
Xylan
Heparin
b
Diet
Normal Chow
Low Fiber
0
7000
14000
Antibody Binding (MFI)
Serum IgA
*
Empty I
Empty II
Arabinogalactan A
Methylcellulose
Amylopectin M
Levan E
Arabinan B
Mannan
Pullulan
Beta-Glucan
Mucin
Galactan Pectic
Chia Seed
Dextran
Laminarin
Amylopectin P
Carrageenan
Resistant Starch 4
Chitosan
Cyclodextrin
Inulin D
Levan T
Soy Fiber
Corn Bran
Rice Bran
Galactomannan G
Galactomannan C
Inulin Low MW
Glucomannan
Acacia Extract
Arabinogalactan L
Rhamnogalactouronan P
Psyllium
Orange Fiber Fine
Citrus Peel
Orange Fiber Coarse
Rhamnogalactouronan K
Arabinan G
Citrus Pectin
Polygalacturonate C
Arabinan T
Apple Fiber
Polygalacturonate A
Apple Pectin
Galactan
Xyloglucan
Sugar Cane Fiber
Wheat Aleurone
Oat Beta-Glucan
Barley Beta-Glucan
Barley Bran
Rye Bran
Oat Hull Fiber
Arabinoxylan
Yellow Mustard Bran
Xylan
Heparin

Extended Data Fig. 2. Induction of anti-psyllium antibodies does not require T cells.

(a) Serum from wild-type or *Tcrb*$^{-/-}$*Tcrd*$^{+/-}$ C57BL/6 mice collected fed normal chow (day -2) was tested using a glycan-coated bead library to measure baseline anti-fiber IgM differences (*, Student's t test, q < 0.05, FC >= 1.5). Each row shows the average of 15 mice. (b) Individual values for anti-psyllium IgM in serum on day -2. (c) Anti-fiber IgM in serum on day 17 after eating a control or 9.2% w/w psyllium-supplemented diet for 12 days followed by a low fiber diet for 5 days. Each row shows the average of 5 mice. Results are representative of 3 independent experiments. (d) Individual values for anti-psyllium IgM in serum on day 17 (Student's t test, *p < 0.05 and ***p < 0.001). Heatmap values are corrected by subtracting the average of 3 secondary-only controls and the average of 2 empty bead populations. Bars, mean + SD.

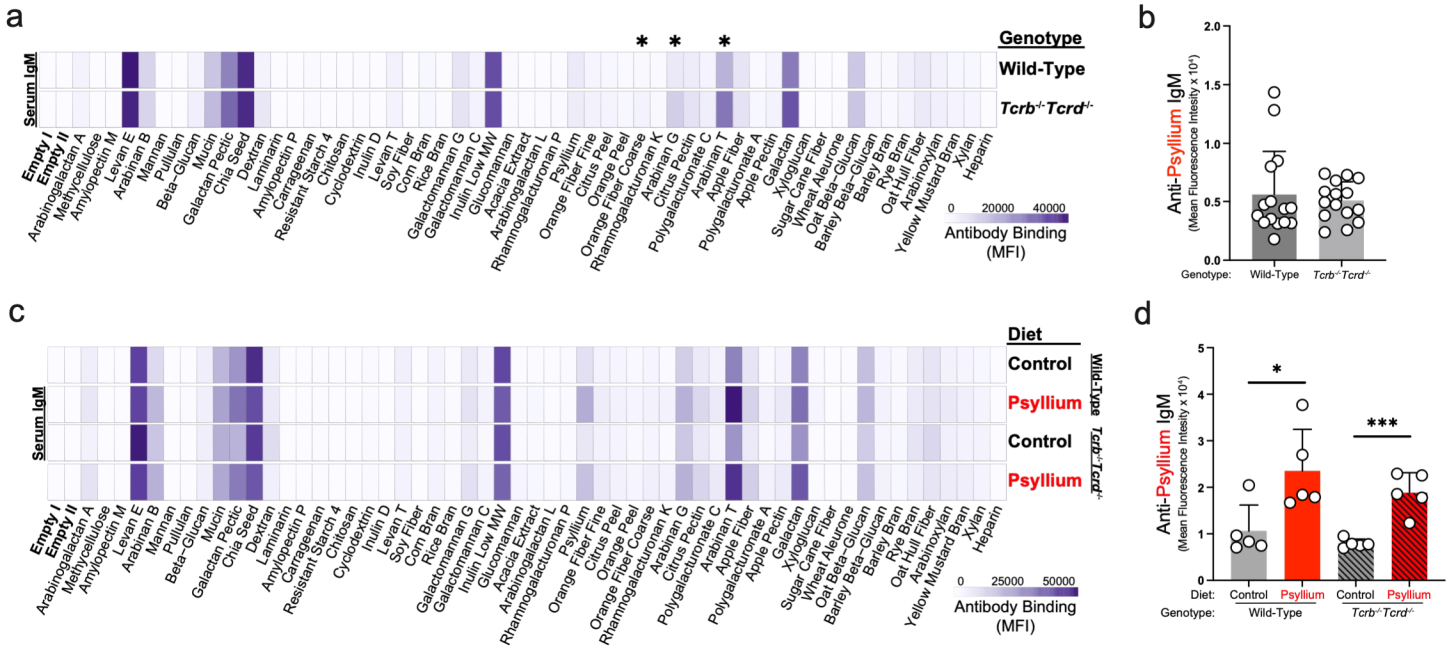
a
Genotype
Wild-Type
Tcrb-/-Tcrd+/-
Serum IgM
Empty I
Empty II
Arabinogalactan A
Methylcellulose
Amylopectin M
Levan E
Arabinan B
Mannan
Pullulan
Beta-Glucan
Mucin
Galactan Pectic
Chia Seed
Dextran
Laminarin
Amylopectin P
Carrageenan
Resistant Starch 4
Chitosan
Cyclodextrin
Inulin D
Levan T
Soy Fiber
Corn Bran
Rice Bran
Galactomannan G
Galactomannan C
Inulin Low MW
Glucomannan
Acacia Extract
Arabinogalactan L
Rhamnogalacturonan P
Psyllium
Orange Fiber Fine
Citrus Peel
Orange Peel
Orange Fiber Coarse
Rhamnogalacturonan K
Arabinan G
Citrus Pectin
Polygalacturonate C
Arabinan T
Apple Fiber
Polygalacturonate A
Apple Pectin
Galactan
Xyloglucan
Sugar Cane Fiber
Wheat Aleurone
Oat Beta-Glucan
Barley Beta-Glucan
Barley Bran
Rye Bran
Oat Hull Fiber
Arabinoxylan
Yellow Mustard Bran
Xylan
Heparin
0 20000 40000
Antibody Binding (MFI)
b
Anti-Psyllium IgM
(Mean Fluorescence Intesity x 10⁴)
2.0
1.5
1.0
0.5
0.0
Genotype: Wild-Type Tcrb-/-Tcrd+/-
c
Diet
Control
Psyllium
Control
Psyllium
Wild-Type
Tcrb-/-Tcrd+/-
Serum IgM
0 25000 50000
Antibody Binding (MFI)
d
Anti-Psyllium IgM
(Mean Fluorescence Intesity x 10⁴)
*
***
Diet: Control Psyllium Control Psyllium
Genotype: Wild-Type Tcrb-/-Tcrd+/-

Induction of anti-fiber antibodies requires exposure to gut microbes

Ingested plant cell wall polysaccharides are not regarded as immunogenic, and there are no known innate recognition pathways involved in the detection of these glycans by B cells. However, we reasoned that gut bacterial products could provide co-stimulation during B cell responses to dietary plant glycans, especially if those bacteria physically associate with fiber (Patnode et al. 2021). The impact of the gut microbiota on the baseline levels of anti-fiber IgM was modest, with reactivity against 10 fiber types reduced in germ-free mice, including fructans (levan E, levan T, inulin low MW), beta-glucans (low viscosity beta-glucan, oat beta-glucan), and arabinoxylans (low viscosity arabinoxylan, corn bran, rye bran, oat hull fiber) **(Extended Data Fig. 3a and Table S5a)**. To determine whether microbes are required for the induction of anti-fiber antibodies, germ-free and conventionally raised mice were fed a control or psyllium-supplemented diet for 12 days. Germ-free mice failed to produce circulating anti-psyllium IgM in response to psyllium feeding **(Fig. 3a)**. Baseline measurements of anti-fiber IgM analyzed 4 days before the fiber feedings confirmed that induction was restricted to conventionally raised mice fed psyllium and that psyllium did not influence the abundance of antibodies against unrelated glycans, such as galactomannan **(Fig. 3b-c, Extended Data Fig. 3b and Table S5b)**. In conventionally raised Swiss Webster (SW) mice, increased circulating anti-psyllium IgM was observed in response to psyllium feeding **(Extended Data Fig. 4a-f and Table S6a-b)**, and the high variance and lack of a detectable IgA response is consistent with the more variable antibody responses in this genetically diverse outbred strain (Enriquez et al. 2020; Sunagar et al. 2018). Like C57BL/6 mice, germ-free SW mice failed to generate anti-psyllium antibodies after psyllium feedings **(Extended Data Fig. 4g-i and Table S6c)**. We also confirmed that the high-temperature autoclave protocol used for sterilizing germ-free food and bedding did not abrogate the anti-psyllium response in conventionally raised C57BL/6 mice **(Extended Data Fig. 5a-c and**

Table S7). Thus, microbial exposure is required for the diet-induced production of circulating anti-fiber antibodies in multiple genetic backgrounds.

To determine the impact of fiber-induced changes to the gut microbiota on the induction of fiber-specific antibodies, antibiotics (ampicillin and neomycin) were added to the drinking water of conventionally raised mice (starting 4 days before the psyllium feeding). The treatment depleted bacterial biomass as assessed by measuring fecal DNA on day -4 through 12 **(Extended Data Fig. 6a)**. Mice exhibited an induction of anti-psyllium antibodies regardless of antibiotic treatment (2.6-fold increase versus 3-fold increase; **Fig. 3d, Extended Data Fig. 6b-c, and Table S8**). The induction of anti-fiber antibodies was specific to psyllium as neither psyllium feeding nor antibiotic treatment influenced anti-galactomannan IgM levels **(Fig. 3e)**. These results are consistent with a limited role for microbes during fiber supplementation and suggest microbial exposure before dietary intervention is necessary for generating anti-fiber responses.

Although microbial changes induced by psyllium did not appear to be involved in the induction of circulating anti-psyllium IgM, fiber-induced changes in microbiota composition could be involved in IgM induction against other fiber types that are more readily degraded by the gut microbiota, such as karaya gum, rich in rhamnogalacturonan II (Ndeh et al. 2017). Mice were fed a control, psyllium-supplemented, or karaya gum-supplemented diet for 12 days and the fecal microbiota composition was analyzed by performing 16S rDNA sequencing (Bolyen et al. 2019). As expected, both diets produced alterations in microbiota composition that were dependent on the fiber type consumed, with psyllium increasing the relative abundance of *Akkermansia*, *Parasutterella*, and *Bacteroides* within the first 5 days **(Extended Data Fig. 7a-b and Table S9)**, consistent with previous studies (Bretin et al. 2023; Pontifex et al. 2021). Since mice in our facility typically lack representatives of the *Proteobacteria* phylum, all mice were additionally inoculated with commensal *Escherichia coli* on day 5. By day 12, psyllium continued to induce distinct microbiota compositions **(Extended Data Fig. 7c)**. Both diets resulted in the production of anti-fiber antibodies

compared to the control diet, with psyllium inducing a 5.2-fold increase in anti-psyllium IgM and karaya inducing a 2.8-fold increase in anti-karaya IgM **(Fig. 3f-g)**. The induction of anti-psyllium IgM by karaya (2.4-fold increase) and anti-karaya IgM by psyllium (3.3-fold increase) is likely due to presence of similar glycan antigens in both fiber types (Patnode et al. 2021). Consistent with our previous feeding results, neither diet increased anti-fiber antibodies against galactomannan **(Fig. 3h)**.

To test an additional readily fermentable fiber with a distinct monosaccharide composition, we fed mice a diet containing 9.2% w/w guar gum (galactomannan G) composed of a beta-1,4-mannan backbone with alpha-1,6-galactose side chains (Balascio et al. 1981; Barber et al. 2023). We observed a 2.4-fold increase in circulating anti-galactomannan IgM in mice eating a galactomannan-containing diet compared to the control diet **(Fig. 3i, Extended Data Fig. 8a, and Table S10)**. The induction of anti-galactomannan was validated by ELISA **(Extended Data Fig. 8b)** and was not due to a global increase in total serum IgM **(Extended Data Fig. 8c)**. As expected based on the lack of induction of anti-galactomannan antibodies when mice were fed psyllium **(Fig. 2d)**, galactomannan did not induce anti-psylium antibodies **(Fig. 3j)**. We detected modestly higher anti-karaya antibodies (1.5-fold) in mice fed galactomannan, which may be due to the abundant galactose side chains in karaya **(Fig. 3k)**. These data, along with the results of antibiotic treatment, argue against the notion that a single stereotyped microbiota alteration during fiber exposure is responsible for the induction of fiber-specific antibodies.

To assess which microbial taxa were sufficient for enabling anti-fiber immune responses, germ-free mice were colonized with minimal communities containing *Bacteroides ovatus* (ATCC-8483) in combination with (i) *E. coli* (TSDC17.2), (ii) *E. coli* (TSDC17.2) plus *Akkermansia muciniphila* (NSD001), or (iii) *Bacteroides ovatus* (WH514), and fed a control or psyllium-containing diet. None of these highly simplified yet phylogenetically diverse collections of taxa were sufficient to permit significant antibody responses against ingested psyllium **(Extended Data Fig. 9a-d and Table S11a-b)**. Together, these results indicate that

the induction of circulating anti-fiber antibodies results from immune activation by ingested dietary fiber glycans in a manner dependent on particular microbial taxa prior to oral fiber exposure.

Fig. 3. Microbes are required for the induction of anti-fiber antibodies

(a) Anti-psyllium IgM in serum from conventionally raised or germ-free C57BL/6 mice eating a control or 9.2% w/w psyllium-supplemented diet for 12 days (Student's t test, *$p < 0.05$ and **$p < 0.01$). Results are representative of >3 independent experiments. (b and c) Serum from conventionally raised or germ-free C57BL/6 mice collected before (day -4) and after eating a control or psyllium-supplemented diet (day 12) was tested using a glycan-coated bead library to measure baseline differences of circulating anti-psyllium IgM (b) and anti-galactomannan IgM (c). Dots represent individual mice, with lines connecting paired samples, and unpaired samples were plotted with no connecting line (Paired t test, *$p < 0.05$ and ***$p < 0.001$). (d) Anti-psyllium IgM and (e) anti-galactomannan IgM in serum from conventionally raised C57BL/6 mice, with or without continuous antibiotic treatment, eating a control or 9.2% w/w psyllium-supplemented diet for 12 days (Student's t test, **$p < 0.01$). (f - h) Anti-psylium IgM (f), anti-karaya IgM (g), or anti-galactomannan IgM (h) in serum from C57BL/6 mice eating a control, 9.2% w/w psyllium-, or 9.2% w/w karaya-supplemented diet for 12 days (Student's t test, ***$p < 0.001$ and ****$p < 0.0001$). (I - K) Anti-galactomannan IgM (i), anti-psyllium IgM (j), or anti-karaya IgM (k) in serum from C57BL/6 mice eating a control or 9.2% w/w galactomannan-supplemented diet for 11 days (Student's t test, *$p < 0.05$ and ***$p < 0.001$). Results are representative of 3 independent experiments. Plotted MFI values are normalized by subtracting the average of 3 secondary-only controls and the average of 2 empty bead populations. Dotted lines, background signal (average of 3 secondary-only controls); bars, mean + SD.

Fig. 3

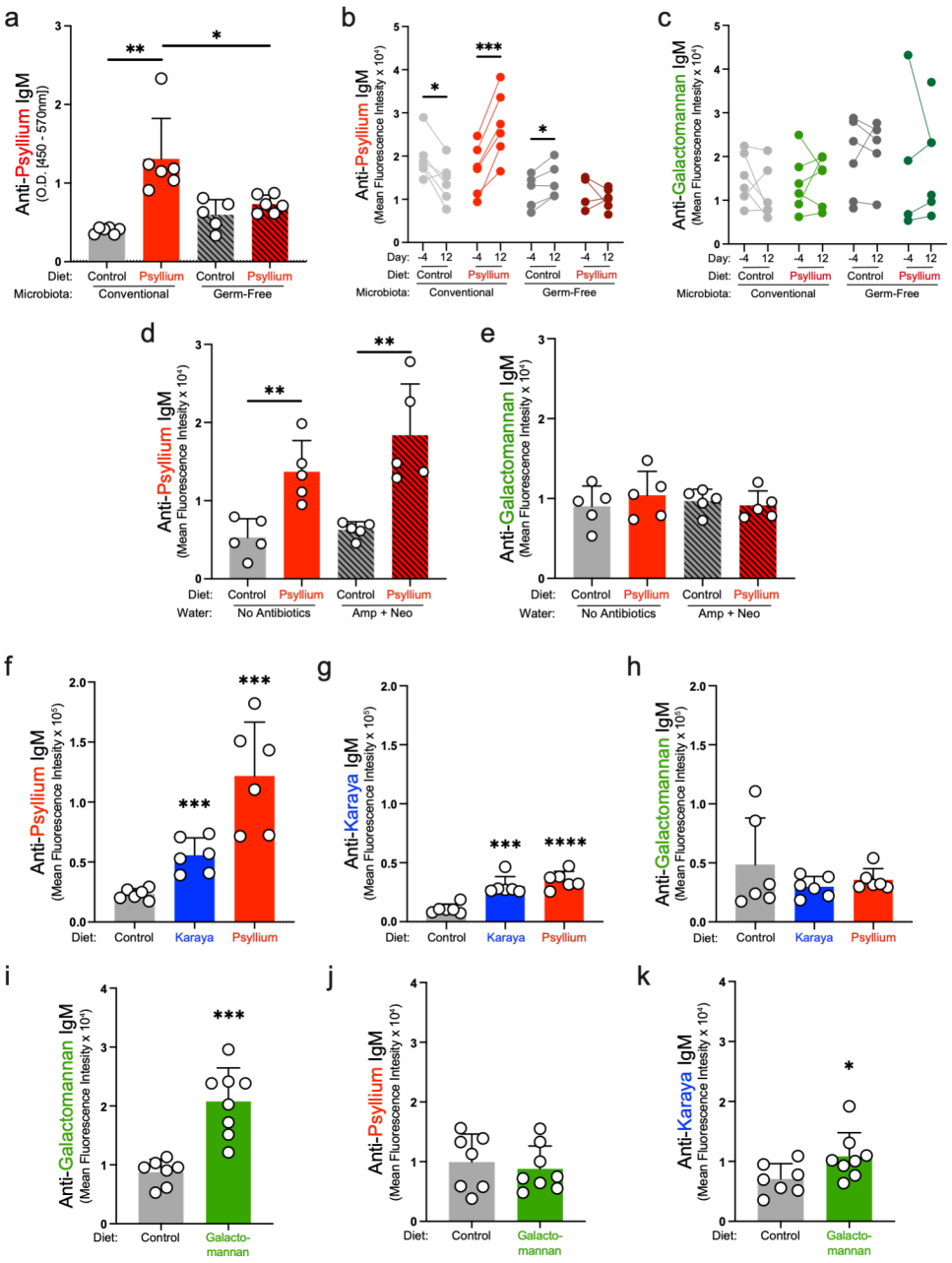
a
Anti-Psyllium IgM
(O.D. [450 - 570nm])
Diet: Control Psyllium Control Psyllium
Microbiota: Conventional Germ-Free
b
Anti-Psyllium IgM
(Mean Fluorescence Intesity x 10⁴)
Day: -4 12 -4 12 -4 12 -4 12
Diet: Control Psyllium Control Psyllium
Microbiota: Conventional Germ-Free
c
Anti-Galactomannan IgM
(Mean Fluorescence Intesity x 10⁴)
Day: -4 12 -4 12 -4 12 -4 12
Diet: Control Psyllium Control Psyllium
Microbiota: Conventional Germ-Free
d
Anti-Psyllium IgM
(Mean Fluorescence Intesity x 10⁴)
Diet: Control Psyllium Control Psyllium
Water: No Antibiotics Amp + Neo
e
Anti-Galactomannan IgM
(Mean Fluorescence Intesity x 10⁴)
Diet: Control Psyllium Control Psyllium
Water: No Antibiotics Amp + Neo
f
Anti-Psyllium IgM
(Mean Fluorescence Intesity x 10⁵)
Diet: Control Karaya Psyllium
g
Anti-Karaya IgM
(Mean Fluorescence Intesity x 10⁵)
Diet: Control Karaya Psyllium
h
Anti-Galactomannan IgM
(Mean Fluorescence Intesity x 10⁴)
Diet: Control Karaya Psyllium
i
Anti-Galactomannan IgM
(Mean Fluorescence Intesity x 10⁴)
Diet: Control Galacto-mannan
j
Anti-Psyllium IgM
(Mean Fluorescence Intesity x 10⁴)
Diet: Control Galacto-mannan
k
Anti-Karaya IgM
(Mean Fluorescence Intesity x 10⁴)
Diet: Control Galacto-mannan

Extended Data Fig. 3. Absence of anti-fiber response in Germ-free mice.

(a and b) Circulating anti-fiber IgM from conventional or germ-free C57BL/6 mice before (a, day -4) and after eating a control or 9.2% w/w psyllium-supplemented diet for 12 days (b) was tested using a glycan-coated bead library. Each row shows the average of 10-12 mice (a) or 5-6 mice (b) (*, Student's t test, $q < 0.05$, FC >= 1.5). Results are representative of >3 independent experiments. Heatmap values are corrected by subtracting the average of 3 secondary-only controls and the average of 2 empty bead populations.

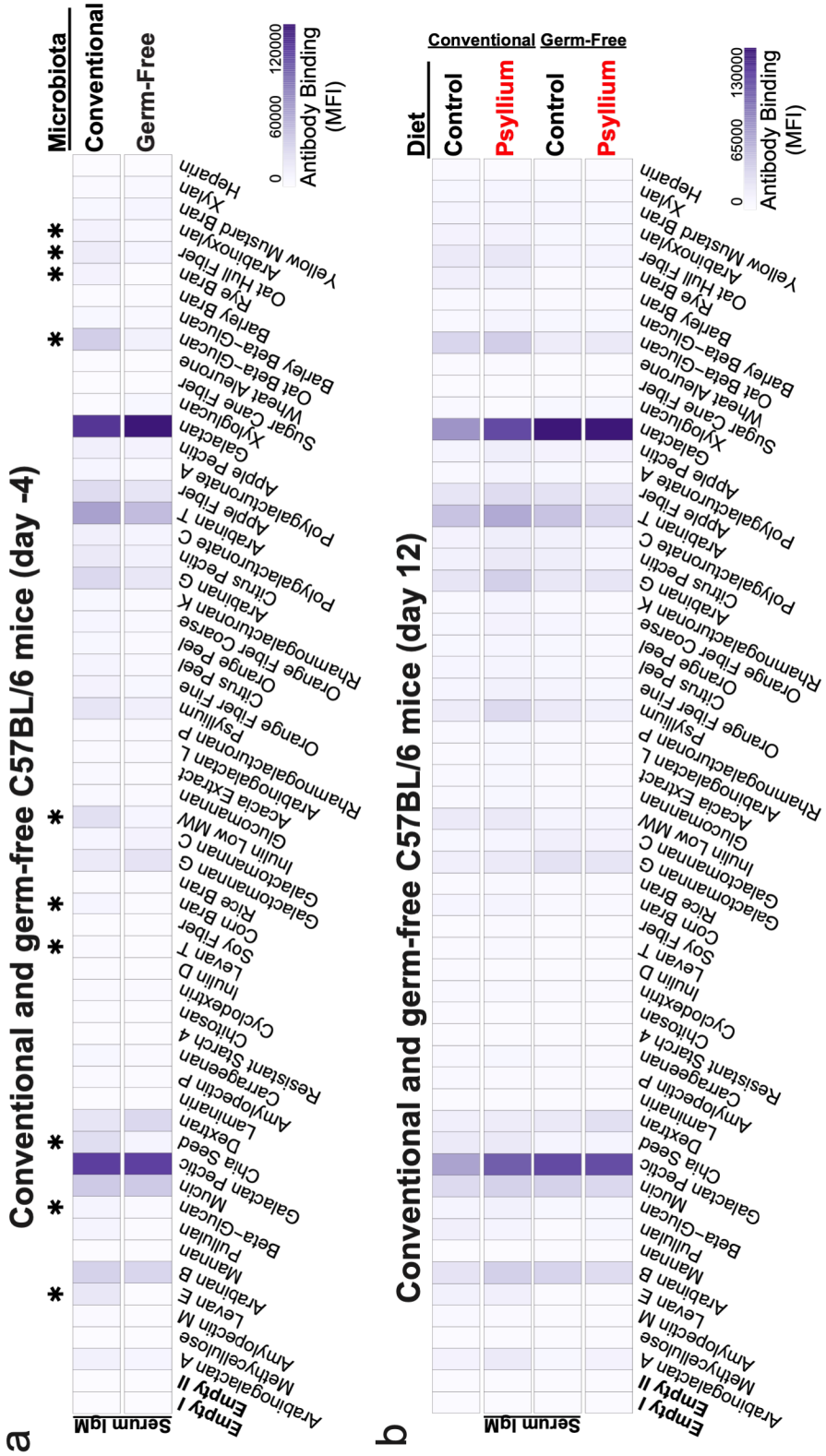
a
Conventional and germ-free C57BL/6 mice (day -4)
Microbiota
Conventional
Germ-Free
Antibody Binding (MFI)
0
60000
120000
Serum IgM
Empty I
Empty II
Arabinogalactan A
Methylcellulose
Amylopectin M
Levan E
Arabinan B
Mannan
Pullulan
Beta-Glucan
Galactan
Pectic
Chia Seed
Dextran
Laminarin
Amylopectin P
Carrageenan
Resistant Starch 4
Chitosan
Cyclodextrin
Inulin D
Levan T
Soy Fiber
Corn Bran
Rice Bran
Galactomannan G
Galactomannan C
Inulin Low MW
Glucomannan
Acacia Extract
Arabinogalactan L
Rhamnogalactouronan P
Psyllium
Orange Fiber Fine
Citrus Peel
Orange Fiber Coarse
Rhamnogalactouronan K
Arabinan G
Citrus Pectin
Polygalacturonate C
Arabinan T
Apple Fiber
Polygalacturonate A
Apple Pectin
Galactan
Xyloglucan
Sugar Cane Fiber
Wheat Alleurone
Oat Beta-Glucan
Barley Beta-Glucan
Rye Bran
Barley Bran
Oat Hull Fiber
Arabinoxylan
Yellow Mustard Bran
Xylan
Heparin
b
Conventional and germ-free C57BL/6 mice (day 12)
Diet
Conventional
Germ-Free
Control
Psyllium
Control
Psyllium
Antibody Binding (MFI)
0
65000
130000
Serum IgM
Empty I
Empty II
Arabinogalactan A
Methylcellulose
Amylopectin M
Levan E
Arabinan B
Mannan
Pullulan
Beta-Glucan
Galactan
Pectic
Chia Seed
Dextran
Laminarin
Amylopectin P
Carrageenan
Resistant Starch 4
Chitosan
Cyclodextrin
Inulin D
Levan T
Soy Fiber
Corn Bran
Rice Bran
Galactomannan G
Galactomannan C
Inulin Low MW
Glucomannan
Acacia Extract
Arabinogalactan L
Rhamnogalactouronan P
Psyllium
Orange Fiber Fine
Citrus Peel
Orange Fiber Coarse
Rhamnogalactouronan K
Arabinan G
Citrus Pectin
Polygalacturonate C
Arabinan T
Apple Fiber
Polygalacturonate A
Apple Pectin
Galactan
Xyloglucan
Sugar Cane Fiber
Wheat Alleurone
Oat Beta-Glucan
Barley Beta-Glucan
Rye Bran
Barley Bran
Oat Hull Fiber
Arabinoxylan
Yellow Mustard Bran
Xylan
Heparin

Extended Data Fig. 4. Circulating response against psyllium in conventionally-raised Swiss Webster mice.

(a) Circulating anti-fiber IgM from conventional Swiss Webster (SW) mice eating a control or 9.2% w/w psyllium-supplemented diet for 12 days followed by a low fiber diet for 5 days was tested using a glycan-coated bead library. Each row shows the average of 5 mice. (b) Individual values for anti-psyllium IgM in serum on day 17 (Student's t test, *p < 0.05). (c) ELISA for anti-psyllium IgM in serum on day 17. (d) Bead library showing cecal anti-fiber IgA signals. Each row shows the average of 5 mice. (e) Individual values for anti-psyllium IgA in cecal contents on day 17. (f) ELISA for anti-psyllium IgA in cecal contents on day 17. (g) Circulating anti-fiber IgM from germ-free SW mice eating a control or 9.2% w/w psyllium-supplemented diet for 12 days was tested using a glycan-coated bead library. Each row shows the average of 5 mice. (h) Individual values for anti-psyllium IgM in serum on day 12. (i) ELISA for anti-psyllium IgM in serum on day 12. Heatmap values are corrected by subtracting the average of 3 secondary-only controls and the average of 2 empty bead populations. Dotted lines, background signal (average of 3 secondary-only controls); bars, mean + SD.

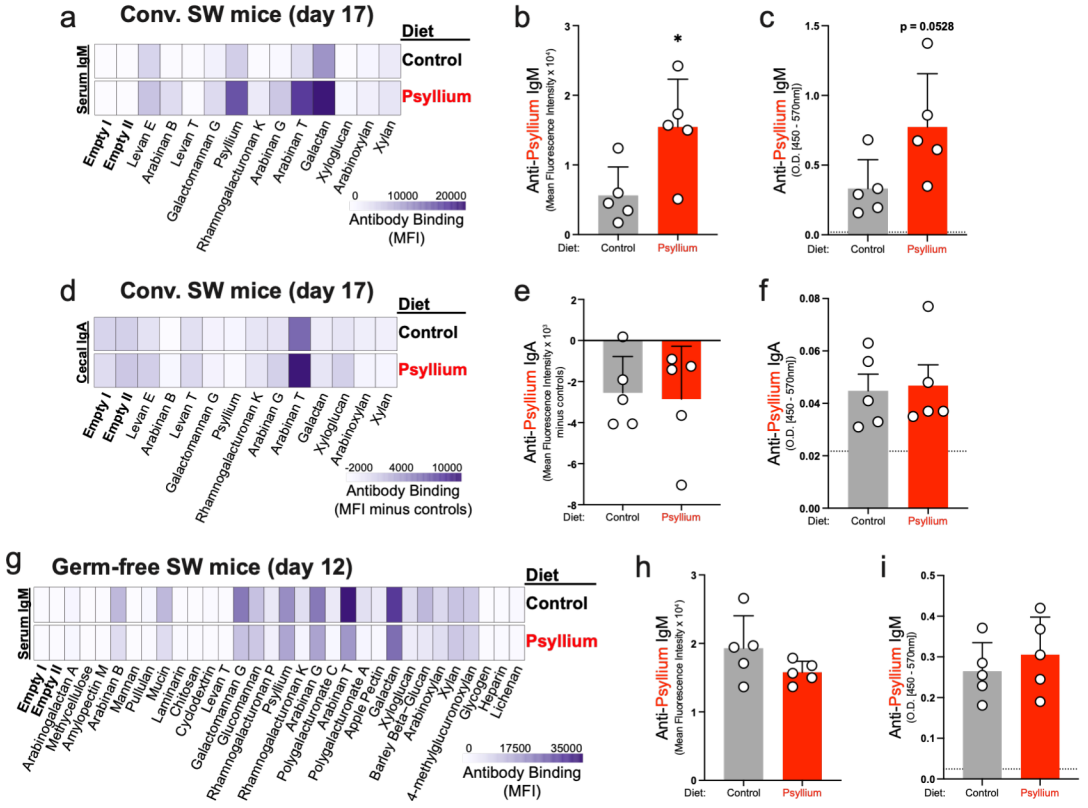

Extended Data Fig. 5. Germ-free husbandry conditions do not inhibit the induction of anti-psyllium antibodies.

(a) Circulating anti-fiber IgM from conventionally raised C57BL/6 mice (raised from birth using the same autoclave-sterilized bedding and chow used for germ-free mice) eating a control or 9.2% w/w psyllium-supplemented diet for 12 days was tested using a glycan-coated bead library. Each row represents the average of 7 mice. (b) Individual values for anti-psyllium IgM in serum on day 12 (Student's t test, $^{**}p < 0.01$). (c) ELISA for anti-psyllium IgM in serum on day 12 (Student's t test, $^{**}p < 0.01$). Heatmap values are corrected by subtracting the average of 3 secondary-only controls and the average of 2 empty bead populations. Dotted lines, background signal (average of 3 secondary-only controls); bars, mean + SD.

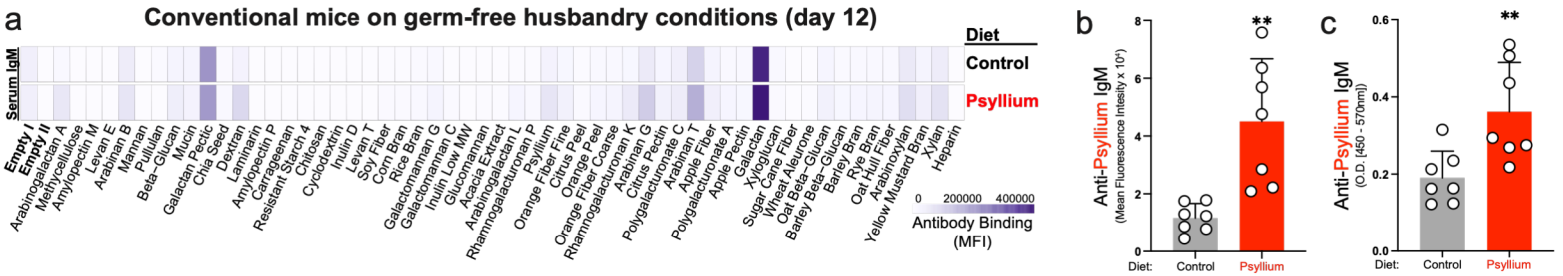
a
Conventional mice on germ-free husbandry conditions (day 12)
Diet
Control
Psyllium
Serum IgM
Empty I
Empty II
Arabinogalactan A
Methylcellulose
Amylopectin M
Levan E
Arabinan B
Mannan
Pullulan
Beta-Glucan
Mucin
Galactan Pectic
Chia Seed
Dextran
Laminarin
Amylopectin P
Carrageenan
Resistant Starch 4
Chitosan
Cyclodextrin
Inulin D
Levan T
Soy Fiber
Corn Bran
Rice Bran
Galactomannan G
Galactomannan C
Inulin Low MW
Glucomannan
Acacia Extract
Arabinogalactan L
Rhamnogalacturonan P
Psyllium
Orange Fiber Fine
Citrus Peel
Orange Peel
Orange Fiber Coarse
Rhamnogalacturonan K
Arabinan G
Citrus Pectin
Polygalacturonate C
Arabinan T
Apple Fiber
Polygalacturonate A
Apple Pectin
Galactan
Xyloglucan
Sugar Cane Fiber
Wheat Aleurone
Oat Beta-Glucan
Barley Beta-Glucan
Barley Bran
Rye Bran
Oat Hull Fiber
Arabinoxylan
Yellow Mustard Bran
Xylan
Heparin
0
200000
400000
Antibody Binding
(MFI)
b
Anti-Psyllium IgM
(Mean Fluorescence Intesity x 10⁴)
8
6
4
2
0
**
Diet:
Control
Psyllium
c
Anti-Psyllium IgM
(O.D. [450 - 570nm])
0.6
0.4
0.2
0.0
**
Diet:
Control
Psyllium

Extended Data Fig. 6. Antibiotic treatment does not inhibit the induction of circulating anti-psyllium IgM.

(a) Fecal DNA from C57BL/6 mice with or without antibiotic treatment (eating a control or 9.2% w/w psyllium-supplemented diet for 12 days) was quantified before starting the fiber feedings (day -4) and throughout the feedings as a proxy for microbial abundance in the gut. (b) Circulating anti-fiber IgM was tested using a glycan-coated bead library. Each row represents the average of 5 mice. (c) ELISA for anti-psyllium IgM in serum on day 12 (Student's t test, *$p < 0.05$). Heatmap values are corrected by subtracting the average of 3 secondary-only controls and the average of 2 empty bead populations. Dotted lines, background signal (average of 3 secondary-only controls); bars, mean + SD.

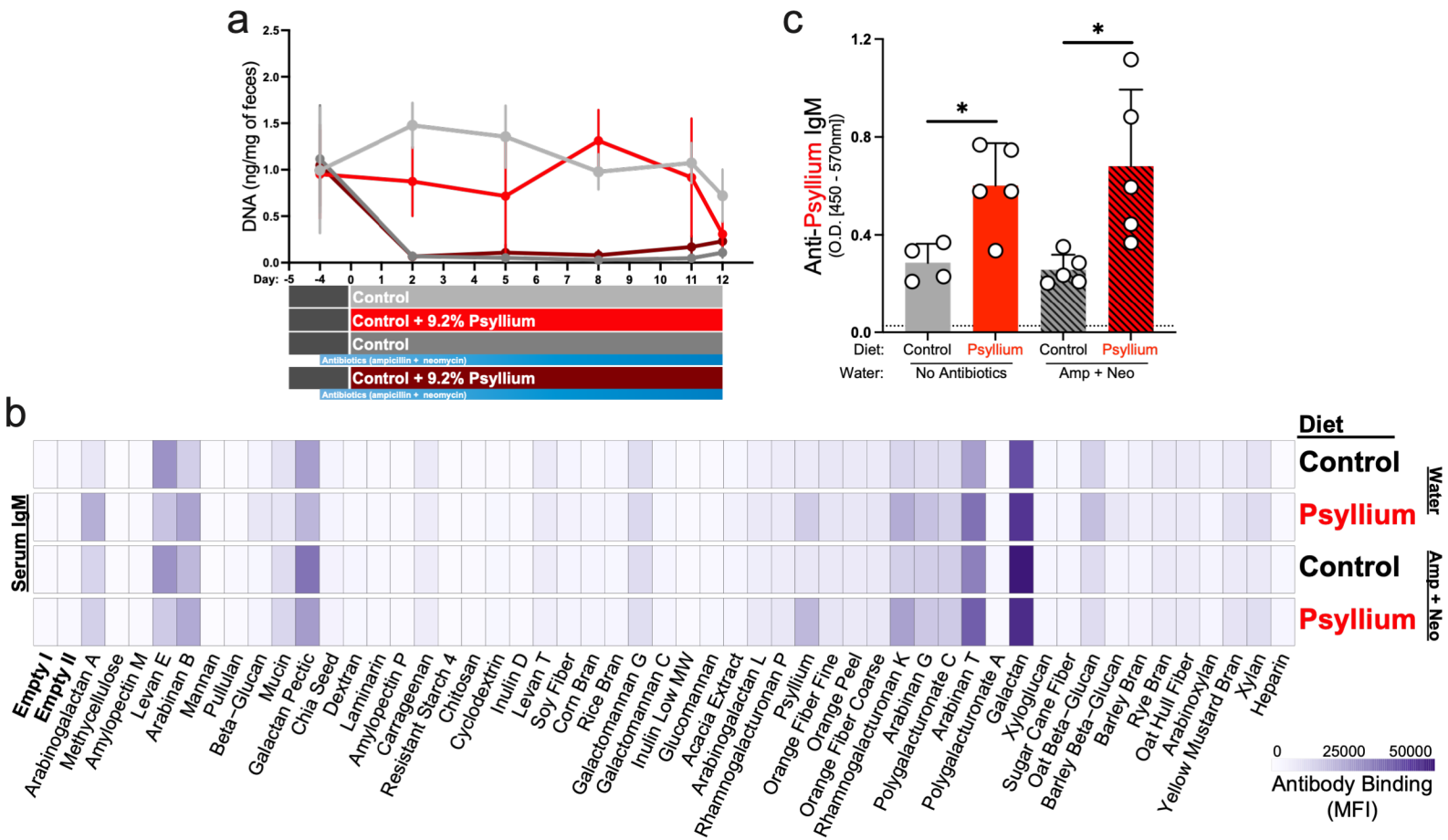
a
DNA (ng/mg of feces)
Day: -5 -4 0 1 2 3 4 5 6 7 8 9 10 11 12
Control
Control + 9.2% Psyllium
Control
Antibiotics (ampicillin + neomycin)
Control + 9.2% Psyllium
Antibiotics (ampicillin + neomycin)
c
Anti-Psyllium IgM
(O.D. [450 - 570nm])
Diet: Control Psyllium Control Psyllium
Water: No Antibiotics Amp + Neo
b
Serum IgM
Diet
Control
Psyllium
Control
Psyllium
Water
Amp + Neo
Empty I
Empty II
Arabinogalactan A
Methylcellulose
Amylopectin M
Levan E
Arabinan B
Mannan
Pullulan
Beta-Glucan
Mucin
Galactan Pectic
Chia Seed
Dextran
Laminarin
Amylopectin P
Carrageenan
Resistant Starch 4
Chitosan
Cyclodextrin
Inulin D
Levan T
Soy Fiber
Corn Bran
Rice Bran
Galactomannan G
Galactomannan C
Inulin Low MW
Glucomannan
Acacia Extract
Arabinogalactan L
Rhamnogalacturonan P
Psyllium
Orange Fiber Fine
Orange Peel
Orange Fiber Coarse
Rhamnogalacturonan K
Arabinan G
Polygalacturonate C
Arabinan T
Polygalacturonate A
Galactan
Xyloglucan
Sugar Cane Fiber
Oat Beta-Glucan
Barley Beta-Glucan
Barley Bran
Rye Bran
Oat Hull Fiber
Arabinoxylan
Yellow Mustard Bran
Xylan
Heparin
0 25000 50000
Antibody Binding
(MFI)

Extended Data Fig. 7. Psyllium feeding alters gut microbiota composition.

(a - c) Relative abundance of bacterial taxa at the genus level in control, 9.2% w/w karaya, and 9.2% w/w psyllium fed mice at day 0 (a), day 5 (b), and day 12 (c) (control, n = 6; karaya, n = 6; psyllium, n = 6). The stacked bar plots display the top 15 most abundant taxa determined from day 12 sequences, with the remaining taxa classified as “other”.

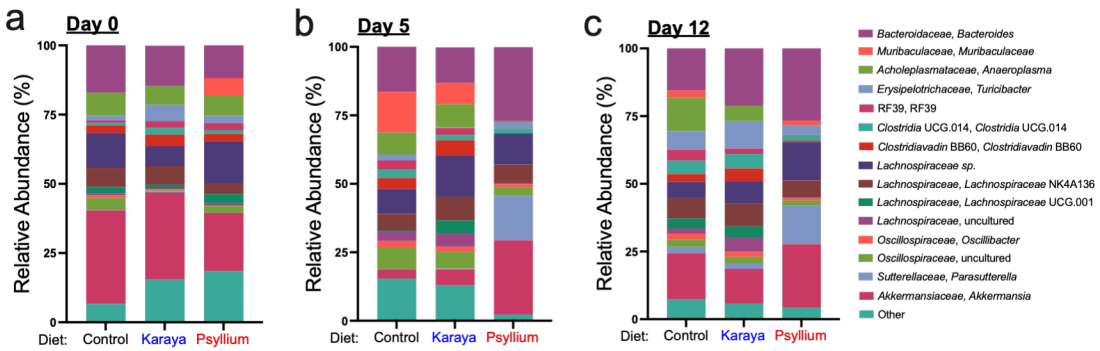

Extended Data Fig. 8. Galactomannan feeding induces circulating anti-galactomannan IgM.

(a) Circulating anti-fiber IgM from C57BL/6 mice eating a control or 9.2% w/w galactomannan-supplemented diet for 11 days was tested using a glycan-coated bead library. Each row represents the average of 7-8 mice. Results are representative of >3 independent experiments. (b) ELISA for anti-galactomannan IgM in serum on day 11 (Student's t test, **$p < 0.01$). (c) Quantification of total serum IgM on day 11. Heatmap values are corrected by subtracting the average of 3 secondary-only controls and the average of 2 empty bead populations. Dotted lines, background signal (average of 3 secondary-only controls); bars, mean + SD.

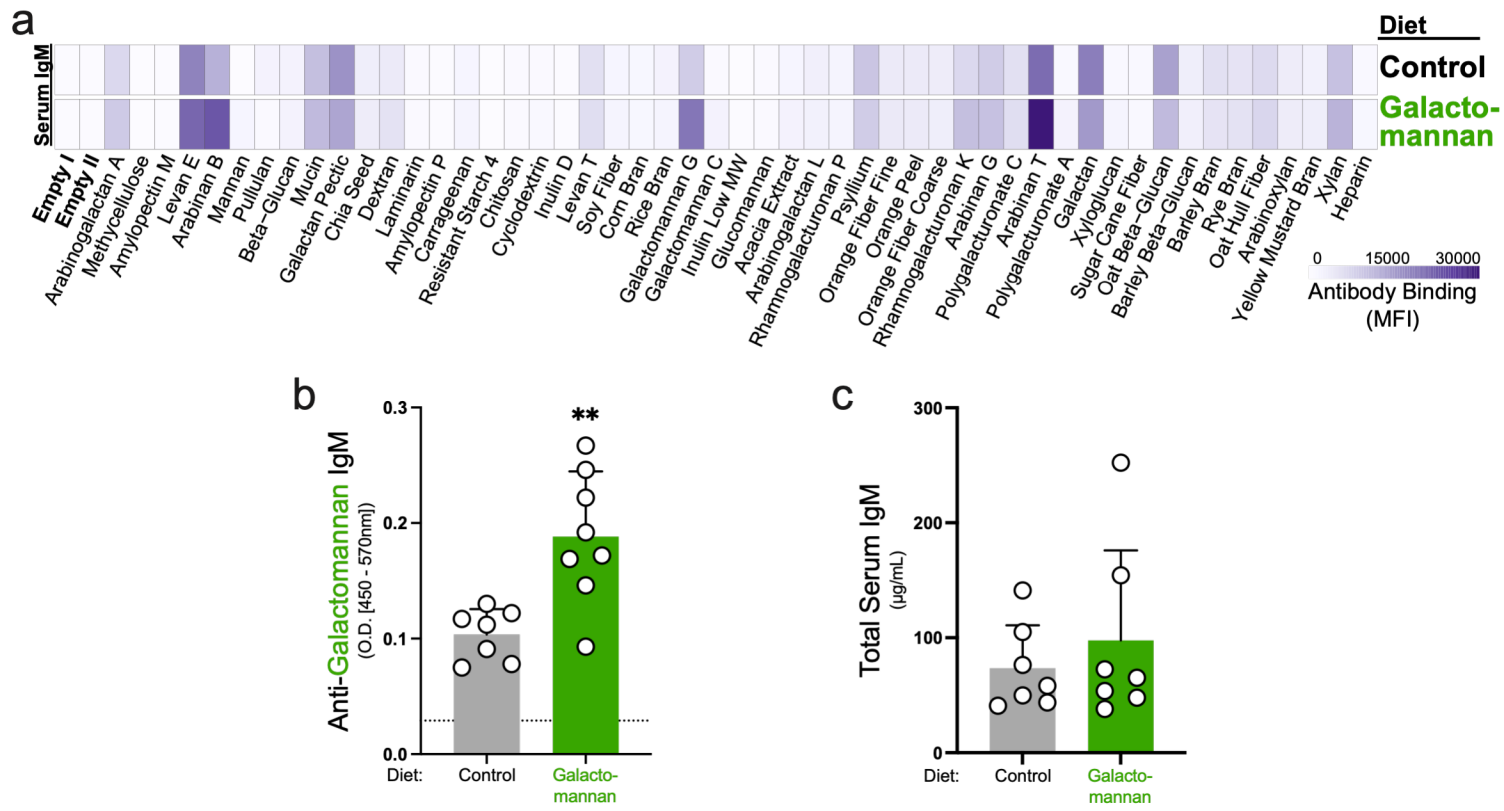
a
Diet
Control
Galacto-
mannan
Serum IgM
Empty I
Empty II
Arabinogalactan A
Methylcellulose
Amylopectin M
Levan E
Arabinan B
Mannan
Pullulan
Beta-Glucan
Mucin
Galactan Pectic
Chia Seed
Dextran
Laminarin
Amylopectin P
Carrageenan
Resistant Starch 4
Chitosan
Cyclodextrin
Inulin D
Levan T
Soy Fiber
Corn Bran
Rice Bran
Galactomannan G
Galactomannan C
Inulin Low MW
Glucomannan
Acacia Extract
Arabinogalactan L
Rhamnogalacturonan P
Psyllium
Orange Fiber Fine
Orange Peel
Orange Fiber Coarse
Rhamnogalacturonan K
Arabinan G
Polygalacturonate C
Arabinan T
Polygalacturonate A
Galactan
Xyloglucan
Sugar Cane Fiber
Oat Beta-Glucan
Barley Beta-Glucan
Barley Bran
Rye Bran
Oat Hull Fiber
Arabinoxylan
Yellow Mustard Bran
Xylan
Heparin
0
15000
30000
Antibody Binding
(MFI)
b
Anti-Galactomannan IgM
(O.D. [450 - 570nm])
0.3
0.2
0.1
0.0
**
Diet:
Control
Galacto-
mannan
c
Total Serum IgM
(µg/mL)
300
200
100
0
Diet:
Control
Galacto-
mannan

Extended Data Fig. 9. Diverse bacterial isolates are not sufficient for the induction of circulating anti-psyllium IgM.

(a) Circulating anti-fiber IgM from germ-free Swiss Webster mice colonized with a 2 (*Bacteroides ovatus* ATCC8483 and *E. coli* TSDC17.2) or 3 (*B. ovatus* ATCC8483, *E. coli* TSDC17.2, and *Akkermansia muciniphila* NSD001) member community eating a control or 9.2% w/w psyllium-supplemented diet for 12 days was tested using a glycan-coated bead library. Each row represents the average of 5-6 mice. (b) Individual values for anti-psyllium IgM in serum on day 12. (c) Circulating anti-fiber IgM from germ-free C57BL/6 mice colonized with a 2-member community (*B. ovatus* WH514 and *B. ovatus* ATCC8483) eating a control or 9.2% w/w psyllium-supplemented diet for 12 days was tested using a glycan-coated bead library. Each row represents the average of 7 mice. (d) Individual values for anti-psyllium IgM in serum on day 12. Heatmap values are corrected by subtracting the average of 3 secondary-only controls and the average of 2 empty bead populations. Bars, mean + SD.

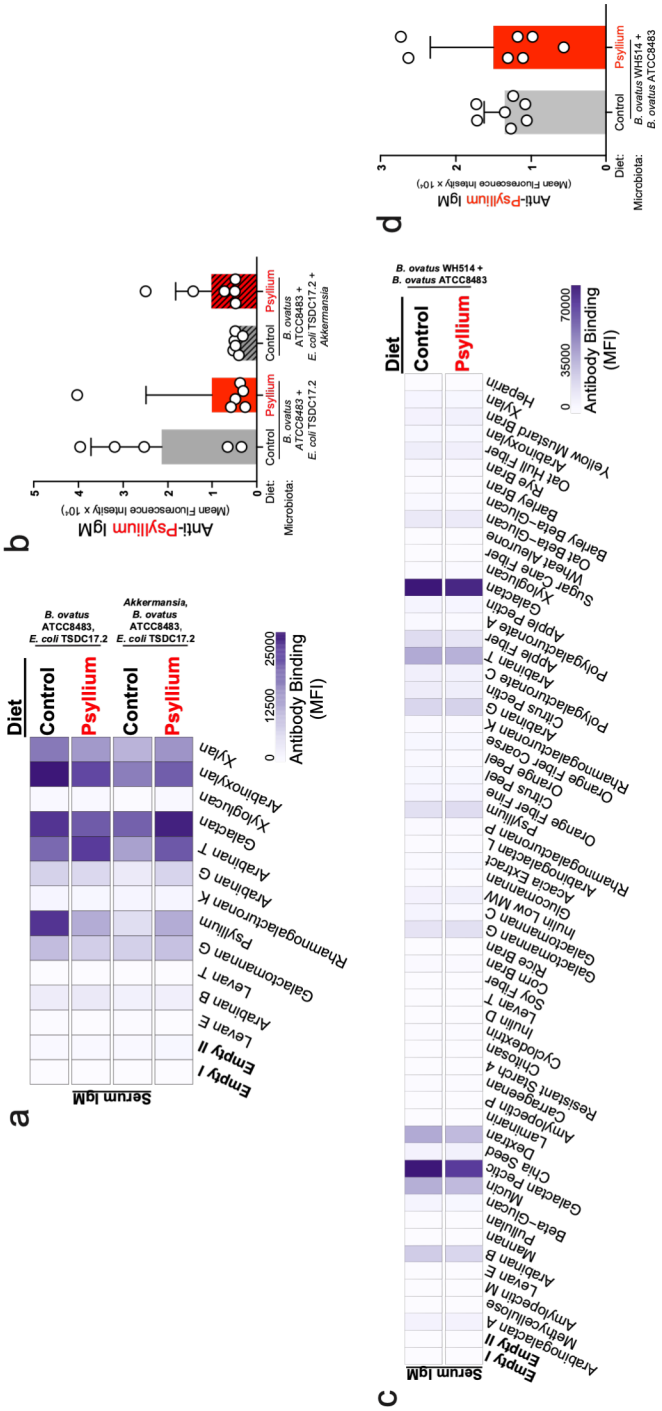
a
Diet
Control
Psyllium
Control
Psyllium
B. ovatus ATCC8483, E. coli TSDC17.2
Akkermansia, B. ovatus ATCC8483, E. coli TSDC17.2
Antibody Binding (MFI)
0
12500
25000
Serum IgM
Empty I
Empty II
Levan E
Arabinan B
Levan T
Galactomannan G
Psyllium
Rhamnogalacturonan K
Arabinan G
Arabinan T
Galactan
Xyloglucan
Arabinoxylan
Xylan
b
Anti-Psyllium IgM
(Mean Fluorescence Intesity x 10³)
0
1
2
3
4
5
Diet:
Microbiota:
Control
Psyllium
Control
Psyllium
B. ovatus ATCC8483 + E. coli TSDC17.2
B. ovatus ATCC8483 + E. coli TSDC17.2 + Akkermansia
c
Diet
Control
Psyllium
B. ovatus WH514 + B. ovatus ATCC8483
Antibody Binding (MFI)
0
35000
70000
Serum IgM
Empty I
Empty II
Arabinogalactan A
Methylcellulose
Amylopectin M
Levan E
Arabinan B
Mannan
Pullulan
Beta-Glucan
Mucin
Galactan Pectic
Chia Seed
Dextran
Laminarin
Amylopectin P
Carrageenan
Resistant Starch 4
Chitosan
Cyclodextrin
Inulin D
Levan T
Soy Fiber
Corn Bran
Rice Bran
Galactomannan G
Inulin Low MW
Glucomannan C
Acacia Extract
Arabinogalactan L
Rhamnogalacturonan P
Psyllium
Orange Fiber Fine
Citrus Peel
Orange Fiber Coarse
Rhamnogalacturonan K
Arabinan G
Citrus Pectin
Polygalacturonate C
Arabinan T
Apple Fiber
Polygalacturonate A
Apple Pectin
Galactan
Xyloglucan
Sugar Cane Fiber
Wheat Arabinoxylan
Oat Beta-Glucan
Barley Beta-Glucan
Rye Bran
Oat Hull Fiber
Arabinoxylan
Yellow Mustard Bran
Xylan
Heparin
d
Anti-Psyllium IgM
(Mean Fluorescence Intesity x 10³)
0
1
2
3
Diet:
Microbiota:
Control
Psyllium
B. ovatus WH514 + B. ovatus ATCC8483

Culturable commensal gut bacteria enable the induction of fiber-specific antibodies

While minimal bacterial communities appeared to lack the necessary signals to sensitize mice to produce anti-fiber antibodies, we wondered whether a broader collection of culturable members of the endogenous mouse microbiota was sufficient. Fecal bacteria from mice eating a low fiber diet were plated on BHI blood agar and then combined to create a pooled "culture collection". Male and female germ-free mice colonized with this culture collection were bred and their progeny were fed a control or psyllium-supplemented diet for 12 days followed by a low fiber diet for 5 days. Psyllium feeding induced 1.4-fold higher anti-psyllium IgM levels in the serum of culture collection colonized mice **(Fig. 4a, Extended Data Fig. 10a-b, and Table S12a)**. In a parallel arm of the experiment, fecal pellets collected from these mice 2 weeks prior to psyllium feeding were used to colonize age-matched germ-free mice. The mice colonized as adults also exhibited an increase in anti-psyllium IgM (1.9-fold) compared to mice eating a control diet **(Fig. 4a, Extended Data Fig. 10a-b, and Table S12a)**. Neither group of mice colonized with the culture collection fully recapitulated the anti-psyllium IgA response seen in conventionally raised animals **(Fig. 4b)**. These results reveal that a complex community of culturable members can sensitize mice to generate an IgM response against ingested plant glycans, whether colonized at birth or as adults.

A fully defined gut microbial community offers opportunities to understand the mechanisms driving antibody induction. The OMM12 (Oligo-Mouse-Microbiota) model community is reproducible for multiple generations, encompasses broad phylogenetic diversity, and has been fully sequenced (Eberl et al. 2019) **(Fig. 4c)**. We colonized C57BL/6 mice with the OMM12 community and fed their progeny a control or psyllium-containing diet for 12 days followed by a low fiber diet for 5 days. The mice fed psyllium exhibited a 1.6-fold increase in circulating anti-psyllium IgM **(Fig. 4d, Extended Data Fig. 10c-d, and Table S12b)**, and this was not due to a global increase in circulating IgM **(Fig. 4e)**. In contrast to the mice colonized with the complete culture collection, we detected a 1.4-fold increase in anti-

psyllium IgA as a result of psyllium feeding **(Fig. 4f)**, despite the reduced IgA^+ plasma cell numbers in mice harboring OMM12 strains (Afrizal et al. 2022). Together, these results show that a fully defined, simplified microbial community sensitizes germ-free mice to produce anti-fiber antibodies in response to a fiber-supplemented diet.

Fig. 4. Mouse-derived communities of culturable isolates sensitize mice to psyllium

(a and b) Anti-psyllium IgM in serum (a) and anti-psyllium IgA in cecal contents (b) from germ-free C57BL/6 mice colonized with a conventionally raised mouse culture collection from birth or as adults and fed control or 9.2% w/w psyllium-supplemented diet for 12 days followed by a low fiber diet for 5 days (Student's t test, $^{**}p < 0.01$). (c) Schematic showing the OMM12 model community experimental design. (d) Anti-psyllium IgM in serum (Student's t test, $^{***}p < 0.001$). Results are representative of 2 independent experiments. (e) Total IgM in serum. (f) Anti-psyllium IgA in cecal contents (Student's t test, $^{*}p < 0.05$). Dotted lines, background signal (average of 3 secondary-only controls); bars, mean + SD or mean + 95% confidence interval (d - f).

Fig. 4

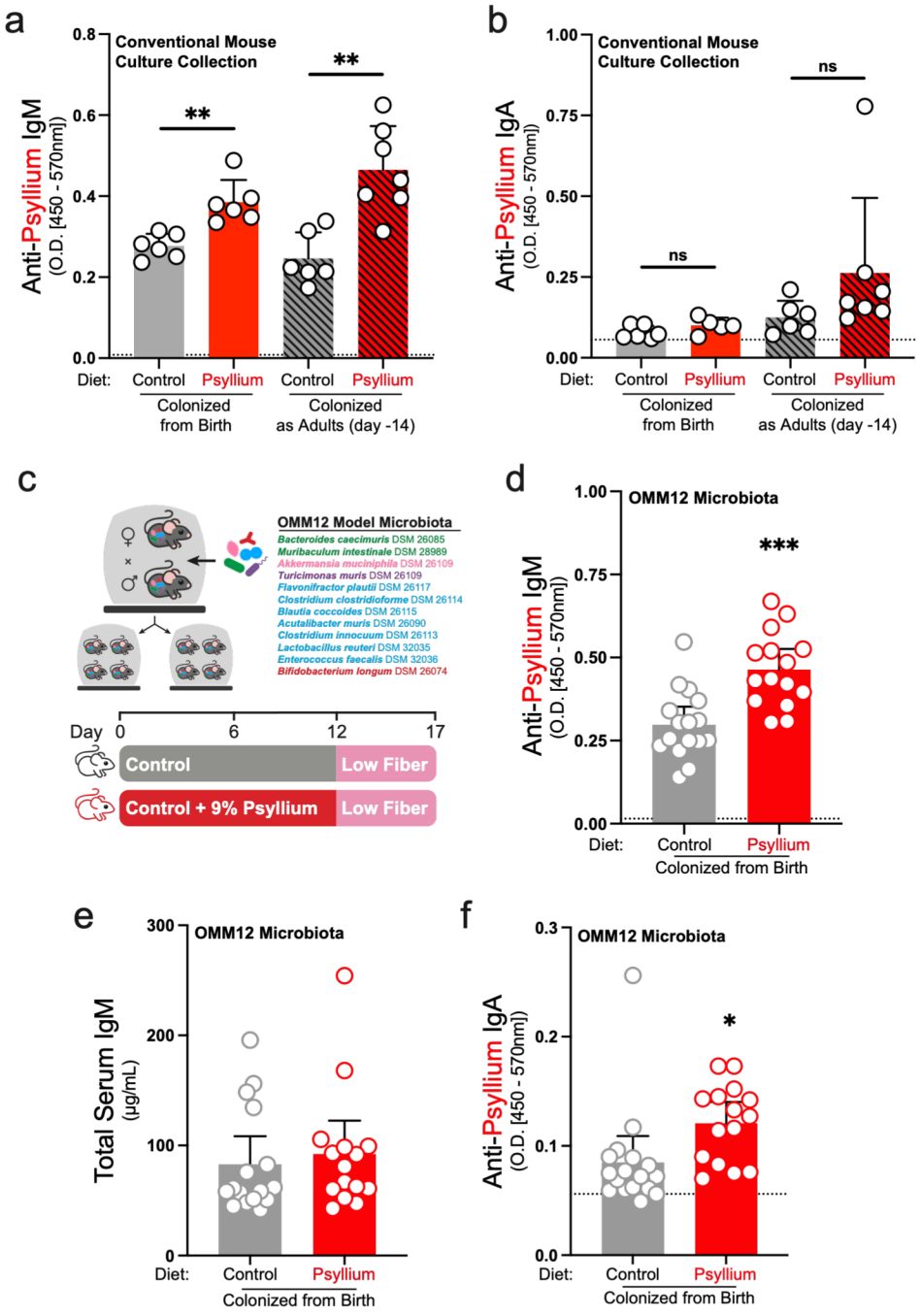
a
Conventional Mouse Culture Collection
Anti-Psyllium IgM (O.D. [450 - 570nm])
0.8
0.6
0.4
0.2
0.0
**
**
Diet: Control Psyllium Control Psyllium
Colonized from Birth
Colonized as Adults (day -14)
b
Conventional Mouse Culture Collection
Anti-Psyllium IgA (O.D. [450 - 570nm])
1.00
0.75
0.50
0.25
0.00
ns
ns
Diet: Control Psyllium Control Psyllium
Colonized from Birth
Colonized as Adults (day -14)
c
OMM12 Model Microbiota
Bacteroides caecimuris DSM 26085
Muribaculum intestinale DSM 28989
Akkermansia muciniphila DSM 26109
Turicimonas muris DSM 26109
Flavonifractor plautii DSM 26117
Clostridium clostridioforme DSM 26114
Blautia coccoides DSM 26115
Acutalibacter muris DSM 26090
Clostridium innocuum DSM 26113
Lactobacillus reuteri DSM 32035
Enterococcus faecalis DSM 32036
Bifidobacterium longum DSM 26074
Day 0 6 12 17
Control
Low Fiber
Control + 9% Psyllium
Low Fiber
d
OMM12 Microbiota
Anti-Psyllium IgM (O.D. [450 - 570nm])
1.00
0.75
0.50
0.25
0.00
***
Diet: Control Psyllium
Colonized from Birth
e
OMM12 Microbiota
Total Serum IgM (µg/mL)
300
200
100
0
Diet: Control Psyllium
Colonized from Birth
f
OMM12 Microbiota
Anti-Psyllium IgA (O.D. [450 - 570nm])
0.3
0.2
0.1
0.0
*
Diet: Control Psyllium
Colonized from Birth

Extended Data Fig. 10. Culturable mouse microbiota enables germ-free mice to generate anti-psyllium antibodies.

(a) Circulating anti-fiber IgM from germ-free C57BL/6 mice colonized with a conventionally raised mouse culture collection from birth or as adults eating a control or 9.2% w/w psyllium-supplemented diet for 12 days followed by a low fiber diet for 5 days was tested using a glycan-coated bead library. Each row represents the average of 6-7 mice. (b) Individual values for anti-psyllium IgM in serum on day 17 (Student's t test, *$p < 0.05$). (c) Circulating anti-fiber IgM from germ-free C57BL/6 mice colonized with an OMM12 community eating a control or 9.2% w/w psyllium-supplemented diet for 12 days followed by a low fiber diet for 5 days was tested using a glycan-coated bead library. Each row represents the average of 15-17 mice. Results are representative of 2 independent experiments. (d) Individual values for anti-psyllium IgM in serum on day 17 (Student's t test, ***$p < 0.001$). Heatmap values are corrected by subtracting the average of 3 secondary-only controls and the average of 2 empty bead populations. Bars, mean + SD or mean + 95% confidence interval (d).

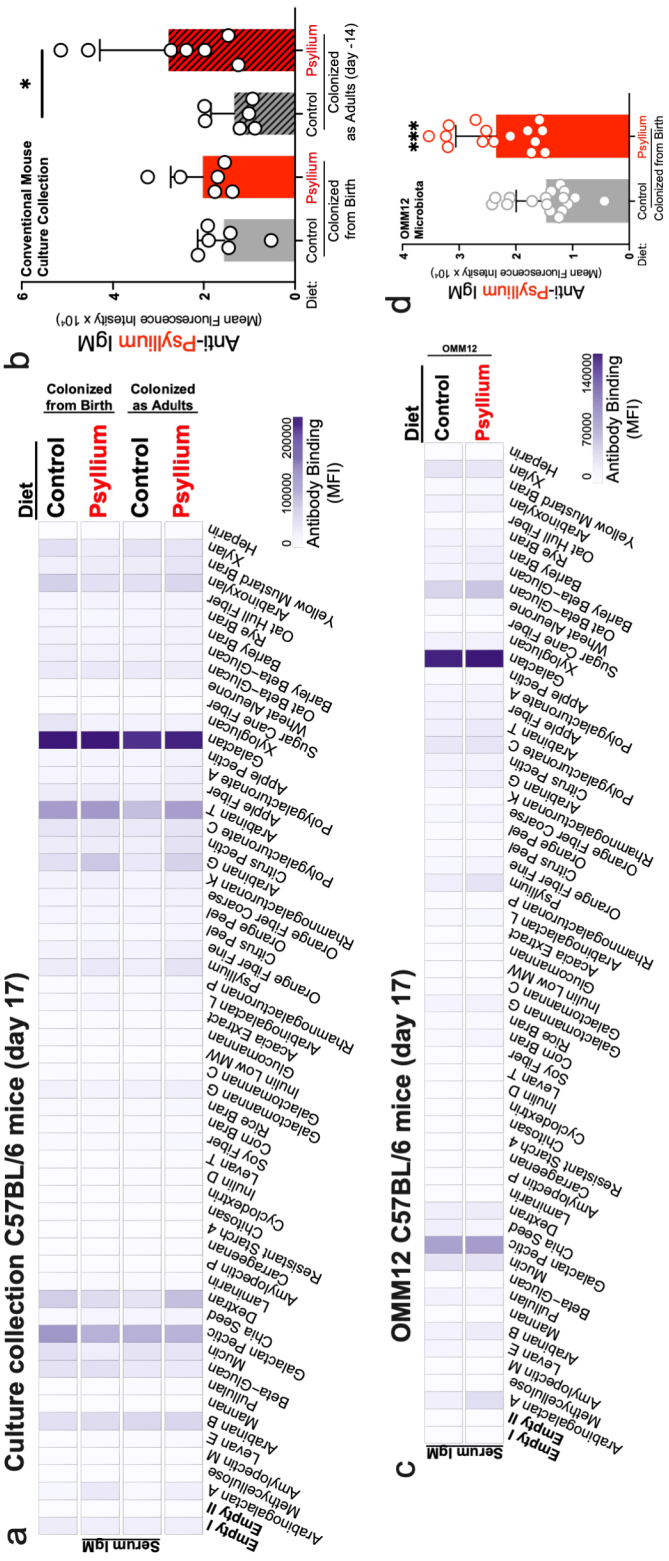
a
Culture collection C57BL/6 mice (day 17)
Diet
Control
Psyllium
Control
Psyllium
Colonized from Birth
Colonized as Adults
Serum IgM
Empty I
Empty II
Arabinogalactan A
Methylcellulose
Amylopectin M
Levan E
Arabinan B
Mannan
Pullulan
Beta-Glucan
Mucin
Galactan Pectic
Chia Seed
Dextran
Laminarin
Amylopectin P
Carrageenan
Resistant Starch 4
Chitosan
Cyclodextrin
Inulin D
Levan T
Soy Fiber
Corn Bran
Rice Bran
Galactomannan G
Galactomannan C
Inulin Low MW
Glucomannan
Acacia Extract
Arabinogalactan L
Rhamnogalactouronan P
Psyllium
Orange Fiber Fine
Citrus Peel
Orange Peel
Orange Fiber Coarse
Rhamnogalactouronan K
Arabinan G
Citrus Pectin
Polygalacturonate C
Arabinan T
Apple Fiber
Polygalacturonate A
Apple Pectin
Galactan
Xyloglucan
Sugar Cane Fiber
Wheat Aleurone
Oat Beta-Glucan
Barley Beta-Glucan
Barley Bran
Rye Bran
Oat Hull Fiber
Arabinoxylan
Yellow Mustard Bran
Xylan
Heparin
0
100000
200000
Antibody Binding (MFI)
b
Anti-Psyllium IgM
(Mean Fluorescence Intensity x 10⁴)
Conventional Mouse Culture Collection
Diet:
Control
Psyllium
Colonized from Birth
Control
Psyllium
Colonized as Adults (day -14)
*
c
OMM12 C57BL/6 mice (day 17)
OMM12
Diet
Control
Psyllium
Serum IgM
0
70000
140000
Antibody Binding (MFI)
d
Anti-Psyllium IgM
(Mean Fluorescence Intensity x 10⁴)
OMM12 Microbiota
***
Diet:
Control
Psyllium
Colonized from Birth

Monoclonal antibodies specific for diverse plant glycans bind the surfaces of gut microbes

Human gut strains from the *Bacteroidales* order adhere to particles covered with dietary fiber glycans with high affinity both *in vitro* and in the gut lumen (Patnode et al. 2021), raising the possibility that bacteria initiate bystander immune responses against fiber glycans on their surfaces. To comprehensively map the fiber glycans bound to microbial cell surfaces in the intestines of mice, we used a collection of 144 monoclonal antibodies specific for plant polysaccharides. These antibodies were generated by immunizing mice with glycans, carrier proteins, and microbial adjuvants via repeated intraperitoneal injection (Pattathil et al. 2010) and recognize a wide breadth of epitopes found in hemicellulose and pectin (including galactans, arabinans, mannans, xylans, galacturonans, and glucans). To first assess the specificities of these antibodies for our library of fiber glycans with defined monosaccharide and linkage composition, we incubated each antibody with the bead library and quantified binding by flow cytometry **(Fig. 5a)**. Hierarchical clustering revealed that beads coated with fibers from similar sources such as oat/wheat/barely (group I), apples (group II), and citrus (groups III and IV) exhibited similar antibody binding profiles **(Fig. 5b and Table S13)**. The discrete specificities represented in this collection of monoclonal antibodies also allowed us to detect subtle distinctions in multiple glycans from different sources, including arabinans (from sugar beet, ghatti gum, and tagaranth), arabinogalactans (from acacia and larch), galactomannans (from carob and guar), and rhamnogalacturonans (from potato and karaya). Thus, this antibody collection detects a wide range of dietary plant polysaccharides and can distinguish between epitopes with subtle structural differences.

The antibody panel was next used to identify which dietary polysaccharides are bound to the surfaces of microbes collected directly from the gut lumen. Fecal pellets were harvested from mice (n = 3 mice) eating a low fiber diet to decrease the likelihood of free dietary glycans sequestering the monoclonal antibodies and reducing binding to dietary

glycans on bacterial surfaces. Of the 144 tested antibodies, 31 bound both a significantly larger fraction than isotype control and also greater than 25% of the microbial community, and their specificities spanned diverse antigens including, arabinan, galactan, rhamnogalacturonan, xylan, and xyloglucan **(Fig. 5b and Table S13)**. To account for antibody staining of microbes that are present at low abundance (less than 25% of the community), we assessed the MFI (geometric mean fluorescence intensity) of this fraction for those that were significantly higher than the respective isotype control. This revealed 17 additional antibodies that strongly bound to microbial populations with low abundances. Overall, the percentage and MFI profiles were largely consistent with the exception of a low-abundance microbial population stained by antibodies recognizing chia seed. Sets of antibodies that shared similar specificity in the bead-binding assay showed discrepant binding to the same gut microbiota sample, which could be due to the sensitivity of some fiber glycan epitopes to microbial processing. Despite the high specificity of many of these antibodies for linkages unique to plants, it is possible that they exhibit cross-reactivity to microbially synthesized glycans with distinct linkage composition. We used glycoside hydrolases specific for beta-1,4-xylan (xylanase) and beta-1,4-xyloglucan (xyloglucanase) to cleave glycans on microbial surfaces before staining. Treatment with each enzyme reduced the binding of the corresponding antibody **(Fig. 5c)**, indicating the presence of stereotypical plant glycan structures. Xylan (21% binding) and xyloglucan (30% binding) were also detected on microbes in fecal pellets from mice colonized with the complete mouse microbiota culture collection **(Fig. 5d)**. In addition, significant populations of OMM12 gut microbes were also recognized by anti-xylan and anti-xyloglucan antibodies (25% binding and 32% binding, respectively) compared to isotype controls **(Fig. 5e)**. Together, these results indicate that microbes with fiber glycans on their surfaces are present in the communities that sensitize the host to produce anti-fiber antibodies.

Fig. 5. Plant glycans are detected on bacterial surfaces

(a) Schematic depicting high-throughput screening of the plant glycan monoclonal antibody library to define carbohydrate epitopes on the fiber bead library and on gut bacterial surfaces. (b) The left heatmap (purple) shows the specificities of monoclonal antibodies using a glycan-coated bead library. The antibodies and bead types are clustered by binding profiles (Ward's minimum variance). Each row represents the average of 2 technical replicates. The right heatmaps (green) depict antibody binding percentage (dark green, Syto+ only) and mean fluorescence intensity (light green, Syto+A488+ only) of gut microbes isolated from fecal samples (n = 3 mice) and stained with DNA-binding dye. The plotted values are background corrected by subtracting the average of 3 isotype control samples. (c) Enzymes specific for linkages in plant glycans were used to validate anti-xylan (xylanase) and anti-xyloglucan (xyloglucanase) antibody binding from the monoclonal antibody screen. Fecal pellets were collected from mice eating a low fiber diet and treated with either enzyme before antibody staining (Student's t test, *$p < 0.05$). (d and e) Anti-xylan (IgG, M140) or anti-xyloglucan (IgG, M104) binding to bacteria in fecal pellets from gnotobiotic mice colonized with the complete culture collection (d) or the defined OMM12 community (e). (Student's t test, ****$p < 0.0001$). Bars, mean + SD.

Fig. 5

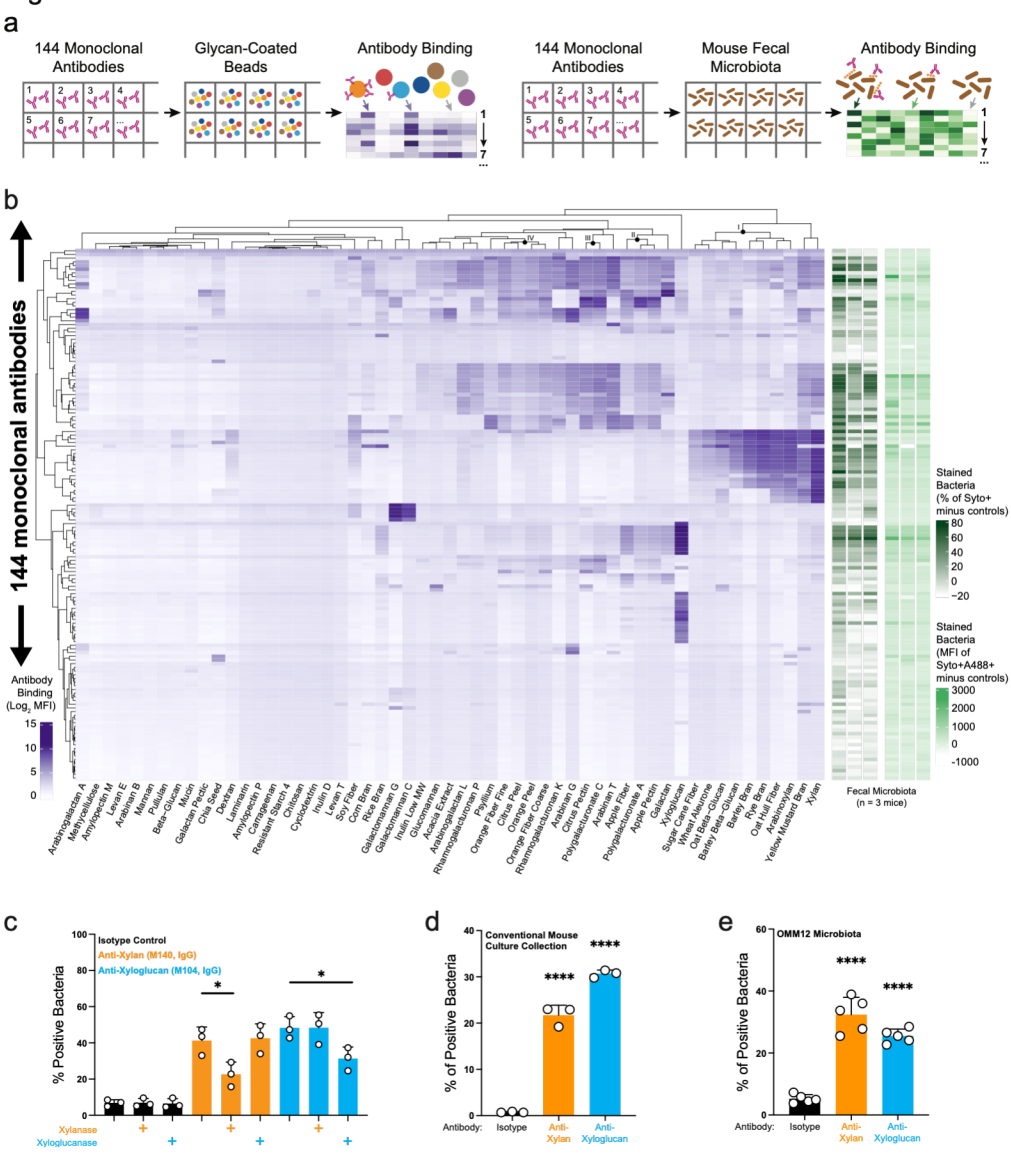
a
144 Monoclonal Antibodies
Glycan-Coated Beads
Antibody Binding
144 Monoclonal Antibodies
Mouse Fecal Microbiota
Antibody Binding
b
144 monoclonal antibodies
Antibody Binding (Log2 MFI)
Stained Bacteria (% of Syto+ minus controls)
Stained Bacteria (MFI of Syto+A488+ minus controls)
Fecal Microbiota (n = 3 mice)
c
Isotype Control
Anti-Xylan (M140, IgG)
Anti-Xyloglucan (M104, IgG)
% Positive Bacteria
Xylanase
Xyloglucanase
d
Conventional Mouse Culture Collection
% of Positive Bacteria
Antibody:
Isotype
Anti-Xylan
Anti-Xyloglucan
e
OMM12 Microbiota
% of Positive Bacteria
Antibody:
Isotype
Anti-Xylan
Anti-Xyloglucan

Discussion

IgA secreted into the intestine functions in part by binding luminal microbes and preventing their adhesion to or translocation across the intestinal epithelium, thereby maintaining mucosal compartmentalization (Mantis et al. 2011; Harris et al. 2006; Corthésy 2013). During homeostasis, anti-fiber IgA could similarly restrict the translocation of dietary glycans and glycan-coated microbes, but these antibodies also have the potential to shape the microbial ecosystem by blocking access to certain nutrients. While a secreted antibody targeting a bacterial protein has the potential to interfere with a limited set of related species (such as in the case of the fructan polysaccharide utilization locus of *Bacteroides thetaiotaomicron* VPI-5482 (Joglekar et al. 2019) a single anti-fiber IgA specificity could conceivably impact fiber harvest by many unrelated microbial taxa. The detection of IgA on gut bacteria (often referred to as “mFLOW” or “BugFACS”) is an increasingly standard assessment of the intestinal immune response. Our data indicate that IgA-positive bacteria identified using these tools include not only those that express targeted bacterial antigens but also those coated in dietary glycan antigens. Future studies will benefit from incorporating the contribution of anti-fiber IgA into the interpretation of IgA binding data. The ability of certain bacterial species to induce IgA responses to exogenous compounds has implications for the development of mucosal vaccines.

Fiber-specific IgM may function similarly to circulating antibodies that bind gut microbial surface structures and limit their dissemination during infection (Wilmore et al. 2018; Zeng et al. 2016). In cases of barrier disruption, anti-fiber antibodies could enable capture and degradation of fiber-coated microbes by immune cells to prevent their accumulation in the lamina propria. In other contexts, anti-fiber IgM could cause complement activation leading to inflammation. Previous work found that antibodies against *Streptococcus pneumonia* serotype 10A cross-react with plant pectin by virtue of a shared glycan epitope (beta-1,6-galactose) (Nahm et al. 2020). Although many of the polysaccharides recognized by the antibodies we report are unique to plants, this raises the prospect that gut bacterial

glycans could mimic these structures. These results highlight the need to further understand the interactions between dietary fiber, the microbiota, and the immune system, especially when considering the immense diversity of dietary glycans in human diets. Our approach using libraries of polysaccharide-coated beads will enable future studies investigating humoral responses against pathogen and vaccine antigens to assess the potential for related epitopes present in the diet.

Microbes synthesize surface proteins and carbohydrates that elicit antibody production. For example, in *Bacteroides fragilis*, genetic deletion of a locus necessary for colonization diminishes IgA coating (Donaldson et al. 2018), while in *Bacteroides thetaiotaomicron*, distinct capsular polysaccharides modulate antibody recognition and colonization (Porter et al. 2017). In addition, *Akkermansia*, *E.coli*, and *Lachnospiraceae* strains also induce microbe specific responses in mice (Zhang et al. 2023; Hapfelmeier et al. 2010; Ansaldo et al. 2019). These findings implicate separate microbial ligands for host pattern recognition receptors in the induction of antibodies against these structures. Our results demonstrating physical associations between dietary glycans and microbial surfaces, as well as rescue of anti-fiber antibody production in germ-free mice colonized with microbes coated in fiber glycans, support the notion that bacterial binding to fiber enhances the host response.

Microbes in the gut lumen are monitored through well-described antigen-sampling pathways, including M-cell transcytosis, dendritic cell uptake, and secretory cell antigen passages (Kulkarni and Newberry 2025). Although there are no established analogous translocation pathways for fiber, it is possible that fibers present on microbial surfaces enter through one or more of these routes. Previous studies have detected unelicited natural antibodies that recognize herbal polysaccharides (Kiyohara et al. 2006) and total IgA can be increased by fiber supplementation (Yamamoto et al. 2015; Yamamoto et al. 2016). However, it is unclear how high molecular weight plant polysaccharides gain access to glycan-specific B cells. Several factors could influence whether B cells are exposed to fiber glycans,

including structural features, lumenal environment (eg. mucus thickness) (Desai et al. 2016), and microbial degradation (Zhang et al. 2023; Hapfelmeier et al. 2010; Palm et al. 2014; Ansaldo et al. 2019). We observed that both poorly fermentable (psyllium) and readily fermentable (karaya and galactomannan) fiber-types induce antibodies, suggesting that fermentability alone does not dictate antibody induction. However, the precise contributions of these factors remain unknown, as does their applicability to different fiber classes.

Dietary fiber is widely recognized as a key contributor to human health and has been shown to modulate immune responses and influence outcomes across several disease contexts (Bindels et al. 2017; Alahmari 2024; Barber et al. 2020). Therapeutic diets with varying amounts of fiber have shown promise as a treatment for patients with inflammatory bowel disease (Barber et al. 2020; Di Rosa et al. 2022). However, the immense variety of glycan structures present across distinct tissues in each plant, and across plant species, has hampered progress in determining which fiber types are beneficial and in which individuals (Juritsch et al. 2026; Koropatkin et al. 2012). It is posited that these therapeutic diets act by altering metabolism in fiber-consuming microbes, but this mechanism has not been definitively confirmed. Furthermore, some dietary interventions appear to exert opposing effects on disease symptoms versus markers of inflammation (Di Rosa et al. 2022). Our findings suggest that anti-psyllium antibodies are present in previous psyllium feeding studies (Llewellyn et al. 2018; Bretin et al. 2023), although their contribution to the observed protection remains to be determined. Fulfilling the promise of personalized therapeutic fiber administration requires a deeper understanding of how plant glycans in fiber alter the immune system as well as the gut microbiota, both in healthy populations and in cases where the epithelial barrier is compromised (Haskey et al. 2023; Grosse et al. 2020).

Methods:

Mice

All experiments involving mice were carried out in accordance with protocols approved by the Animal Studies Committee of the University of California, Santa Cruz and the University of California, Berkeley. C57BL/6 and Swiss Webster mice (6-16 weeks) were reared and maintained in specific pathogen-free (SPF) facilities or, for gnotobiotic mice, maintained in cages located within flexible plastic isolators in the UCSC gnotobiotic facility or at UCB on an Innovive Innorack IVC Mouse 3.5 using Innovive's caging (M-BTM bottom, MVX3 containment lid). Cages contained paper towels for environmental enrichment. For gnotobiotic colonization, pre-colonization fecal pellets were collected and cultured to verify the sterility of the mice. Female and male mice were used, and no sex differences were observed in the reported measures. T cell-deficient mice (B6.129P2-*Tcrb*^{tm1Mom} *Tcrd*^{tm1Mom}/J) were obtained from Jackson Laboratories (002122). All mice were maintained on a strict light cycle (lights on at 0600h, off at 1800h).

Human Samples

Deidentified human serum samples were obtained from healthy adult and child participants enrolled in a collaborative study conducted at the International Centre for Diarrhoeal Disease Research, Bangladesh (icddr,b). The cohort comprised adults (21-41 years old) and children (3-4 years old) with no major gastrointestinal surgery, recurrent intestinal inflammation, recent COVID-19 infection, recent antibiotic use, recent diarrhea, or other recent vaccination. Serum samples were collected at enrollment and again at 1-week post-enrollment. Following collection, serum was processed according to standard clinical procedures, stored at -80°C, and maintained as deidentified specimens until downstream analysis.

Mouse feeding experiments

Dietary fibers (psyllium, karaya gum, and galactomannan) were either included at 9.2% w/w in a control diet during pelleting (Envigo, TD.170694 and Envigo, TD.250449) or mixed at 9.2% w/w with a powdered control diet (Envigo, T.2020XM) in collection cups (Avantor Science Central, 89508-716) or autoclavable bags (Fisher Scientific, 01-812-54). The prepared diets were then autoclaved for sterilization. On day 0, mice were switched from a pellet diet to the experimental diets for 11 or 12 days depending on experimental design. Powdered diets were hydrated with 100 mL of sterile water, and the resulting paste was pressed into a feeding dish and placed on the cage floor as previously described (Patnode et al. 2019). Food levels were monitored daily, and a freshly hydrated serving of the diet was supplied every 2 days. For experiments using antibiotics, ampicillin (1 g/L) and neomycin (0.5 g/L) were administered through the drinking water of mice 4 days before the initiation of experimental diets and continued for the duration of the experiment. Mice were switched to a low-fiber diet (Envigo, TD.130343) where indicated for 5 days.

Bacterial samples for mouse colonization

For preparing the complete mouse microbiota culture collection, cecal contents and fecal pellets were harvested from two separate mice, each eating a low-fiber diet for 15 weeks to limit potential strain candidates. Samples were added to 5 mL of filtered TYG supp (supplemented tryptone yeast glucose) media (Martens et al. 2008), mashed, filtered through a 100 µm cell strainer in an anaerobic chamber, and rinsed with 5 mL of filtered TYG. Filtrate (1 mL) was plated onto aerobic and anaerobic brain-heart-infusion (BHI) blood agar plates and allowed to grow at 37°C. After 5 days, the colonies were scraped and mixed in 5 mL of filtered TYG. The samples were then prepared in 1 mL aliquots for colonization. For colonization with clonal strains, aliquots of bacterial stocks were thawed, and the outer surfaces were sterilized with activated Clidox (Fisher Scientific, NC9122380 and NC0089321)

before transferring into gnotobiotic isolators. Cell suspension (200 uL) was administered through a plastic-tipped oral gavage needle. Equal volumes of bacterial stocks were combined when colonizing germ-free mice with multiple bacterial strains. The colonized mice were bred and maintained in plastic gnotobiotic isolators. Fecal pellets from the progeny were collected and filtered (40 μm) using 5 mL of sterile water. Filtrate (200 uL) was administered to age-matched gnotobiotic mice through a plastic-tipped oral gavage needle. Identities of commensal gut bacterial isolates, *Bacteroides ovatus* ATCC-8483 (ATCC), *Bacteroides ovatus* WH514 (Shoemaker et al. 2001), *Akkermansia muciniphila* NSD001 (Jax C57BL/6 microbiota), and *Escherichia coli* TSDC17.2 (Faith et al. 2013; Faith et al. 2014) were verified by full-length 16S rDNA sequencing. Each strain of the OMM12 community (Eberl et al. 2019) was grown according to the specifications provided by DSMZ, and pooled at equal OD600 for oral gavage of mice. C57BL/6NTac germ-free mice (Taconic Biosciences) were colonized with 200 μL of the OMM12 cocktail once via oral gavage as above. One week post-gavage, fecal samples were collected to confirm colonization using 16S amplicon sequencing.

Mouse sample collections

Blood was collected from live mice via submandibular vein puncture into serum separator tubes (Fisher Scientific, 02-675-185). Blood samples were allowed to clot at room temperature for 30 mins and then centrifuged at 18213xg speed for 5 mins at 4°C to isolate the serum. After centrifugation, sodium azide (0.05% v/v) was added and the serum stored at -80°C until analysis. Mice were euthanized individually by CO_2 asphyxiation followed by bilateral thoracotomy. Following euthanasia, whole blood was collected by cardiac puncture using a 22-gauge needle and processed in the same manner as described above. The cecum was collected, and a small incision was made in the cecal wall. Cecal contents were squeezed from the incision onto a sterile surface. The circular end of a sterile yellow plastic inoculation loop (Fisher Scientific, 22363600) was used to collect cecal contents (~3 loops

per mouse). Each loop was immediately flash-frozen in liquid nitrogen and transferred into a screw-cap tube. Samples were stored at -80°C until processing. For cecal content processing, a freshly made working solution (10 mL) of phosphate-buffered saline containing 0.01% sodium azide and one protease inhibitor tablet (Sigma, 11836170001) was prepared (PBS-SA-PI). Frozen cecal contents were weighed, and PBS-SA-PI was added (3 µL/mg of cecal contents). A sterile 3/8-inch stainless steel grinding ball (McMaster-Carr, 96455k73) was added to each tube. Samples were homogenized using a bead beater (Biospec, 1001) at 14000 rpm for 1 min, then centrifuged at 18213xg speed for 5 mins at 4°C. The resulting supernatant was transferred to a screw-cap tube, and additional sodium azide was added to a final concentration of 0.05% (v/v). Processed samples were stored at -80°C until further analysis.

Fiber glycan bead library

Biotinylated glycans were generated as described previously (Patnode et al. 2019). Briefly, glycan preparations were suspended in water at a concentration of 20 mg/mL, heated by sonicating for 1 min, and then centrifuged at 18213xg speed for 10 min. The resulting solutions were diluted 1:4 in water (v/v). TFPA-PEG3-biotin (Thermofisher, 21303), dissolved in DMSO at 10 mg/mL, was added to the glycan solutions at a ratio of 1:5 (v/v). Samples were subjected to UV irradiation for 10 mins (Fisher Scientific, 13-245-221) and then diluted 1:4 (v/v) to facilitate desalting using 96-well ZEBA plates with a 7kDa molecular weight cut-off (Thermo Scientific, 89808).

Biotinylated glycans were incubated with paramagnetic, streptavidin-coated silica beads (Millipore Sigma, LSKMAGT) at a 1:2 v/v ratio for 1 hr at room temperature. Beads were washed three times with 150 µL HNTB buffer (10 mM HEPES, 150 mM NaCl, 0.05% Tween-20, 0.1% bovine serum albumin) using a magnetic stand. Beads were subsequently incubated for 30 mins with 1 µg/mL streptavidin-fluorophore mixtures in HNTB. The process

of washing, biotin-glycan incubation, and re-washing was repeated for one additional cycle. No impact of streptavidin-fluorophore selection on antibody binding was detected after permutation of color combinations in replicate bead libraries.

Anti-fiber antibody detection assay

An aliquot of the pooled bead library was added to the wells of a 96-well plate. A 10-15 µL sample of monoclonal antibody (CarboSource, SKCMA-AM1 and SKCMA-AM2), serum, cecal contents, or colostrum was added to the beads and incubated at 4°C with constant rotation for 1 hr. The beads were then collected using a magnetic rack and washed three times with 150 µL HNTB. Beads were incubated with the appropriate fluorescent secondary antibodies (1 µg/mL) at 4°C with constant rotation for 30 mins and washed three times with 150 µL HNTB. Beads were run on an LSR II (BD Biosciences), CytoFLEX (Beckman Coulter), or Attune (Thermo Fisher Scientific). The beads were identified based on streptavidin fluorescence, and fluorescence of the secondary antibody was measured for each bead type. Separate aliquots of the bead library were incubated with fluorescent secondary antibodies in the absence of primary antibodies to establish background fluorescence levels.

ELISA

Carbohydrates were diluted with sterile water (1:1000) and 60 µL was plated onto Immulon 2HB 96-well plates (Thermo Fisher Scientific, 3455). The plates were left at 37°C overnight, uncovered to induce complete evaporation. The following day, the plates were washed with 200 µL PBS containing 1% Tween-20 (PBS-T) and blocked for 1 hr at 4°C with 200 µL/well blocking buffer (PBS containing 1-5% bovine serum albumin). The plates were then washed three times with 200 µL PBS-T and incubated with 50 µL diluted serum (1:50, 1:100, or 1:200 with PBS-T) or cecal contents (1:10 or 1:25 with PBS-T) for 1 hr at 4°C. For detection, plates

were washed three times with 200 µL PBS-T, and bound antibodies were detected using 50 µL of the appropriate horseradish peroxidase (HRP)-conjugated secondary antibodies (1 µg/mL) and incubated for 30 mins at 4°C. After washing three times with 200 µL PBS-T, 50 µL/well of 3,3′,5,5′-tetramethylbenzidine (TMB) substrate (Thermo Fisher Scientific, N301) was added, and the reaction was developed for 5-15 mins in the dark. The reaction was stopped with 50 µL/well of 0.2 M sulfuric acid, and the absorbance was read at 450 nm and 570 nm using a microplate reader.

Unconjugated capture antibodies were diluted to 0.5 µg/mL with PBS and plated onto Immulon 2HB 96-well plate(s) (Thermo Fisher Scientific, 3455) and incubated overnight at 4°C with 60 µL/well. The following day, the plates were blocked as described above. The plates were then washed three times with 200 µL PBS-T, and samples were diluted with PBS-T and added at 50 µL/well. A standard curve was prepared using serial dilutions (1:2) of purified antibodies of the same isotype as the target, starting at 2 µg/mL or 0.5 µg/mL. Plates were incubated for 1 hr at 4°C, followed by three washes with 200 µL PBS-T. The plates were then processed for detection as described above.

Microbial flow cytometry

Fresh fecal pellets were collected from mice and weighed. Fecal pellets received 1 mL of PBS containing 1% bovine serum albumin and 0.05% sodium azide (BS-PBS). A sterile 3/8-inch stainless steel grinding ball (McMaster-Carr, 96455k73) was placed into each tube, and samples were homogenized using a bead beater (Biospec, 1001) at 1,400 rpm for 1 min. Following homogenization, the homogenized samples were filtered twice through a 70 µm nylon mesh filter to remove debris. Filtrates were then transferred to a U-bottom 96-well plate with volumes adjusted based on sample weights to achieve a final concentration of 0.5-1 mg of fecal material per well. Bacterial pellets were washed twice by centrifugation at 3,220xg for 5 mins at 4 °C. Where indicated, bacterial pellets were incubated with 50 µL BS-PBS, diluted

xylanase (1 U/mL with BS-PBS [Neogen, E-XYLNP]), or diluted xyloglucanase (1 U/mL with BS-PBS [Neogen, E-XEGP]) for 15 mins at 37 °C on a plate shaker at 250 rpm (SCILOGEX, 822000049999) and then washed twice by centrifugation at 3,220xg for 5 mins at 4°C. Bacterial pellets were resuspended with 20 µL of diluted monoclonal antibodies (1 µg/mL with BS-PBS) or the respective isotype control (1 µg/mL) and incubated for 1 hr at 4°C on a plate shaker at 250 rpm. Following incubation, samples were washed twice with 200 µL BS-PBS by centrifugation (3,220xg, 5 mins, 4 °C). 50 µL of fluorescent secondary antibodies (1 µg/mL) stained bacterial pellets for 30 mins at 4 °C with shaking. After washing twice, the samples were stained with 50µL of 10 µM Syto62 (Thermo Fisher Scientific, S11344) and incubated for 5 mins at room temperature in the dark with shaking. Samples were washed twice and resuspended with a final volume of 150 µL BS-PBS. The final suspensions were passed through a 70 µm filter into a U-bottom plate to remove aggregates.

V4 16S rDNA sequencing

Fecal DNA was isolated using the DNeasy PowerSoil Pro Kit (Qiagen, 47014). Extracted DNA was quantified using Qubit, normalized, and the V4 region was PCR amplified. Each V4 amplicon was annealed to a sample-specific i5 and i7 Illumina adapter index. The samples were pooled at equal concentration and run on a 2x250 MiSeq Illumina instrument. Reads were demultiplexed and analyzed using QIIME2 (version 2021.4). Sequences were singlet filtered and used to generate amplicon sequence variants (ASVs). The taxonomy was assigned by the Silva 138 classifier for the 515F/806R region (V4). These results were then summarized to produce sequence counts and the relative abundance of taxa per sample.

Statistics and Reproducibility

Statistical analysis was performed in GraphPad Prism 11 and R (v4.5.2) using RStudio (v2026.01.0+392). All glycan bead flow cytometry data is presented in supplementary tables

including empty bead values, which were averaged and used for background subtraction unless otherwise indicated. For statistical testing, bead types were filtered for those where the raw signal was significantly greater than that of empty beads (Paired t-test and Benjamini-Hochberg (BH) FDR p value correction, $q < 0.1$) and exceeded a minimum fold change threshold (FC >= 1.5) in at least one of the two groups being compared. After filtering, differences between groups were calculated using a Student's t test and BH FDR p value correction ($q < 0.05$) and exceeding a minimum fold change threshold (FC >= 1.5 for mouse samples and FC >= 1.25 for human samples), unless otherwise indicated. For analysis of correlations between antibody responses to glycans in human samples, a Spearman's rank correlation coefficient was calculated for each glycan-glycan pair across individuals. For anti-fiber bar plots, antibody binding to bacteria, and ELISAs, significance was determined using Student's t test. For anti-psyllium antibody comparisons collected from mice at different time points, significance was determined using a paired t-test. All t-tests were two-tailed with a p-value cutoff of 0.05. Mean values and standard deviations or 95% confidence intervals are shown in the figures as indicated.

Chapter 3: Antibody-mediated interactions with gut microbes

Giovanni Vega[1,2] and Michael L. Patnode[1,*]

[1] Department of Microbiology and Environmental Toxicology, University of California, Santa Cruz, Santa Cruz, CA, 95064 USA.

[2] Graduate Program in Biological Sciences and Engineering, University of California, Santa Cruz, Santa Cruz, CA, 95064 USA.

* Correspondence: mpatnode@ucsc.edu

Introduction:

Due to the abundance of carbon sources in the mammalian gut, nitrogen often serves as a limiting nutrient for microbes (Reese et al. 2018). Nitrogen is an essential element for the growth of bacteria and contributes to the synthesis of proteins, nucleic acids, and peptidoglycan. Soluble nitrogen sources, including dietary nitrate and excreted urea, are harvested by bacteria in the intestine. Isotope tracing studies demonstrated that Firmicutes obtain nitrogen from host urea while Bacteroidota (formerly Bacteroidetes) rely more on host mucin in a simplified diet context (Zeng et al. 2022). Although the delineation of nitrogen sources that support gut microbes in a typical, complex human diet context is not easily determined, the importance of nitrogen is made clear by the expression of nitrogen acquisition genes induced by fiber supplementation (Wu et al. 2015).

Animal-derived foods typically contain higher total protein content than plant foods, and as such, the majority of protein in most adult human diets comes from consuming mammals, fish, poultry, and dairy (Mariotti and Gardner 2019). While host proteases are capable of breaking down a majority of the protein from animal-derived foods, collagen is not highly soluble in water (Telis et al. 2006), and has been shown to survive digestion processes (Xu et al. 2021). Bacteria from the *Staphylococcus*, *Streptococcus*, *Enterococcus*, and *Bacillus* genera have been shown to encode proteins that bind to human collagen for tissue colonization and host infection (Arora et al. 2021), demonstrating that collagen can act as a substratum for adhesion. In addition, mice fed a high-fat diet supplemented with collagen from fish skin exhibited an increase in the abundance of *Bacteroides*, *Streptococcus*, *Faecalibaculum*, and *Clostridium* in the intestine (Baek et al. 2023).

Bacteria can also obtain nitrogen from sources originating from the epithelium. The epithelial mucus layer undergoes constant renewal as mucin glycoproteins are secreted and form a gel in the gut lumen (Pelaseyed et al. 2014). Some human gut microbes are known to utilize mucin as a nitrogen source, including *Akkermansia muciniphila* and members of the

Bacteroides genus (Pan et al. 2022; Tailford et al. 2015). *Akkermansia* and *B. thetaiotaomicroniotamicron* compete with one another *in vitro* and *in vivo*, and genes involved in carbohydrate metabolism, glycan biosynthesis, and antimicrobial activity were associated with their interactions (Kostopoulos et al. 2021). In addition to secreted proteins, epithelial cells themselves that are sloughed into the lumen (Ngo et al. 2022) contain abundant protein, nucleic acids, glycosaminoglycans, and membrane-derived phospholipids, such as phosphatidylethanolamine, that can form concentrated regions rich in nitrogen-containing compounds (Pickard et al. 2017; Anderson et al. 2021). Phosphatidylethanolamine in the membranes of these cells can be broken down by phosphodiesterases into ethanolamine and glycerol, which provide nutrient sources for certain gut microbes, including species in the Pseudomonadota (formerly Proteobacteria) phylum (Pickard et al. 2017; Anderson et al. 2021; Rowley et al. 2018). Nonpathogenic *E. coli* strains were observed to outcompete pathogenic *E. coli* (EHEC) when cultivated in minimal media containing ethanolamine plus glucose or glycerol (Rowley et al. 2018).

In addition to mucins and sloughed epithelial cells, antibodies represent another class of abundant host-derived proteins encountered by gut microbes within the intestinal lumen. Secretory IgA (sIgA) is the predominant antibody isotype at mucosal surfaces and accounts for the majority of antibodies secreted at mucosal tissues (Mantis et al. 2011; Pabst 2012). Consequently, gut microbes are continuously exposed to these glycoproteins. One of the primary functions of sIgA is to coat microbes, limiting their interaction with the intestinal epithelium and facilitating their removal through normal peristaltic movements, thereby contributing to immune exclusion and shaping microbiota composition (Mantis et al. 2011; Pabst 2012; Macpherson et al. 2018). In addition to recognizing microbial surfaces, we showed in Chapter 2 that antibodies recognize dietary polysaccharides, positioning them at the interface between host immunity and microbial nutrient acquisition.

Antibodies are continuously secreted into the intestinal lumen, where they undergo continual turnover through both host- and microbe-derived proteolytic processes. Moon and colleagues demonstrated that gut microbial communities possess proteolytic activity capable of degrading the secretory component of sIgA, indicating that members of the mouse intestinal microbiota can directly modulate antibody levels within the gut lumen (Moon et al. 2015). Numerous bacterial species, particularly mucosal pathogens, encode sIgA-degrading proteases, which are primarily characterized as immune-evasion factors that facilitate bacterial persistence and mucosal colonization (Plaut 1983; Lu et al. 2024; Mistry and Stockley 2006). Although bacterial antibody degradation has been well documented, the ecological consequences of this process remain poorly understood. In particular, it is unclear whether antibody degradation solely promotes immune evasion or whether it also provides a nitrogen source to gut microbes living in a nitrogen-limiting environment.

Collectively, these observations suggest that antibodies occupy a unique position connecting host immunity and microbial nutrient acquisition. As abundant host-derived glycoproteins that bind dietary polysaccharides and are susceptible to bacterial proteolysis, antibodies have the potential to influence microbial biology through multiple mechanisms. However, whether antibodies primarily serve as nutrient reservoirs following degradation or modulate microbial interactions with dietary substrates remains unknown. Here, we investigated these possibilities by examining bacterial-mediated antibody degradation, antibody utilization as a nitrogen source, and the effects of antibody binding on bacterial adhesion, substrate hydrolysis, and growth.

Results:

Gut bacteria degrade antibodies through protease-dependent mechanisms

To determine whether cecal contents from mice in our facilities contain antibody-degrading activity, we incubated purified mouse IgA immobilized on an ELISA plate with conventional C57BL/6 cecal contents. The cecal contents were spun down to separate the supernatant from the pelleted material and incubated separately with the plated IgA in the presence or absence of a broad-spectrum protease inhibitor (inhibits serine, cysteine, and metalloproteases). Both the cecal slurry and cecal supernatant reduced detectable IgA to similar levels, and inclusion of the protease inhibitor partially restored IgA signal (Figure 1A). Germ-free Swiss albino cecal contents similarly reduced detectable IgA levels, and the activity was likewise diminished by the protease inhibitor. Together, these findings demonstrate that intestinal contents from mice contain soluble protease-dependent activity capable of degrading IgA.

Since cecal contents contain a complex mixture of host- and microbially-derived proteins, we next sought to determine whether individual human gut bacterial isolates possess antibody-degrading activity. Eight representative human gut bacterial isolates, including strains of *Bacteroides cellulosilyticus* and *Phocaeicola vulgatus*, were grown in either tryptone-yeast extract-glucose (TYG) or minimal medium (MM), and incubated with purified mouse IgA as described above. Antibody degradation varied considerably among the tested isolates and depended on growth conditions. Several isolates consistently reduced detectable IgA, whereas others exhibited little or no degradation under the tested conditions (Figure 1B). In addition, antibody degradation differed between TYG and MM, suggesting that antibody degradation is a strain-dependent phenotype that is influenced by bacterial growth conditions.

To determine whether antibody degradation by representative gut bacterial isolates was protease-dependent, the eight representative strains were incubated with immobilized mouse IgA in the presence or absence of a protease inhibitor. The inclusion of a protease inhibitor significantly restored detectable IgA for several isolates, demonstrating that antibody degradation was largely protease-dependent (Figure 1C). However, the extent of rescue varied among isolates, indicating that the contribution of protease activity differs between strains. Similar results were obtained using purified mouse IgG, as representative isolates likewise reduced detectable IgG and protease inhibition restored antibody signal (Figure 1D), indicating that this degradative activity is not restricted to IgA.

Figure 1. Gut bacterial communities degrade antibodies through protease-dependent mechanisms.

(A) Cecal slurries and clarified cecal supernatants from germ-free Swiss albino (blue) and conventional C57BL/6 (red) mice were incubated with plate-bound mouse IgA in the presence or absence of a broad-spectrum protease inhibitor (white dashed lines). PBS-T and pepsin served as negative and positive controls, respectively. Bars represent the mean ± SD, and individual points represent biological replicates (n = 3). Statistical significance was determined by Welch's t-test. $p < 0.01$ (**) and $p < 0.001$ (***). (B) Eight representative human gut bacterial isolates were grown in either tryptone-yeast extract-glucose (TYG) or minimal medium before incubation with plate-bound mouse IgA. Remaining IgA was quantified by ELISA. PBS-T and pepsin served as negative and positive controls, respectively. Each strain was screened once. (C and D) Representative human gut bacterial isolates were grown in TYG medium, normalized by optical density, and incubated with plate-bound mouse IgA (C) or IgG (D) in the presence or absence of a broad-spectrum protease inhibitor. TYG medium and pepsin served as negative and positive controls, respectively. Bars represent the mean ± SD, and individual points represent biological replicates (n = 3). Statistical significance was determined by Welch's t-test. $p < 0.05$ (*), $p < 0.01$ (**), and $p < 0.001$ (***).

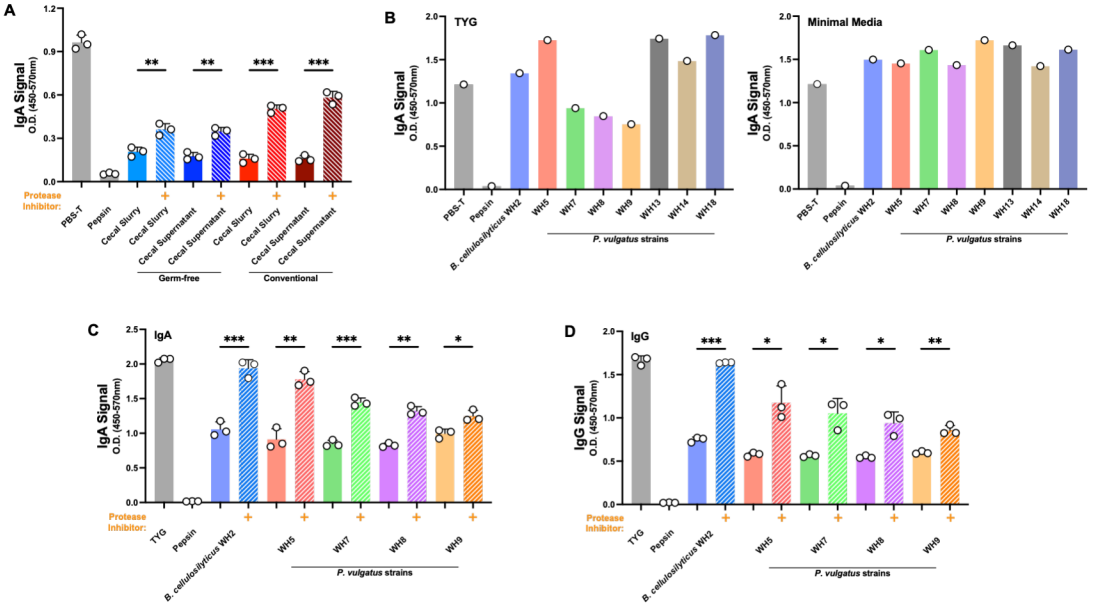

Human IgG does not broadly support bacterial growth under nitrogen-limited conditions

Having established that representative human gut bacterial isolates proteolytically degrade both IgA and IgG, we next investigated whether human IgG supports bacterial growth as the sole nitrogen source. To test this, a collection of human gut bacterial isolates was cultured in nitrogen-limited minimal medium supplemented with purified human IgG as the only exogenously supplied nitrogen source. Bacterial growth was monitored over 48 hours to determine whether IgG was sufficient to support growth. Under these conditions, the isolates exhibited little or no increase in optical density (Figure 2 and Table 1) and indicate that human IgG supplementation does not support bacterial growth under the conditions tested.

Figure 2. Human IgG does not support bacterial growth.

Representative human gut bacterial isolates were cultured in nitrogen-limited minimal medium containing purified human IgG as the sole nitrogen source. Bacterial growth was monitored by measuring optical density at 595 nm over 48 h. Data represent a representative screen, and Table 1 summarizes the complete bacterial strain collection.

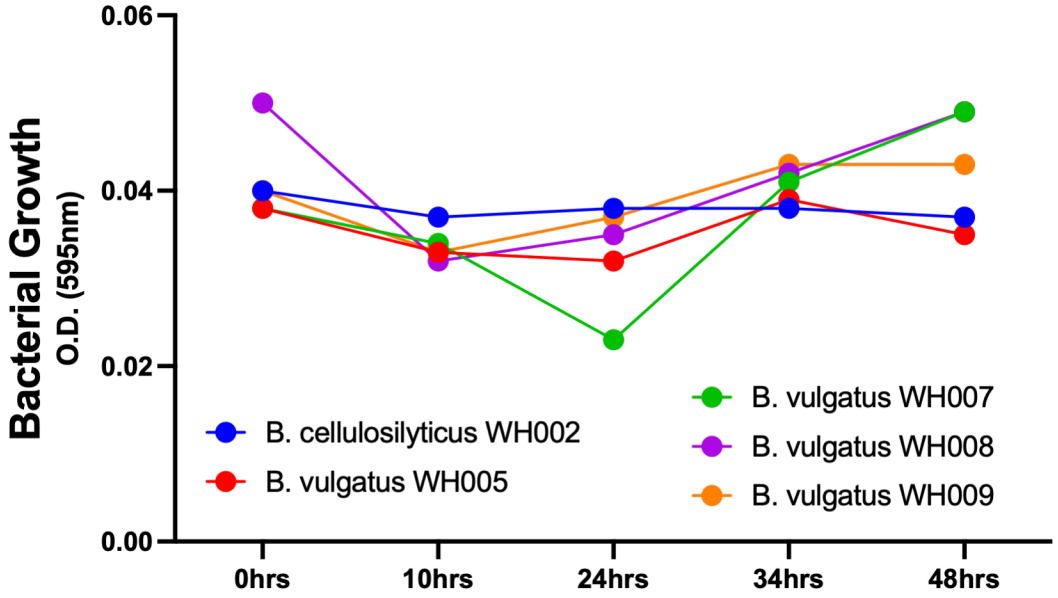

Table 1. Human IgG does not support bacterial growth

Sample	0hrs	10hrs	24hrs	34hrs	48hrs	48hrs - 0hrs
BLANK	0.039	0.033	0.032	0.033	0.033	-0.006
BLANK	0.04	0.033	0.033	0.034	0.042	0.002
BLANK	0.039	0.033	0.04	0.046	0.049	0.01
BLANK	0.051	0.032	0.037	0.044	0.05	-0.001
BLANK	0.034	0.033	0.039	0.042	0.041	0.007
BLANK	0.034	0.033	0.035	0.033	0.036	0.002
BLANK	0.034	0.022	0.033	0.047	0.033	-0.001
B. cellulosilyticus WH002	0.04	0.037	0.038	0.038	0.037	-0.003
B. vulgatus WH019	0.027	0.031	0.032	0.035	0.041	0.014
B. ovatus WH208	0.035	0.042	0.042	0.041	0.038	0.003
B. thetaiotaomicron WH502	0.039	0.039	0.043	0.045	0.046	0.007
B. vulgatus WH515	0.039	0.032	0.042	0.037	0.041	0.002
B. ovatus WH713	0.039	0.038	0.051	0.042	0.052	0.013
P. distasonis VPI-C19-17	0.039	0.034	0.037	0.035	0.03	-0.009
B. thetaiotaomicron VPI-C11-15	0.039	0.04	0.041	0.047	0.044	0.005
B. vulgatus VPI-4245	0.038	0.033	0.029	0.046	0.047	0.009
B. dorei VPI-3776A	0.039	0.033	0.033	0.04	0.043	0.004
B. vulgatus VPI-4506	0.038	0.032	0.033	0.033	0.034	-0.004
B. xylanisolvens VPI-BOv7991	0.039	0.034	0.041	0.043	0.047	0.008
B. vulgatus WH005	0.038	0.033	0.032	0.039	0.035	-0.003
B. faecis WH021	0.041	0.04	0.048	0.049	0.05	0.009
B. xylanisolvens WH213	0.04	0.037	0.039	0.039	0.037	-0.003
B. thetaiotaomicron WH503	0.04	0.04	0.044	0.052	0.046	0.006
B. vulgatus WH516	0.038	0.037	0.034	0.028	0.048	0.01
B. vulgatus WH715	0.039	0.043	0.042	0.042	0.047	0.008
P. distasonis VPI-C14-2	0.041	0.03	0.04	0.043	0.05	0.009
B. ovatus VPI-435	0.04	0.035	0.044	0.045	0.044	0.004
B. dorei VPI-2277	0.039	0.032	0.037	0.039	0.037	-0.002
B. thetaiotaomicron VPI-3164	0.048	0.043	0.044	0.042	0.042	-0.006
B. ovatus VPI-4496.2	0.048	0.033	0.038	0.041	0.036	-0.012
B. fragilis VPI-BV8526	0.05	0.036	0.043	0.045	0.045	-0.005
B. vulgatus WH007	0.038	0.034	0.023	0.041	0.049	0.011
B. cellulosilyticus WH101	0.038	0.035	0.035	0.042	0.043	0.005
B. ovatus WH214	0.04	0.039	0.045	0.045	0.042	0.002
B. thetaiotaomicron WH507	0.041	0.04	0.046	0.047	0.047	0.006

Sample	0hrs	10hrs	24hrs	34hrs	48hrs	48hrs - 0hrs
P. distasonis WH517	0.043	0.037	0.036	0.036	0.035	-0.008
B. vulgatus WH716	0.039	0.033	0.033	0.035	0.039	0
P. distasonis VPI-C18-7	0.042	0.036	0.036	0.037	0.037	-0.005
. VPI-C2-26	0.039	0.033	0.033	0.033	0.034	-0.005
B. thetaiotaomicron VPI-2808B	0.041	0.038	0.042	0.042	0.042	0.001
B. thetaiotaomicron VPI-BT-DOT2	0.041	0.04	0.043	0.047	0.047	0.006
P. distasonis WAL8975	0.041	0.034	0.036	0.041	0.046	0.005
B. vulgatus WH008	0.05	0.032	0.035	0.042	0.049	-0.001
B. dorei WH106	0.044	0.034	0.04	0.045	0.05	0.006
. WH303	0.04	0.033	0.032	0.033	0.042	0.002
B. thetaiotaomicron WH508	0.039	0.033	0.039	0.04	0.041	0.002
B. ovatus WH601	0.04	0.039	0.043	0.043	0.043	0.003
P. distasonis VPI-4243	0.03	0.033	0.033	0.033	0.034	0.004
B. thetaiotaomicron VPI-5482A	0.035	0.039	0.043	0.045	0.047	0.012
B. ovatus VPI-C16-22	0.04	0.054	0.047	0.047	0.053	0.013
B. vulgatus VPI-5710	0.04	0.035	0.044	0.048	0.058	0.018
B. thetaiotaomicron VPI-0633-1	0.039	0.04	0.056	0.047	0.049	0.01
P. distasonis VPI-BD6803	0.04	0.035	0.041	0.038	0.032	-0.008
P. distasonis WAL9063	0.04	0.038	0.044	0.036	0.029	-0.011
B. vulgatus WH009ab	0.04	0.033	0.037	0.043	0.043	0.003
B. vulgatus WH108	0.038	0.034	0.034	0.038	0.045	0.007
B. thetaiotaomicron WH509	0.043	0.041	0.046	0.056	0.048	0.005
B. ovatus WH604	0.039	0.04	0.045	0.054	0.041	0.002
P. distasonis VPI-B1-20	0.04	0.035	0.035	0.038	0.035	-0.005
Staphylococcus pasteuri VPI-J19-343	0.04	0.049	0.043	0.047	0.048	0.008
B. ovatus VPI-B4-11	0.04	0.043	0.038	0.042	0.041	0.001
B. vulgatus VPI-C1-13	0.039	0.035	0.033	0.023	0.042	0.003
B. ovatus VPI-3049	0.039	0.033	0.041	0.041	0.047	0.008
P. merdae VPI-BD6944	0.04	0.024	0.036	0.04	0.044	0.004
B. thetaiotaomicron WAL8713	0.04	0.033	0.043	0.046	0.046	0.006
B. vulgatus WH013	0.039	0.044	0.05	0.044	0.053	0.014
B. vulgatus WH109	0.039	0.04	0.048	0.043	0.047	0.008
B. xylanisolvens WH404	0.04	0.039	0.04	0.039	0.033	-0.007
B. thetaiotaomicron WH510	0.04	0.041	0.046	0.048	0.038	-0.002
B. dorei WH607	0.039	0.034	0.025	0.04	0.035	-0.004
P. distasonis VPI-C30-45	0.039	0.034	0.03	0.04	0.044	0.005

Sample	0hrs	10hrs	24hrs	34hrs	48hrs	48hrs - 0hrs
B. thetaiotaomicron VPI-11984	0.04	0.04	0.045	0.046	0.045	0.005
B. dorei VPI-6598B	0.041	0.034	0.039	0.046	0.045	0.004
B. ovatus VPI-4104	0.04	0.04	0.043	0.046	0.045	0.005
P. distasonis VPI-BD6781	0.04	0.035	0.035	0.036	0.036	-0.004
B. thetaiotaomicron WAL8669	0.04	0.041	0.043	0.049	0.044	0.004
B. vulgatus WH014	0.04	0.035	0.041	0.049	0.057	0.017
B. dorei WH111	0.039	0.033	0.035	0.025	0.038	-0.001
B. thetaiotaomicron WH408	0.039	0.028	0.034	0.031	0.034	-0.005
B. dorei WH512	0.039	0.024	0.034	0.038	0.043	0.004
P. distasonis VPI-T3-25	0.049	0.036	0.038	0.038	0.045	-0.004
B. thetaiotaomicron VPI-3443	0.043	0.04	0.043	0.045	0.045	0.002
B. ovatus VPI-C1-45	0.041	0.039	0.044	0.044	0.044	0.003
Staphylococcus caprae VPI-2365	0.04	0.033	0.042	0.053	0.067	0.027
B. salyersiae VPI-2828	0.032	0.038	0.041	0.042	0.043	0.011
B. thetaiotaomicron VPI-BT7853	0.033	0.04	0.042	0.045	0.043	0.01
B. faecis WAL8736	0.039	0.043	0.047	0.048	0.055	0.016
B. vulgatus WH018	0.039	0.034	0.034	0.035	0.036	-0.003
B. vulgatus WH202	0.039	0.043	0.034	0.036	0.053	0.014
B. thetaiotaomicron WH501	0.04	0.04	0.046	0.051	0.055	0.015
B. ovatus WH514	0.039	0.043	0.044	0.05	0.048	0.009
B. ovatus WH711	0.04	0.042	0.045	0.047	0.048	0.008
VPI-56A-56	0.04	0.044	0.035	0.036	0.037	-0.003
B. thetaiotaomicron VPI-0940-1	0.039	0.037	0.112	0.04	0.043	0.004
B. ovatus VPI-8653	0.04	0.04	0.044	0.043	0.045	0.005
B. vulgatus VPI-4025	0.04	0.036	0.054	0.074	0.085	0.045
B. thetaiotaomicron VPI-6186	0.039	0.033	0.034	0.055	0.059	0.02
VPI-BT8702	0.039	0.05	0.041	0.046	0.041	0.002
B. thetaiotaomicron WAL8655	0.039	0.04	0.033	0.037	0.051	0.012
B. thetaiotaomicron 22866	0.034	0.04	0.053	0.042	0.042	0.008
B. thetaiotaomicron 23113	0.033	0.037	0.045	0.039	0.041	0.008
B. thetaiotaomicron 23190	0.034	0.039	0.034	0.043	0.042	0.008
B. thetaiotaomicron 23272	0.033	0.039	0.034	0.044	0.054	0.021
B. thetaiotaomicron 23580	0.042	0.04	0.041	0.049	0.046	0.004
B. vulgatus 23673	0.043	0.032	0.034	0.032	0.032	-0.011
B. thetaiotaomicron 23692	0.036	0.04	0.043	0.043	0.041	0.005
B. faecis 23730	0.035	0.031	0.039	0.044	0.042	0.007

Sample	0hrs	10hrs	24hrs	34hrs	48hrs	48hrs - 0hrs
B. thetaiotaomicron TS20APG1.1	0.029	0.051	0.045	0.046	0.043	0.014
B. thetaiotaomicron TS120APG1.1	0.025	0.043	0.042	0.043	0.045	0.02
B. thetaiotaomicron BT7330-1	0.032	0.042	0.045	0.054	0.049	0.017
DH4119	0.034	0.023	0.032	0.044	0.033	-0.001
B. thetaiotaomicron 22911	0.034	0.04	0.045	0.044	0.041	0.007
B. thetaiotaomicron 23114	0.034	0.037	0.041	0.041	0.042	0.008
B. caccae 23205	0.033	0.032	0.033	0.034	0.033	0
B. thetaiotaomicron 23367	0.035	0.038	0.043	0.043	0.046	0.011
B. thetaiotaomicron 23584	0.034	0.038	0.043	0.044	0.045	0.011
B. faecis 23677	0.034	0.039	0.042	0.042	0.039	0.005
B. vulgatus 23693	0.033	0.035	0.043	0.046	0.047	0.014
B. ovatus 23734	0.035	0.041	0.057	0.045	0.039	0.004
B. thetaiotaomicron TS21APG1.1	0.034	0.04	0.043	0.043	0.041	0.007
B. thetaiotaomicron TS61APG1.1	0.035	0.037	0.041	0.041	0.039	0.004
B. thetaiotaomicron DH4108	0.034	0.038	0.038	0.041	0.04	0.006
B. thetaiotaomicron 22913	0.045	0.036	0.04	0.037	0.039	-0.006
B. thetaiotaomicron 23149	0.023	0.04	0.042	0.039	0.041	0.018
B. fragilis 23212	0.03	0.039	0.039	0.039	0.04	0.01
B. thetaiotaomicron 23368	0.035	0.033	0.04	0.04	0.042	0.007
B. thetaiotaomicron 23586	0.035	0.029	0.042	0.047	0.045	0.01
B. faecis 23680	0.034	0.034	0.039	0.052	0.044	0.01
23698	0.033	0.033	0.033	0.034	0.043	0.01
B. ovatus 23735	0.034	0.042	0.045	0.033	0.039	0.005
B. thetaiotaomicron TS130APG1.1	0.034	0.039	0.042	0.037	0.052	0.018
B. thetaiotaomicron TS62APG1.1	0.035	0.037	0.04	0.048	0.045	0.01
B. thetaiotaomicron BT8702	0.035	0.039	0.041	0.044	0.031	-0.004
B. thetaiotaomicron DH4111	0.035	0.039	0.042	0.044	0.039	0.004
B. faecis 22953	0.035	0.041	0.046	0.04	0.041	0.006
B. faecis 23150	0.034	0.042	0.045	0.042	0.044	0.01
B. thetaiotaomicron 23213	0.037	0.038	0.063	0.041	0.044	0.007
B. salyersiae 23369	0.034	0.034	0.05	0.039	0.043	0.009
B. thetaiotaomicron 23596	0.035	0.034	0.041	0.039	0.039	0.004
B. faecis 23681	0.034	0.041	0.043	0.042	0.044	0.01

Sample	0hrs	10hrs	24hrs	34hrs	48hrs	48hrs - 0hrs
B. thetaiotaomicron 23699	0.034	0.035	0.034	0.04	0.043	0.009
B. ovatus 23736	0.031	0.04	0.033	0.04	0.039	0.008
B. thetaiotaomicron TS131APG1.1	0.046	0.038	0.038	0.043	0.044	-0.002
B. caccae TS4APG1.1	0.039	0.033	0.034	0.033	0.034	-0.005
B. thetaiotaomicron BT8713	0.036	0.039	0.044	0.038	0.046	0.01
B. ovatus DH4140	0.035	0.037	0.041	0.042	0.045	0.01
B. thetaiotaomicron 22959	0.035	0.043	0.045	0.035	0.058	0.023
B. faecis 23218	0.035	0.038	0.041	0.041	0.034	-0.001
B. thetaiotaomicron 23447	0.034	0.041	0.045	0.04	0.041	0.007
B. fragilis 23618	0.035	0.039	0.053	0.042	0.049	0.014
B. thetaiotaomicron 23682	0.036	0.033	0.035	0.038	0.038	0.002
B. ovatus 23708	0.035	0.036	0.039	0.04	0.045	0.01
Megasphaera cerevisiae 23742	0.035	0.041	0.043	0.039	0.04	0.005
B. thetaiotaomicron TS132APG1.1	0.034	0.04	0.047	0.045	0.041	0.007
B. thetaiotaomicron TS6APG1.1	0.035	0.036	0.041	0.041	0.041	0.006
B. thetaiotaomicron BT8669	0.035	0.041	0.046	0.042	0.046	0.011
B. thetaiotaomicron DH3730	0.035	0.04	0.042	0.042	0.045	0.01
B. thetaiotaomicron 22967	0.034	0.043	0.047	0.052	0.046	0.012
B. thetaiotaomicron 23156	0.033	0.04	0.043	0.043	0.043	0.01
B. thetaiotaomicron 23243	0.046	0.049	0.042	0.044	0.045	-0.001
B. thetaiotaomicron 23566	0.041	0.042	0.039	0.037	0.043	0.002
B. ovatus 23621	0.036	0.042	0.044	0.047	0.049	0.013
B. thetaiotaomicron 23685	0.024	0.04	0.043	0.041	0.039	0.015
B. ovatus ATCC-8483	0.028	0.041	0.039	0.041	0.043	0.015
B. ovatus 23748	0.033	0.04	0.042	0.044	0.039	0.006
B. thetaiotaomicron TS31APG1.1	0.034	0.028	0.034	0.052	0.033	-0.001
B. faecis BT8736	0.035	0.042	0.044	0.053	0.042	0.007
B. thetaiotaomicron DH3731	0.034	0.04	0.043	0.035	0.055	0.021
B. thetaiotaomicron 22987	0.034	0.039	0.051	0.045	0.043	0.009
B. thetaiotaomicron 23161	0.035	0.04	0.044	0.045	0.047	0.012
B. faecis 23251	0.036	0.041	0.046	0.046	0.048	0.012
B. ovatus 23575	0.036	0.038	0.044	0.048	0.051	0.015
B. vulgatus 23668	0.033	0.034	0.034	0.034	0.038	0.005
B. faecis 23688	0.035	0.04	0.042	0.043	0.045	0.01

Sample	0hrs	10hrs	24hrs	34hrs	48hrs	48hrs - 0hrs
B. thetaiotaomicron 23722	0.035	0.04	0.053	0.044	0.046	0.011
B. uniformis 23836	0.034	0.034	0.043	0.033	0.034	0
B. thetaiotaomicron TS118APG1.1	0.035	0.042	0.047	0.045	0.043	0.008
B. thetaiotaomicron TS32APG1.1	0.034	0.034	0.034	0.041	0.033	-0.001
B. thetaiotaomicron BT8655	0.033	0.034	0.035	0.034	0.038	0.005
B. thetaiotaomicron DH3941	0.034	0.039	0.032	0.045	0.046	0.012
B. fragilis 22998	0.037	0.03	0.046	0.05	0.055	0.018
B. thetaiotaomicron 23188	0.034	0.032	0.043	0.046	0.049	0.015
B. thetaiotaomicron 23269	0.036	0.041	0.044	0.045	0.045	0.009
B. fragilis 23576	0.038	0.036	0.038	0.03	0.055	0.017
B. ovatus 23689	0.034	0.04	0.042	0.042	0.045	0.011
B. faecis 23723	0.034	0.036	0.044	0.046	0.033	-0.001
B. faecis TS19APG1.1	0.035	0.04	0.043	0.045	0.038	0.003
B. thetaiotaomicron TS119APG1.2	0.036	0.04	0.044	0.046	0.046	0.01
B. thetaiotaomicron TS33APG1.1	0.034	0.041	0.045	0.049	0.051	0.017
B. thetaiotaomicron DH4087	0.034	0.043	0.047	0.05	0.05	0.016
B. thetaiotaomicron DH3956	0.035	0.045	0.048	0.049	0.055	0.02

Anti-fiber antibodies modulate bacterial interactions with dietary glycans

Previous work demonstrated that human gut bacteria exhibit strain-specific adhesion to dietary polysaccharides through interactions with glycan-coated artificial food particles (Patnode et al. 2021). Since mammals produce antibodies directed against many of these same dietary glycans (Chapter 2), we hypothesized that antibody binding could alter bacterial interactions with dietary polysaccharides. To test this, glycan-coated beads were incubated with glycan-specific antibodies before incubation with *Bacteroides thetaiotaomicron* DH4087, and bacterial adhesion was quantified by flow cytometry. In the absence of any antibodies, DH4087 adhered most strongly to galactan-coated particles compared with arabinoxylan- and xyloglucan-coated beads (Figure 3A). Pre-incubation with anti-galactan antibodies selectively reduced bacterial adhesion to galactan-coated beads and had little effect on adhesion to the other beads. In contrast, anti-xyloglucan antibodies did not reduce adhesion to xyloglucan-coated particles Together, these findings demonstrate that anti-fiber antibodies can alter bacterial interactions with dietary glycans in an antigen-dependent manner.

Because antibody binding altered bacterial adhesion to dietary glycans, we next investigated whether antibodies can limit enzyme activity against glycans. To test this, xylan-coated beads were pre-incubated with a xylan-specific blocking antibody before exposure to purified endo-1,4-β-xylanase. The blocking antibody was removed through pH-shocking and residual xylan was quantified using a second xylan-specific detecting antibody. In the absence of the blocking antibody, xylanase treatment reduced detection-antibody binding, consistent with enzymatic degradation of the xylan substrate (Figure 3B). Pre-incubation with the blocking antibody did not preserve detection-antibody binding following xylanase treatment, indicating that antibody occupancy was insufficient to prevent enzymatic access to the glycan. Together, these findings suggest that although anti-fiber antibodies can alter bacterial adhesion to dietary polysaccharides, they do not interfere with glycan hydrolysis under the conditions tested.

Although glycan-specific antibodies did not limit hydrolysis by a purified xylanase, bacterial glycan utilization relies on coordinated polysaccharide utilization systems composed of multiple glycan-binding proteins and carbohydrate-active enzymes. We therefore next investigated whether anti-fiber antibodies alter bacterial growth on dietary polysaccharides. *Bacteroides ovatus* has been shown to grow using polygalacturonate as a sole carbon source (Desai et al. 2016) and therefore provided a suitable model to determine whether antibody binding interferes with bacterial access to dietary glycans. To establish conditions for these assays, representative *B. ovatus* strains were first cultured in minimal medium containing increasing concentrations of polygalacturonate (PPC). A concentration of 1 mg/mL consistently supported robust bacterial growth across the majority of tested strains and was therefore selected for subsequent growth inhibition experiments (Table 2). Glycan-specific monoclonal antibodies were mixed with polygalacturonate-containing media before inoculation with the representative *B. ovatus* strains, and bacterial growth was monitored over 24 hours. None of the tested anti-glycan antibodies inhibited bacterial growth compared to the no-antibody control across the tested strains (Figure 3C). These findings indicate that antibody binding to dietary glycans is insufficient to inhibit bacterial growth on polygalacturonate. Together, these findings demonstrate that antibody-microbe interactions extend beyond immune recognition to include bacterial proteolysis of antibodies and modulation of bacteria-glycan interactions, although these effects do not broadly alter glycan hydrolysis or utilization under the conditions tested.

Table 2. Bacterial isolates using polygalacturonate (PPC) as a sole carbon source

Growth of gut bacterial isolates in minimal medium supplemented with 1 mg/mL PPC. Optical density at 595 nm was measured at the indicated time points over 49 h. The final column indicates the change in optical density between 49 h and 0 h.

Sample	0hrs	6hrs	9hrs	24hrs	30hrs	35hrs	49hrs	49hrs - 0hrs
BLANK	0.1067	0.1067	0.1067	0.1033	0.1033	0.1033	0.1033	-0.0033
B. ovatus VPI435	0.1100	0.1867	0.1967	0.1867	0.1800	0.1767	0.1567	0.0467
B. ovatus WH214	0.1067	0.1833	0.2167	0.1833	0.1800	0.1867	0.1500	0.0433
B. ovatus WH208	0.1067	0.1900	0.1900	0.1867	0.1833	0.1800	0.1267	0.0200
B. ovatus VPI3049	0.1067	0.1900	0.1900	0.1800	0.1900	0.1800	0.1900	0.0833
B. ovatus VPIC1622	0.1033	0.1233	0.1933	0.1767	0.1533	0.2067	0.1267	0.0233
B. ovatus WH514	0.1067	0.1100	0.1167	0.1867	0.1833	0.1767	0.1933	0.0867
B. ovatus WH601	0.1033	0.1300	0.1933	0.1933	0.1833	0.1867	0.1833	0.0800
B. ovatus VPI8653	0.1067	0.1867	0.1933	0.1933	0.1800	0.1733	0.1400	0.0333
B. ovatus WH711	0.1033	0.1900	0.1967	0.1800	0.1800	0.1800	0.1967	0.0933
B. ovatus WH604	0.1033	0.1500	0.1933	0.1900	0.1900	0.1633	0.1833	0.0800
B. ovatus WH713	0.1133	0.1700	0.2000	0.1933	0.1900	0.1867	0.1333	0.0200
B. ovatus VPIB411	0.1067	0.1700	0.1767	0.1933	0.1867	0.1667	0.1367	0.0300
B. ovatus VPIC145	0.1067	0.1767	0.1833	0.1867	0.1900	0.1800	0.1500	0.0433
B. ovatus VPI4104	0.1067	0.2000	0.1833	0.1900	0.1667	0.1733	0.1800	0.0733
B. ovatus DH4140	0.1067	0.1067	0.1100	0.1900	0.1867	0.1767	0.1500	0.0433
B. ovatus 23621	0.1067	0.1033	0.1067	0.1033	0.1033	0.1067	0.1033	-0.0033
B. ovatus 23708	0.1067	0.2033	0.2100	0.1900	0.1867	0.1733	0.1833	0.0767
B. ovatus 23734	0.1067	0.1333	0.1867	0.1867	0.1767	0.1800	0.1767	0.0700
B. ovatus 23689	0.1067	0.1100	0.1167	0.1167	0.1167	0.1167	0.1200	0.0133
B. ovatus 23735	0.1233	0.1033	0.1067	0.1033	0.1033	0.1033	0.1033	-0.0200
B. ovatus 23575	0.1067	0.2000	0.2133	0.1900	0.1600	0.1567	0.1533	0.0467
B. ovatus 23736	0.1067	0.1900	0.1967	0.1800	0.1500	0.1433	0.1400	0.0333

Sample	0hrs	6hrs	9hrs	24hrs	30hrs	35hrs	49hrs	49hrs - 0hrs
B. ovatus 23748	0.1067	0.2100	0.2000	0.2000	0.1700	0.1867	0.1600	0.0533
B. ovatus ATCC8483	0.1067	0.1567	0.2100	0.2067	0.1833	0.1767	0.1700	0.0633
B. thetaiotaomicron VPI5482	0.1033	0.1167	0.2000	0.2467	0.1567	0.1567	0.1600	0.0567

Figure 3. Fiber-specific monoclonal antibodies inhibit bacterial adhesion but do not prevent glycan hydrolysis or bacterial growth.

(A) *B. thetaiotaomicron*iotamicron DH4887 was incubated with arabinoxylan-, galactan-, or xyloglucan-coated beads in the presence of no antibody, a purified anti-galactan monoclonal antibody, or a purified anti-xyloglucan monoclonal antibody. Bacterial adhesion was quantified by measuring the mean fluorescence intensity (MFI) of Syto-82-positive events by flow cytometry. Bars represent the mean ± SD, and individual points represent biological replicates (n = 3). Statistical significance was determined using Student's t-test. $p < 0.05$ (*) and $p < 0.01$ (**). (B) Purified xylan-coated beads were incubated with xylanase in the presence or absence of a purified blocking anti-xylan IgM monoclonal antibody. Following enzymatic hydrolysis, bound IgM was removed by pH shock, and the remaining xylan epitopes were quantified using a purified detecting anti-xylan IgG monoclonal antibody by flow cytometry. Bars represent the mean ± SD, and individual points represent biological replicates (n = 5). Statistical significance was determined using Welch's t-test. $p < 0.05$ (*) and $p < 0.01$ (**). (C) Representative *B. ovatus* strains were cultured in minimal medium supplemented with citrus polygalacturonate in the presence of no antibody, a purified anti-polygalacturonate monoclonal antibody, or an unrelated purified anti-xylan monoclonal antibody. Bacterial growth was monitored by measuring optical density at 595 nm over 24 h. Data represent the mean ± SD of biological replicates (n = 3).

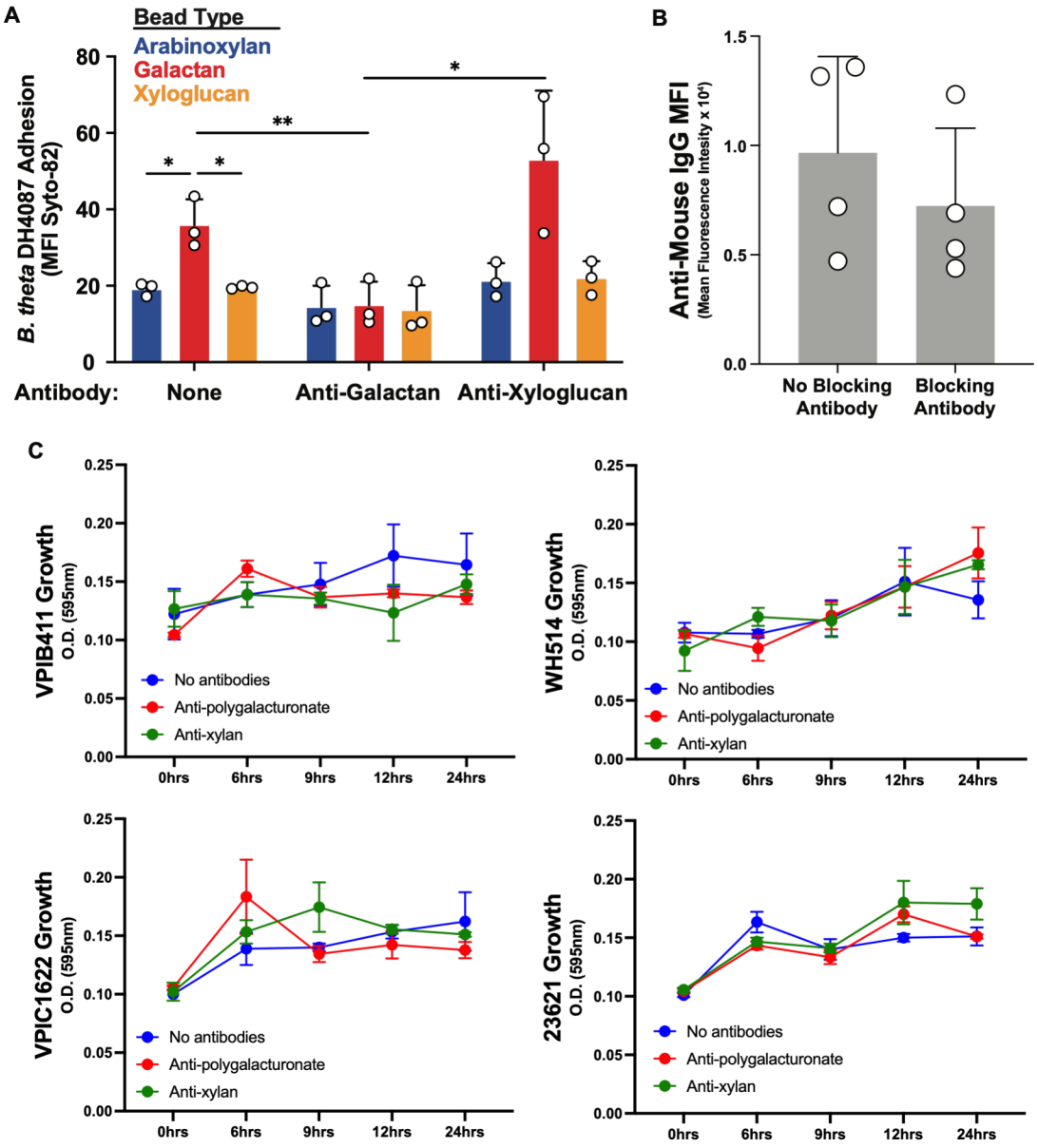
A
Bead Type
Arabinoxylan
Galactan
Xyloglucan
B. theta DH4087 Adhesion (MFI Syto-82)
Antibody:
None
Anti-Galactan
Anti-Xyloglucan
B
Anti-Mouse IgG MFI
(Mean Fluorescence Intesity x 10⁴)
No Blocking Antibody
Blocking Antibody
C
VPIB411 Growth
O.D. (595nm)
WH514 Growth
VPIC1622 Growth
23621 Growth
No antibodies
Anti-polygalacturonate
Anti-xylan
0hrs
6hrs
9hrs
12hrs
24hrs

Discussion:

Antibodies are classically viewed as immune effector molecules that protect the host by targeting pathogens and preventing their dissemination. In the intestinal lumen, secretory IgA (sIgA) is the predominant antibody isotype and is continuously encountered by the gut microbiota. Despite this constant exposure, little is known about how antibodies influence microbial ecology beyond their canonical functions, such as immune exclusion. Here, we investigated whether antibodies serve as (i) nitrogen sources for gut bacteria and (ii) whether glycan-specific antibodies alter bacterial interactions with dietary glycans. We found that gut bacteria, including individual human isolates and native microbial communities, proteolytically degrade antibodies. However, human antibodies supplied as the sole exogenous nitrogen source did not support growth of the tested human gut isolates. Furthermore, although glycan-specific antibodies reduced bacterial adhesion to dietary glycans, they had limited effects on glycan hydrolysis and bacterial growth. Together, these findings reveal that antibodies participate in multiple interactions with the gut microbiota beyond their established roles in host immunity.

Native gut bacterial communities and human isolates proteolytically degraded antibodies, yet this degradation did not support bacterial growth. At first glance, these findings appear contradictory, as degradation of proteins is often associated with nutrient acquisition. Antibody degradation has primarily been studied as an immune evasion strategy employed by pathogenic bacteria. In contrast, antibody degradation by commensal bacteria has received comparatively little attention, although native mouse gut bacterial communities have been shown to degrade intestinal antibodies and generate low-IgA phenotypes (Moon et al. 2015). As such, the biological significance of antibody degradation by commensal bacteria remains unclear. Our findings suggest that proteolytic cleavage of antibodies does not necessarily generate metabolically accessible nutrients and instead distinguish antibody proteolysis from complete antibody catabolism. One possible explanation is that proteolytic

cleavage produces relatively large antibody fragments that require additional processing before peptides and amino acids become metabolically accessible. Consequently, antibody cleavage alone may not liberate sufficient accessible nitrogen to broadly support bacterial growth. Complete degradation may require additional proteolytic activities beyond those encoded by a single organism.

Although anti-glycan antibodies reduced adhesion of the tested bacterium to glycan-coated beads, they did not inhibit microbial growth or glycan hydrolysis. The reduced adhesion could be due to antibodies masking glycan epitopes and limiting access to bacterial adhesion receptors, suggesting that bacterial adhesion and glycan utilization can be functionally uncoupled. One possible explanation is that carbohydrate-active enzymes retain access to glycan substrates despite antibody occupancy, allowing glycan degradation to proceed even when bacterial adhesion is diminished. These results suggest that anti-glycan antibodies selectively modulate initial bacteria-glycan interactions without broadly disrupting glycan utilization under the conditions tested.

Collectively, our findings expand the view of antibodies beyond their established roles in host defense by demonstrating that they participate in diverse interactions with the gut microbiota. Unlike antibodies directed against bacterial surface antigens, which are typically considered in the context of individual microbial species, glycan-specific antibodies may instead recognize shared dietary glycans that can be encountered by multiple bacterial taxa. Consequently, a single antibody specificity has the potential to influence interactions across diverse members of the microbial community rather than targeting a single bacterial species. Determining the physiological relevance of these interactions will require identification of the bacterial proteases responsible for antibody degradation, characterization of antibody-derived degradation products, and investigation if glycan-specific antibodies influence microbial ecology and dietary glycan utilization *in vivo*. Together, these studies

provide a new understanding of how adaptive immunity can contribute to the dynamic interactions between the host, diet, and gut microbiota within the intestinal lumen.

Methods:

Mouse sample collections (cecal contents)

Mice were euthanized individually by CO_2 asphyxiation followed by bilateral thoracotomy. Following euthanasia, the cecum was collected, and a small incision was made in the cecal wall. Cecal contents were squeezed from the incision onto a sterile surface.

Antibody degradation assays

Purified mouse IgA (BD Biosciences, 553472) and IgG (BD Biosciences, 554054) were diluted in PBS and plated onto Immulon 2HB 96-well plates (Thermo Fisher Scientific, 3455) at 100 µL/well. Antibodies were used at 0.25 µg/mL for assays using mouse cecal contents and 0.5 µg/mL for assays using bacterial culture supernatants. Plates were incubated overnight at 4°C. The following day, plates were washed with 200 µL PBS containing 1% Tween-20 (PBS-T), blocked with 200 µL/well blocking buffer (PBS containing 1% bovine serum albumin), and washed three times with 200 µL PBS-T. Plates were blocked for 1.5 h for cecal-content assays and 1 h for bacterial culture-supernatant assays.

Mouse cecal contents

Freshly collected cecal contents (10 mg) from germ-free Swiss albino or conventional C57BL/6 mice were suspended in 150 µL molecular-grade water, homogenized by vortexing, filtered through a sterile 100-µm nylon mesh, and centrifuged at 2,000 × g for 2 min to separate the clarified supernatant from the particulate fraction. A fresh protease inhibitor solution was prepared immediately before each experiment by dissolving one protease inhibitor tablet (Sigma, 11836170001) in 10 mL molecular-grade water. Cecal slurries and clarified supernatants were mixed 1:1 (v/v) with either the protease inhibitor solution or

molecular-grade water. Fifty microliters of each sample were added to antibody-coated wells and incubated anaerobically at 37°C for 5 h.

Bacterial culture supernatants

Overnight bacterial cultures were subcultured by inoculating 50 µL into 1 mL of brain heart infusion (BHI), tryptone-yeast extract-glucose (TYG), or minimal medium (MM) and incubated anaerobically at 37°C for 7 h. For the assays shown in Figure 1B, bacterial growth was monitored by measuring optical density at 595 nm before culture supernatants were collected. For the protease inhibition assays (Figure 1C-D), bacterial cultures were grown in TYG medium, subcultured in 900 µL TYG for 4 h, normalized by optical density at 595 nm, and culture supernatants were collected. Fifty microliters of clarified culture supernatant were added to antibody-coated wells and incubated anaerobically at 37°C overnight. For protease inhibition assays, culture supernatants were incubated with or without protease inhibitor before addition to the ELISA plates.

Pepsin (1 mg/mL in 10 mM HCl) was included as a positive control for antibody degradation, while PBS-T served as the negative control. Following incubation, plates were washed three times with PBS-T and incubated with biotin-conjugated anti-mouse detection antibodies diluted to 5 ng/mL. Anti-mouse IgA (Southern Biotech, 1040-05) and anti-mouse IgG (Jackson ImmunoResearch, 115-066-071) were used for the cecal-content assays (30 min at 4°C), whereas anti-mouse IgA alone was used for the bacterial culture-supernatant assays (15 min at 4°C). After washing, streptavidin-horseradish peroxidase (0.25 µg/mL) was added for 30 min at 4°C for cecal-content assays or 15 min at room temperature for bacterial culture-supernatant assays. Plates were washed three additional times with PBS-T, developed using 3,3′,5,5′-tetramethylbenzidine (TMB), and the reactions were stopped with 0.2 M sulfuric acid. Absorbance was measured at 450 nm with background correction at 570 nm using a microplate reader.

Bacterial growth assays

Minimal medium containing purified human IgG as the sole nitrogen source was prepared by combining 2X minimal medium, molecular-grade water, and a 5X human IgG stock solution. Aliquots were dispensed into deep-well plates and inoculated with 5 µL of each bacterial stock culture. Cultures were incubated anaerobically at 37°C for 72 h. Bacterial growth was monitored throughout the incubation period and optical density was measured at 595 nm using a microplate reader. All strains were screened once.

A collection of 25 Bacteroides ovatus strains, Bacteroides thetaiotaomicron VPI5482, and a no-bacteria control were inoculated into 500 µL tryptone-yeast extract-glucose (TYG) medium and grown anaerobically overnight at 37°C. Cultures were diluted 1:100 into minimal medium containing citrus polygalacturonate at 0, 1, 2.5, or 5 mg/mL and incubated anaerobically at 37°C for 72 h. Bacterial growth was monitored at multiple time points by measuring optical density at 595 nm.

Representative Bacteroides ovatus strains (23621, VPIB411, VPIC1622, and WH514) were grown anaerobically overnight in TYG medium. Cultures were subcultured into minimal medium containing 0.5 mg/mL citrus polygalacturonate, incubated for 1.5 h, normalized by optical density at 595 nm, and inoculated into assay wells containing polygalacturonate that had been pre-incubated with desalted, normalized glycan-specific CCRC monoclonal antibodies or molecular-grade water as a no-antibody control. Three independent biological replicates were performed for each condition. Bacterial growth was monitored over 24 h by measuring optical density at 595 nm using a microplate reader.

Blocking microbial adhesion

Bacterial strains were inoculated into 5 mL tryptone-yeast extract-glucose (TYG) medium and grown anaerobically overnight at 37°C. Three independent cultures were prepared for each

strain. Glycan-coated beads were aliquoted into 96-well plates and incubated for 1 h at room temperature with glycan-specific CCRC monoclonal antibodies or HNTB buffer as a no-antibody control. Following incubation, beads were washed three times with HNTB. Overnight bacterial cultures were normalized by optical density at 595 nm, harvested by centrifugation (4,000 × g, 5 min), washed with HNTB, and stained with 40 μM Syto82 for 10 min at room temperature in the dark. Stained bacteria were washed twice with HNTB and resuspended in HNTB. Twenty microliters of each bacterial suspension were added to antibody-treated glycan-coated beads and incubated for 30 min at 4°C on a rotator. Beads were washed once with HNTB to remove unbound bacteria, resuspended in HNTB, and analyzed by flow cytometry. Adhesion was quantified as the Syto82 median fluorescence intensity (MFI) associated with each bead population.

Blocking glycan hydrolysis

Xylan-coated beads were incubated overnight at 4°C on a rotator with the anti-xylan IgM monoclonal antibody M137 or HNTB buffer as a no-blocking control. The following day, beads were washed three times with HNTB and incubated with endo-1,4-β-xylanase (0.01 U/mL in 3.2 M ammonium sulfate) or ammonium sulfate alone for 10 min at 37°C. Following three washes with HNTB, bound antibodies were removed by incubation with glycine-HCl (pH 1.5) or glycine control for 30 min at room temperature. Beads were then incubated for 1 h at 4°C with the anti-xylan IgG monoclonal antibody M140 or HNTB, washed, and stained with Alexa Fluor 488-conjugated anti-mouse IgG and PE-Cy7-conjugated anti-mouse IgM secondary antibodies (1 μg/mL each). Following three washes with HNTB, beads were filtered through a 70-μm nylon mesh and analyzed by flow cytometry. Glycan hydrolysis was quantified by measuring the mean fluorescence intensity (MFI) of the M140 detection antibody, with increased fluorescence indicating preservation of xylan epitopes following enzyme treatment.

Bibliography:

Afrizal, Afrizal, Susan A. V. Jennings, Thomas C. A. Hitch, et al. 2022. “Enhanced Cultured Diversity of the Mouse Gut Microbiota Enables Custom-Made Synthetic Communities.” *Cell Host & Microbe* 30 (11): 1630–1645.e25.

Alahmari, Layla A. 2024. “Dietary Fiber Influence on Overall Health, with an Emphasis on CVD, Diabetes, Obesity, Colon Cancer, and Inflammation.” *Frontiers in Nutrition* 11 (December): 1510564.

Allman, David, Joel R. Wilmore, and Brian T. Gaudette. 2019. “The Continuing Story of T-Cell Independent Antibodies.” *Immunological Reviews* 288 (1): 128–135.

Anderson, Christopher J., Christopher B. Medina, Brady J. Barron, et al. 2021. “Microbes Exploit Death-Induced Nutrient Release by Gut Epithelial Cells.” *Nature* 596 (7871): 262–267.

Ansaldo, Eduard, Leianna C. Slayden, Krystal L. Ching, et al. 2019. “Akkermansia Muciniphila Induces Intestinal Adaptive Immune Responses during Homeostasis.” *Science (New York, N.Y.)* 364 (6446): 1179–1184.

Arora, Srishtee, Jay Gordon, and Magnus Hook. 2021. “Collagen Binding Proteins of Gram-Positive Pathogens.” *Frontiers in Microbiology* 12 (February): 628798.

Astronomo, Rena D., and Dennis R. Burton. 2010. “Carbohydrate Vaccines: Developing Sweet Solutions to Sticky Situations?” *Nature Reviews. Drug Discovery* 9 (4): 308–324.

Baek, Ga Hyeon, Ki Myeong Yoo, Seon-Yeong Kim, et al. 2023. “Collagen Peptide Exerts an Anti-Obesity Effect by Influencing the Firmicutes/Bacteroidetes Ratio in the Gut.” *Nutrients* 15 (11). https://doi.org/10.3390/nu15112610.

Balascio, J. R., J. K. Palmer, and A. A. Salyers. 1981. “Degradation of Guar Gum by Enzymes Produced by a Bacterium from the Human Colon.” *Journal of Food Biochemistry* 5 (4): 271–282.

Barber, Claudia, Carlos Sabater, Francisco Guarner, Abelardo Margolles, and Fernando Azpiroz. 2023. “Metabolic Response of Intestinal Microbiota to Guar Gum Consumption.” *Frontiers in Nutrition* 10 (June): 1160694.

Barber, Thomas M., Stefan Kabisch, Andreas F. H. Pfeiffer, and Martin O. Weickert. 2020. “The Health Benefits of Dietary Fibre.” *Nutrients* 12 (10): 3209.

Basha, Saleem, Naveen Surendran, and Michael Pichichero. 2014. “Immune Responses in Neonates.” *Expert Review of Clinical Immunology* 10 (9): 1171–1184.

Bayram, Rumeysa Olcay, Hülya Özdemir, Ayça Emsen, Hatice Türk Dağı, and Hasibe Artaç. 2019. “Reference Ranges for Serum Immunoglobulin (IgG, IgA, and IgM) and IgG Subclass Levels in Healthy Children.” *Turkish Journal of Medical Sciences* 49 (2): 497–505.

Bergqvist, P., A. Stensson, L. Hazanov, et al. 2013. “Re-Utilization of Germinal Centers in Multiple Peyer’s Patches Results in Highly Synchronized, Oligoclonal, and Affinity-Matured Gut IgA Responses.” *Mucosal Immunology* 6 (1): 122–135.

Bindels, Laure B., Rafael R. Segura Munoz, João Carlos Gomes-Neto, et al. 2017. "Resistant Starch Can Improve Insulin Sensitivity Independently of the Gut Microbiota." *Microbiome* 5 (1): 12.

Bolyen, Evan, Jai Ram Rideout, Matthew R. Dillon, et al. 2019. "Reproducible, Interactive, Scalable and Extensible Microbiome Data Science Using QIIME 2." *Nature Biotechnology* 37 (8): 852–857.

Bos, N. A., H. Kimura, C. G. Meeuwsen, et al. 1989. "Serum Immunoglobulin Levels and Naturally Occurring Antibodies against Carbohydrate Antigens in Germ-Free BALB/c Mice Fed Chemically Defined Ultrafiltered Diet." *European Journal of Immunology* 19 (12): 2335–2339.

Bourges, Dorothée, François Meurens, Mustapha Berri, et al. 2008. "New Insights into the Dual Recruitment of IgA+ B Cells in the Developing Mammary Gland." *Molecular Immunology* 45 (12): 3354–3362.

Bovin, Nicolai, Polina Obukhova, Nadezhda Shilova, et al. 2012. "Repertoire of Human Natural Anti-Glycan Immunoglobulins. Do We Have Auto-Antibodies?" *Biochimica et Biophysica Acta* 1820 (9): 1373–1382.

Bretin, Alexis, Jun Zou, Beng San Yeoh, et al. 2023. "Psyllium Fiber Protects against Colitis via Activation of Bile Acid Sensor Farnesoid X Receptor." *Cellular and Molecular Gastroenterology and Hepatology* 15 (6): 1421–1442.

Castigli, Emanuela, Stephen A. Wilson, Lilit Garibyan, et al. 2005. "TACI Is Mutant in Common Variable Immunodeficiency and IgA Deficiency." *Nature Genetics* 37 (8): 829–834.

Cerutti, Andrea. 2008. "The Regulation of IgA Class Switching." *Nature Reviews. Immunology* 8 (6): 421–434.

Chiang, Bo Huey, Giovanni Vega, Sarah C. Dunwoody, and Michael L. Patnode. 2024. "Bacterial Interactions on Nutrient-Rich Surfaces in the Gut Lumen." *Infection and Immunity* 92 (9): e00480-23. https://doi.org/10.1128/iai.00480-23.

Corthésy, Blaise. 2013. "Role of Secretory IgA in Infection and Maintenance of Homeostasis." *Autoimmunity Reviews* 12 (6): 661–665.

Czerkinsky, C., S. J. Prince, S. M. Michalek, et al. 1987. "IgA Antibody-Producing Cells in Peripheral Blood after Antigen Ingestion: Evidence for a Common Mucosal Immune System in Humans." *Proceedings of the National Academy of Sciences of the United States of America* 84 (8): 2449–2453.

Desai, Mahesh S., Anna M. Seekatz, Nicole M. Koropatkin, et al. 2016. "A Dietary Fiber-Deprived Gut Microbiota Degrades the Colonic Mucus Barrier and Enhances Pathogen Susceptibility." *Cell* 167 (5): 1339–1353.e21.

Di Rosa, Claudia, Annamaria Altomare, Elena Imperia, Chiara Spiezia, Yeganeh Manon Khazrai, and Michele Pier Luca Guarino. 2022. "The Role of Dietary Fibers in the Management of IBD Symptoms." *Nutrients* 14 (22): 4775.

Donaldson, G. P., M. S. Ladinsky, K. B. Yu, et al. 2018. “Gut Microbiota Utilize Immunoglobulin A for Mucosal Colonization.” *Science (New York, N.Y.)* 360 (6390): 795–800.

Eberl, Claudia, Diana Ring, Philipp C. Münch, et al. 2019. “Reproducible Colonization of Germ-Free Mice with the Oligo-Mouse-Microbiota in Different Animal Facilities.” *Frontiers in Microbiology* 10: 2999.

Enriquez, Josue, Brianyell Mc Daniel Mims, Scott Trasti, Kathryn L. Furr, and Matthew B. Grisham. 2020. “Genomic, Microbial and Environmental Standardization in Animal Experimentation Limiting Immunological Discovery.” *BMC Immunology* 21 (1): 50.

Faith, Jeremiah J., Philip P. Ahern, Vanessa K. Ridaura, Jiye Cheng, and Jeffrey I. Gordon. 2014. “Identifying Gut Microbe-Host Phenotype Relationships Using Combinatorial Communities in Gnotobiotic Mice.” *Science Translational Medicine* 6 (220): 220ra11.

Faith, Jeremiah J., Janaki L. Guruge, Mark Charbonneau, et al. 2013. “The Long-Term Stability of the Human Gut Microbiota.” *Science* 341 (6141): 1237439.

Finn, Adam. 2004. “Bacterial Polysaccharide-Protein Conjugate Vaccines.” *British Medical Bulletin* 70 (1): 1–14.

Flint, Harry J., Karen P. Scott, Sylvia H. Duncan, Petra Louis, and Evelyne Forano. 2012. “Microbial Degradation of Complex Carbohydrates in the Gut.” *Gut Microbes* 3 (4): 289–306.

Foote, Jeremy B., and John F. Kearney. 2009. “Generation of B Cell Memory to the Bacterial Polysaccharide Alpha-1,3 Dextran.” *Journal of Immunology (Baltimore, Md.: 1950)* 183 (10): 6359–6368.

Galili, U., R. E. Mandrell, R. M. Hamadeh, S. B. Shohet, and J. M. Griffiss. 1988. “Interaction between Human Natural Anti-Alpha-Galactosyl Immunoglobulin G and Bacteria of the Human Flora.” *Infection and Immunity* 56 (7): 1730–1737.

Grosse, Charlene S. J., Claus T. Christophersen, Amanda Devine, and Ian C. Lawrance. 2020. “The Role of a Plant-Based Diet in the Pathogenesis, Etiology and Management of the Inflammatory Bowel Diseases.” *Expert Review of Gastroenterology & Hepatology* 14 (3): 137–145.

Hapfelmeier, Siegfried, Melissa A. E. Lawson, Emma Slack, et al. 2010. “Reversible Microbial Colonization of Germ-Free Mice Reveals the Dynamics of IgA Immune Responses.” *Science (New York, N.Y.)* 328 (5986): 1705–1709.

Harris, Nicola L., Iris Spoerri, Jacqueline F. Schopfer, et al. 2006. “Mechanisms of Neonatal Mucosal Antibody Protection.” *The Journal of Immunology* 177 (9): 6256–6262.

Haskey, Natasha, Stephanie L. Gold, Jeremiah J. Faith, and Maitreyi Raman. 2023. “To Fiber or Not to Fiber: The Swinging Pendulum of Fiber Supplementation in Patients with Inflammatory Bowel Disease.” *Nutrients* 15 (5). https://doi.org/10.3390/nu15051080.

Hayakawa, K., and R. R. Hardy. 2000. “Development and Function of B-1 Cells.” *Current Opinion in Immunology* 12 (3): 346–353.

He, Bing, Raul Santamaria, Weifeng Xu, et al. 2010. “The Transmembrane Activator TACI Triggers Immunoglobulin Class Switching by Activating B Cells through the Adaptor MyD88.” *Nature Immunology* 11 (9): 836–845.

He, Bing, Weifeng Xu, Paul A. Santini, et al. 2007. “Intestinal Bacteria Trigger T Cell-Independent Immunoglobulin A(2) Class Switching by Inducing Epithelial-Cell Secretion of the Cytokine APRIL.” *Immunity* 26 (6): 812–826.

Holodick, Nichol E., Nely Rodríguez-Zhurbenko, and Ana María Hernández. 2017. “Defining Natural Antibodies.” *Frontiers in Immunology* 8 (July): 872.

Huflejt, Margaret E., Marko Vuskovic, Daniela Vasiliu, et al. 2009. “Anti-Carbohydrate Antibodies of Normal Sera: Findings, Surprises and Challenges.” *Molecular Immunology* 46 (15): 3037–3049.

Jazayeri, Mir Hadi, Ali Akbar Pourfathollah, Mohammad Javad Rasaee, Zahra Porpak, and Mohammad Ebrahim Jafari. 2013. “The Concentration of Total Serum IgG and IgM in Sera of Healthy Individuals Varies at Different Age Intervals.” *Biomedicine & Aging Pathology* 3 (4): 241–245.

Joglekar, Payal, Hua Ding, Pablo Canales-Herrerias, Pankaj Jay Pasricha, Justin L. Sonnenburg, and Daniel A. Peterson. 2019. “Intestinal IgA Regulates Expression of a Fructan Polysaccharide Utilization Locus in Colonizing Gut Commensal Bacteroides Thetaiotaomicron.” *mBio* 10 (6): e02324–19.

Juritsch, Anthony F., Edward C. Deehan, Anissa M. Armet, Peter J. Mannon, and Amanda E. Ramer-Tait. 2026. “Eating for Inflammatory Bowel Disease: Assessing the Effect of Dietary Carbohydrates on Gut Microbiota and Implications for Disease Management.” *The Journal of Nutrition* 156 (6): 101551.

Kappler, Katharina, and Thierry Hennet. 2020. “Emergence and Significance of Carbohydrate-Specific Antibodies.” *Genes and Immunity* 21 (4): 224–239.

Kawabe, T., T. Naka, K. Yoshida, et al. 1994. “The Immune Responses in CD40-Deficient Mice: Impaired Immunoglobulin Class Switching and Germinal Center Formation.” *Immunity* 1 (3): 167–178.

Kimura, H., M. Umeda, and D. M. Marcus. 1989. “Expression of a Cross-Reactive Idiotope on Naturally Occurring Murine Antibodies against 3-Fucosyllactosamine, Levan, and Dextran.” *Journal of Immunology (Baltimore, Md.: 1950)* 142 (10): 3477–3481.

Kiyohara, H., T. Matsumoto, T. Nagai, S-J Kim, and H. Yamada. 2006. “The Presence of Natural Human Antibodies Reactive against Pharmacologically Active Pectic Polysaccharides from Herbal Medicines.” *Phytomedicine: International Journal of Phytotherapy and Phytopharmacology* 13 (7): 494–500.

Koropatkin, Nicole M., Elizabeth A. Cameron, and Eric C. Martens. 2012. “How Glycan Metabolism Shapes the Human Gut Microbiota.” *Nature Reviews. Microbiology* 10 (5): 323–335.

Kostopoulos, Ioannis, Steven Aalvink, Petia Kovatcheva-Datchary, et al. 2021. “A Continuous Battle for Host-Derived Glycans Between a Mucus Specialist and a Glycan Generalist in Vitro and in Vivo.” *Frontiers in Microbiology* 12 (June): 632454.

Kulkarni, Devesha H., and Rodney D. Newberry. 2025. “Antigen Uptake in the Gut: An Underappreciated Piece to the Puzzle?” *Annual Review of Immunology* 43 (1): 571–588.

Kurosaki, Tomohiro, Yuichi Aiba, Kohei Kometani, Saya Moriyama, and Yoshimasa Takahashi. 2010. “Unique Properties of Memory B Cells of Different Isotypes: Memory B Cells of Different Isotypes.” *Immunological Reviews* 237 (1): 104–116.

Llewellyn, Sean R., Graham J. Britton, Eduardo J. Contijoch, et al. 2018. “Interactions between Diet and the Intestinal Microbiota Alter Intestinal Permeability and Colitis Severity in Mice.” *Gastroenterology* 154 (4): 1037–1046.e2.

Lu, Qiuhe, Thomas C. A. Hitch, Julie Y. Zhou, et al. 2024. “A Host-Adapted Auxotrophic Gut Symbiont Induces Mucosal Immunodeficiency.” *Science (New York, N.Y.)* 385 (6716): eadk2536.

Macpherson, A. J., D. Gatto, E. Sainsbury, G. R. Harriman, H. Hengartner, and R. M. Zinkernagel. 2000. “A Primitive T Cell-Independent Mechanism of Intestinal Mucosal IgA Responses to Commensal Bacteria.” *Science (New York, N.Y.)* 288 (5474): 2222–2226.

Macpherson, Andrew J., Bahtiyar Yilmaz, Julien P. Limenitakis, and Stephanie C. Ganal-Vonarburg. 2018. “IgA Function in Relation to the Intestinal Microbiota.” *Annual Review of Immunology* 36 (1): 359–381.

Mantis, N. J., N. Rol, and B. Corthésy. 2011. “Secretory IgA’s Complex Roles in Immunity and Mucosal Homeostasis in the Gut.” *Mucosal Immunology* 4 (6): 603–611.

Mariotti, François, and Christopher D. Gardner. 2019. “Dietary Protein and Amino Acids in Vegetarian Diets-A Review.” *Nutrients* 11 (11). https://doi.org/10.3390/nu11112661.

Marshall, Jennifer L., Adriana Flores-Langarica, Robert A. Kingsley, et al. 2012. “The Capsular Polysaccharide Vi from Salmonella Typhi Is a B1b Antigen.” *Journal of Immunology (Baltimore, Md.: 1950)* 189 (12): 5527–5532.

Martellet, Mônica Cerutti, Fernanda Majolo, Rodrigo Gay Ducati, Claucia Fernanda Volken de Souza, and Márcia Inês Goettert. 2022. “Probiotic Applications Associated with Psyllium Fiber as Prebiotics Geared to a Healthy Intestinal Microbiota: A Review.” *Nutrition (Burbank, Los Angeles County, Calif.)* 103-104 (111772): 111772.

Martens, Eric C., Herbert C. Chiang, and Jeffrey I. Gordon. 2008. “Mucosal Glycan Foraging Enhances Fitness and Transmission of a Saccharolytic Human Gut Bacterial Symbiont.” *Cell Host & Microbe* 4 (5): 447–457.

Martin, F., and J. F. Kearney. 2001. “B1 Cells: Similarities and Differences with Other B Cell Subsets.” *Current Opinion in Immunology* 13 (2): 195–201.

Martin, F., A. M. Oliver, and J. F. Kearney. 2001. “Marginal Zone and B1 B Cells Unite in the Early Response against T-Independent Blood-Borne Particulate Antigens.” *Immunity* 14 (5): 617–629.

McAdam, A. J., R. J. Greenwald, M. A. Levin, et al. 2001. “ICOS Is Critical for CD40-Mediated Antibody Class Switching.” *Nature* 409 (6816): 102–105.

McDonald, P. J., R. M. Goldblum, G. J. Van Sickle, and G. K. Powell. 1984. “Food Protein-Induced Enterocolitis: Altered Antibody Response to Ingested Antigen.” *Pediatric Research* 18 (8): 751–755.

Miller, Brittany M., and Andreas J. Bäumler. 2021. “The Habitat Filters of Microbiota-Nourishing Immunity.” *Annual Review of Immunology* 39 (1): 1–18.

Mishra, Arjun K., and Roy A. Mariuzza. 2018. “Insights into the Structural Basis of Antibody Affinity Maturation from next-Generation Sequencing.” *Frontiers in Immunology* 9 (February): 117.

Mistry, Dippica, and Robert A. Stockley. 2006. “IgA1 Protease.” *The International Journal of Biochemistry & Cell Biology* 38 (8): 1244–1248.

Moon, Clara, Megan T. Baldridge, Meghan A. Wallace, et al. 2015. “Vertically Transmitted Faecal IgA Levels Determine Extra-Chromosomal Phenotypic Variation.” *Nature* 521 (7550): 90–93.

Mysonhimer, Annemarie R., and Hannah D. Holscher. 2022. “Gastrointestinal Effects and Tolerance of Nondigestible Carbohydrate Consumption.” *Advances in Nutrition (Bethesda, Md.)* 13 (6): 2237–2276.

Nahm, Moon H., Jigui Yu, Jiri Vlach, and Maor Bar-Peled. 2020. “A Common Food Glycan, Pectin, Shares an Antigen with Streptococcus Pneumoniae Capsule.” *mSphere* 5 (2): e00074–20.

Ndeh, Didier, Artur Rogowski, Alan Cartmell, et al. 2017. “Complex Pectin Metabolism by Gut Bacteria Reveals Novel Catalytic Functions.” *Nature* 544 (7648): 65–70.

New, J. Stewart, Brian L. P. Dizon, Christopher F. Fucile, Alexander F. Rosenberg, John F. Kearney, and R. Glenn King. 2020. “Neonatal Exposure to Commensal-Bacteria-Derived Antigens Directs Polysaccharide-Specific B-1 B Cell Repertoire Development.” *Immunity* 53 (1): 172–186.e6.

Ngo, Phuong A., Markus F. Neurath, and Rocío López-Posadas. 2022. “Impact of Epithelial Cell Shedding on Intestinal Homeostasis.” *International Journal of Molecular Sciences* 23 (8). https://doi.org/10.3390/ijms23084160.

Noelle, R. J., and E. C. Snow. 1990. “Cognate Interactions between Helper T Cells and B Cells.” *Immunology Today* 11 (10): 361–368.

Obukhanych, Tetyana V., and Michel C. Nussenzweig. 2006. “T-Independent Type II Immune Responses Generate Memory B Cells.” *The Journal of Experimental Medicine* 203 (2): 305–310.

Pabst, Oliver. 2012. “New Concepts in the Generation and Functions of IgA.” *Nature Reviews. Immunology* 12 (12): 821–832.

Palm, Noah W., Marcel R. de Zoete, Thomas W. Cullen, et al. 2014. “Immunoglobulin A Coating Identifies Colitogenic Bacteria in Inflammatory Bowel Disease.” *Cell* 158 (5): 1000–1010.

Palma, Joanna, Beata Tokarz-Deptuła, Jakub Deptuła, and Wiesław Deptuła. 2018. “Natural Antibodies - Facts Known and Unknown.” *Central-European Journal of Immunology* 43 (4): 466–475.

Pan, Mingfang, Nilakshi Barua, and Margaret Ip. 2022. “Mucin-Degrading Gut Commensals Isolated from Healthy Faecal Donor Suppress Intestinal Epithelial Inflammation and Regulate Tight Junction Barrier Function.” *Frontiers in Immunology* 13 (October): 1021094.

Patnode, Michael L., Zachary W. Beller, Nathan D. Han, et al. 2019. “Interspecies Competition Impacts Targeted Manipulation of Human Gut Bacteria by Fiber-Derived Glycans.” *Cell* 179 (1): 59–73.e13.

Patnode, Michael L., Janaki L. Guruge, Juan J. Castillo, et al. 2021. “Strain-Level Functional Variation in the Human Gut Microbiota Based on Bacterial Binding to Artificial Food Particles.” *Cell Host & Microbe* 29 (4): 664–673.e5.

Pattathil, Sivakumar, Utku Avci, David Baldwin, et al. 2010. “A Comprehensive Toolkit of Plant Cell Wall Glycan-Directed Monoclonal Antibodies.” *Plant Physiology* 153 (2): 514–525.

Pelaseyed, Thaher, Joakim H. Bergström, Jenny K. Gustafsson, et al. 2014. “The Mucus and Mucins of the Goblet Cells and Enterocytes Provide the First Defense Line of the Gastrointestinal Tract and Interact with the Immune System.” *Immunological Reviews* 260 (1): 8–20.

Pickard, Joseph M., Melody Y. Zeng, Roberta Caruso, and Gabriel Núñez. 2017. “Gut Microbiota: Role in Pathogen Colonization, Immune Responses, and Inflammatory Disease.” *Immunological Reviews* 279 (1): 70–89.

Pinegin, B. V., A. V. Kulakov, E. A. Makarov, P. W. Ledger, and R. M. Khaitov. 1995. “The Occurrence of Natural Antibodies to Minimal Component of Bacterial Cell Wall (N-Acetylglucosaminyl-N-Acetylmuramyl Dipeptide) in Sera from Healthy Humans.” *Immunology Letters* 47 (1-2): 33–37.

Plaut, A. G. 1983. “The IgA1 Proteases of Pathogenic Bacteria.” *Annual Review of Microbiology* 37 (1): 603–622.

Pollard, Andrew J., Kirsten P. Perrett, and Peter C. Beverley. 2009. “Maintaining Protection against Invasive Bacteria with Protein-Polysaccharide Conjugate Vaccines.” *Nature Reviews. Immunology* 9 (3): 213–220.

Pontifex, Matthew G., Aleena Mushtaq, Gwenaëlle Le Gall, et al. 2021. “Differential Influence of Soluble Dietary Fibres on Intestinal and Hepatic Carbohydrate Response.” *Nutrients* 13 (12): 4278.

Porter, Nathan T., Pablo Canales, Daniel A. Peterson, and Eric C. Martens. 2017. “A Subset of Polysaccharide Capsules in the Human Symbiont Bacteroides Thetaiotaomicron Promote Increased Competitive Fitness in the Mouse Gut.” *Cell Host & Microbe* 22 (4): 494–506.e8.

Reese, Aspen T., Fátima C. Pereira, Arno Schintlmeister, et al. 2018. “Microbial Nitrogen Limitation in the Mammalian Large Intestine.” *Nature Microbiology* 3 (12): 1441–1450.

Renshaw, B. R., W. C. Fanslow 3rd, R. J. Armitage, et al. 1994. “Humoral Immune Responses in CD40 Ligand-Deficient Mice.” *The Journal of Experimental Medicine* 180 (5): 1889–1900.

Rivera-Chávez, Fabian, Lillian F. Zhang, Franziska Faber, et al. 2016. “Depletion of Butyrate-Producing Clostridia from the Gut Microbiota Drives an Aerobic Luminal Expansion of Salmonella.” *Cell Host & Microbe* 19 (4): 443–454.

Rowley, Carol A., Christopher J. Anderson, and Melissa M. Kendall. 2018. “Ethanolamine Influences Human Commensal Escherichia Coli Growth, Gene Expression, and Competition with Enterohemorrhagic E. Coli O157:H7.” *mBio* 9 (5). https://doi.org/10.1128/mBio.01429-18.

Shoemaker, N. B., H. Vlamakis, K. Hayes, and A. A. Salyers. 2001. “Evidence for Extensive Resistance Gene Transfer among Bacteroides Spp. and among Bacteroides and Other Genera in the Human Colon.” *Applied and Environmental Microbiology* 67 (2): 561–568.

Snapper, Clifford M. 2016. “Differential Regulation of Polysaccharide-Specific Antibody Responses to Isolated Polysaccharides, Conjugate Vaccines, and Intact Gram-Positive versus Gram-Negative Extracellular Bacteria.” *Vaccine* 34 (30): 3542–3548.

Stavnezer, Janet, Jeroen E. J. Guikema, and Carol E. Schrader. 2008. “Mechanism and Regulation of Class Switch Recombination.” *Annual Review of Immunology* 26 (1): 261–292.

Sunagar, Raju, Sudeep Kumar, Prachi Namjoshi, Sarah J. Rosa, Karsten R. O. Hazlett, and Edmund J. Gosselin. 2018. “Evaluation of an Outbred Mouse Model for Francisella Tularensis Vaccine Development and Testing.” *PloS One* 13 (12): e0207587.

Tailford, Louise E., Emmanuelle H. Crost, Devon Kavanaugh, and Nathalie Juge. 2015. “Mucin Glycan Foraging in the Human Gut Microbiome.” *Frontiers in Genetics* 6 (March): 81.

Telis, V., K. Wolf, and P. Sobral. 2006. “Characterizations of Collagen Fibers for Biodegradable Films Production.” Paper presented 13th World Congress of Food Science & Technology, 2006/9/17-2006/9/21, Nantes, France. *13th World Congress of Food Science & Technology*. https://doi.org/10.1051/iufost:20060929.

Usami, Katsuki, Kanae Niimi, Ayumi Matsuo, et al. 2021. “The Gut Microbiota Induces Peyer’s-Patch-Dependent Secretion of Maternal IgA into Milk.” *Cell Reports* 36 (10): 109655.

Vinuesa, Carola G., and Pheh-Ping Chang. 2013. “Innate B Cell Helpers Reveal Novel Types of Antibody Responses.” *Nature Immunology* 14 (2): 119–126.

Wilmore, Joel R., Brian T. Gaudette, Daniela Gomez Atria, et al. 2018. “Commensal Microbes Induce Serum IgA Responses That Protect against Polymicrobial Sepsis.” *Cell Host & Microbe* 23 (3): 302–311.e3.

Wilson, Christopher B., and Tobias R. Kollmann. 2008. “Induction of Antigen-Specific Immunity in Human Neonates and Infants.” *Nestle Nutrition Workshop Series. Paediatric Programme* (Basel) 61: 183–195.

Wong, Jason B., Susannah L. Hewitt, Lynn M. Heltemes-Harris, et al. 2019. “B-1a Cells Acquire Their Unique Characteristics by Bypassing the Pre-BCR Selection Stage.” *Nature Communications* 10 (1): 4768.

Wortis, H. H., M. Teutsch, M. Higer, J. Zheng, and D. C. Parker. 1995. “B-Cell Activation by Crosslinking of Surface IgM or Ligation of CD40 Involves Alternative Signal Pathways and Results in Different B-Cell Phenotypes.” *Proceedings of the National Academy of Sciences of the United States of America* 92 (8): 3348–3352.

Wu, Meng, Nathan P. McNulty, Dmitry A. Rodionov, et al. 2015. “Genetic Determinants of in Vivo Fitness and Diet Responsiveness in Multiple Human Gut Bacteroides.” *Science* 350 (6256): aac5992.

Xu, Rong, Lin Zheng, Guowan Su, Donghui Luo, Chenrong Lai, and Mouming Zhao. 2021. “Protein Solubility, Secondary Structure and Microstructure Changes in Two Types of Undenatured Type II Collagen under Different Gastrointestinal Digestion Conditions.” *Food Chemistry* 343 (May): 128555.

Yamamoto, Yuko, Toru Takahahi, Masahiro To, et al. 2016. “The Salivary IgA Flow Rate Is Increased by High Concentrations of Short-Chain Fatty Acids in the Cecum of Rats Ingesting Fructooligosaccharides.” *Nutrients* 8 (8): E500.

Yamamoto, Yuko, Masahiro To, Takashi Hayashi, et al. 2015. “Intake of Indigestible Carbohydrates Influences IgA Response and Polymeric Ig Receptor Expression in the Rat Submandibular Gland.” *The British Journal of Nutrition* 113 (12): 1895–1902.

Zeng, Melody Y., Daniel Cisalpino, Saranyaraajan Varadarajan, et al. 2016. “Gut Microbiota-Induced Immunoglobulin G Controls Systemic Infection by Symbiotic Bacteria and Pathogens.” *Immunity* 44 (3): 647–658.

Zeng, Xianfeng, Xi Xing, Meera Gupta, et al. 2022. “Gut Bacterial Nutrient Preferences Quantified in Vivo.” *Cell* 185 (18): 3441–3456.e19.

Zhang, Shanshan, Yi Han, Whitman Schofield, et al. 2023. “Select Symbionts Drive High IgA Levels in the Mouse Intestine.” *Cell Host & Microbe* 31 (10): 1620–1638.e7.

Zubler, R. H. 2001. “Naive and Memory B Cells in T-Cell-Dependent and T-Independent Responses.” *Springer Seminars in Immunopathology* 23 (4): 405–419.